

AD-A174 455

EVALUATION OF RADIATION TECHNIQUES FOR IMPROVING THE
MECHANICAL PROPERTIES. (U) MARYLAND UNIV COLLEGE PARK
LAB FOR RADIATION AND POLYMER SCIE.

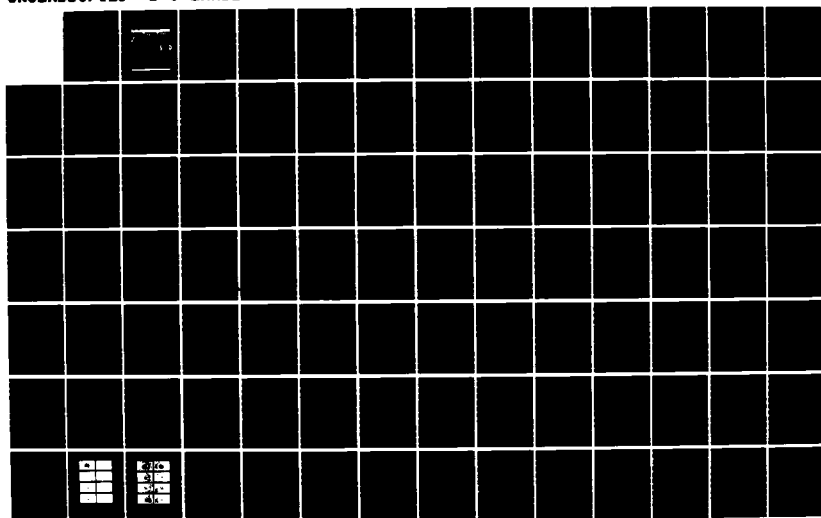
1/2

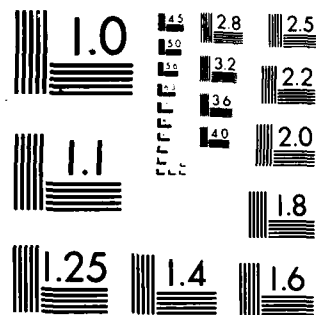
UNCLASSIFIED

B J LAMBERT ET AL. OCT 86 TACOM-TR-13215

F/G 11/10

NL





MICROCOPY RESOLUTION TEST CHART
NATIONAL BUREAU OF STANDARDS-1963-A

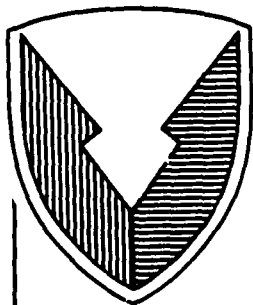
12

AD-A174 455

RD & E

C E N T E R

Technical Report



No. 13215

EVALUATION OF RADIATION TECHNIQUES
FOR IMPROVING THE MECHANICAL PROPERTIES

OF TANK PADS

CONTRACT NUMBER DAAE07-84C-R086

OCTOBER 1986

DTIC
ELECTE
NOV 26 1986
S D

DTIC FILE COPY

Byron J. Lambert & Joseph Silverman
University of Maryland
Laboratory for Radiation and
Polymer Science
Department of Chemical and
Nuclear Engineering

By College Park, MD 20742

APPROVED FOR PUBLIC RELEASE:
DISTRIBUTION IS UNLIMITED.

U.S. ARMY TANK-AUTOMOTIVE COMMAND
RESEARCH, DEVELOPMENT & ENGINEERING CENTER
Warren, Michigan 48397-5000

86 11 26 004

NOTICES

This report is not to be construed as an official Department of the Army position.

Mention of any trade names or manufacturers in this report shall not be construed as an official indorsement or approval of such products or companies by the U.S. Government.

Destroy this report when it is no longer needed. Do not return it to the originator.

UNCLASSIFIED

SECURITY CLASSIFICATION OF THIS PAGE

REPORT DOCUMENTATION PAGE

Form Approved
OMB No 0704-0188
Exp. Date Jun 30, 1986

1a. REPORT SECURITY CLASSIFICATION Unclassified			1b. RESTRICTIVE MARKINGS	
2a. SECURITY CLASSIFICATION AUTHORITY			3. DISTRIBUTION/AVAILABILITY OF REPORT	
2b. DECLASSIFICATION/DOWNGRADING SCHEDULE			Approved for Public Release. Distribution is Unlimited	
4. PERFORMING ORGANIZATION REPORT NUMBER(S) 13215			5. MONITORING ORGANIZATION REPORT NUMBER(S)	
6a. NAME OF PERFORMING ORGANIZATION University of Maryland		6b. OFFICE SYMBOL (If applicable)	7a. NAME OF MONITORING ORGANIZATION U.S. Army Tank-Automotive Command	
6c. ADDRESS (City, State, and ZIP Code) College Park, MD 20742			7b. ADDRESS (City, State, and ZIP Code) Warren, MI 48397-5000	
8a. NAME OF FUNDING/SPONSORING ORGANIZATION		8b. OFFICE SYMBOL (If applicable)	9. PROCUREMENT INSTRUMENT IDENTIFICATION NUMBER	
8c. ADDRESS (City, State, and ZIP Code)			10. SOURCE OF FUNDING NUMBERS	
			PROGRAM ELEMENT NO.	PROJECT NO.
			TASK NO.	WORK UNIT ACCESSION NO.
11. TITLE (Include Security Classification) EVALUATION OF RADIATION TECHNIQUES FOR IMPROVING THE MECHANICAL PROPERTIES OF TANK PADS				
12. PERSONAL AUTHOR(S) Lambert, Byron, J. and Silverman, Joseph				
13a. TYPE OF REPORT Final		13b. TIME COVERED FROM 7/84 TO 8/86		14. DATE OF REPORT (Year, Month, Day) 1986 October
				15. PAGE COUNT 120
16. SUPPLEMENTARY NOTATION				
17. COSATI CODES			18. SUBJECT TERMS (Continue on reverse if necessary and identify by block number)	
FIELD	GROUP	SUB-GROUP		
19. ABSTRACT (Continue on reverse if necessary and identify by block number)				
<p>This report describes the development work involved in processing T-142 tank pads with elastomers cured by high energy electrons. Two hundred such pads have been delivered to Yuma Proving Grounds for field testing. Also presented are the studies which demonstrate that design and manufacture of pads by means of this technology involves commercially available electron beam generators under circumstances where there is no radioactivity in the product or in the radiation installation. Our formulation studies show significant advances and much potential for radiation formulation improvements based on the electron curing technology. One such formulation is the basis of patent action.</p>				
20. DISTRIBUTION/AVAILABILITY OF ABSTRACT			21. ABSTRACT SECURITY CLASSIFICATION	
<input checked="" type="checkbox"/> UNCLASSIFIED/UNLIMITED <input type="checkbox"/> SAME AS RPT <input type="checkbox"/> DTIC USERS			Unclassified	
22a. NAME OF RESPONSIBLE INDIVIDUAL Jack Patt			22b. TELEPHONE (Include Area Code) (313) 574-8687	22c. OFFICE SYMBOL AMSTA-RTT

TABLE OF CONTENTS

Section	Page
1.0. INTRODUCTION	8
2.0. OBJECTIVES	8
3.0. CONCLUSIONS	8
3.1. Electron Beam Processing Feasibility	8
3.2. Residual Activity	8
3.3. Quality of Radiation-Cured Tank Pads	8
3.4. Potential for Improvement of Radiation-Cured Formulations	9
4.0. RECOMMENDATIONS	9
5.0. DISCUSSION	10
5.1. Background	10
5.1.1. Mechanical Properties of Radiation-Cured Elastomers	10
5.1.2. Radiation Cure Advantages	13
5.2. Pad Production by Electron Beam	14
5.2.1. Radioactivity	14
5.2.2. Dose Depth Profiles	14
5.2.3. Temperature Profiles	17
5.2.4. Process Specifications	17
5.3. Contract Deliverables	24
5.4. Optimization Studies: Formulations and Dose Requirements	24
5.4.1. Motivation for Radiation Sensitization	26
5.4.2. Mechanical Property Tests - SBR	26
5.4.3. BR, NR, and SBR with TMPTMA	48
5.4.4. BR plus syndiotactic-1,2-polybutadiene	48
5.4.5. Dose Requirements for Partially Sulfur-Cured Pads.	82
SELECTED BIBLIOGRAPHY	92
APPENDIX A DISCLOSURE DOCUMENT FOR RADIATION CURE OF BR WITH SYNDIOTACTIC-1,2-POLYBUTADIENE	A-1
APPENDIX B THEORETICAL ACTIVATION OF IRRADIATED TANK PADS	B-1
APPENDIX C DOSE DEPTH EXPERIMENTAL MEASUREMENTS	C-1
APPENDIX D DOSE DEPTH THEORETICAL PROFILES	D-1
APPENDIX E PAD FORMULATION AND RHEOMETER CURVE	E-1
APPENDIX F THERMAL GRAVIMETRIC ANALYSIS CURVES	F-1
APPENDIX G RHEOMETER CURVES: TAN δ AND LOSS MODULUS	G-1



Availability Codes	
Dist	Avail and/or Special
A-1	

LIST OF ILLUSTRATIONS

Figure	Title	Page
5-1.	Measured Dose Depth Profiles	16
5-2.	Theoretical Dose Depth Profiles	18
5-3.	One-Sided Irradiation Dose Depth Profiles	19
5-4.	Pad Carrier Design	22
5-5.	Electron Beam Horizontal Dosimetry	23
5-6.	Hot Tear Strength vs. Dose. SBR (A-F)	32
5-7.	Hot Tear Strength vs. Dose. SBR (G'-K)	34
5-8.	200% Modulus vs. Dose. SBR (A-F)	35
5-9.	200% Modulus vs. pphr DTUD. SBR (A-F)	36
5-10.	Hot Tear Strength vs. 200% Modulus. SBR (A-F)	37
5-11.	Hot Tear Strength vs. pphr DTUD. SBR (A-F)	38
5-12.	Tensile Strength vs. 200% Modulus. SBR (A-F)	40
5-13.	Hot Tear Strength vs. 200% Modulus. SBR (G'-K)	43
5-14.	Hot Tear Strength vs. 200% Modulus. SBR (A, GB, LB)	44
5-15.	Mechanical Properties: NR, BR, and SBR	52
5-16.	Carbon Gel% vs. Dose. BR	57
5-17.	Carbon Gel% vs. RB-820 Concentration. BR	58
5-18.	Charlesby-Pinner Plot for BR and RBR	59
5-19.	Tensile Strength vs. Dose. BR	62
5-20.	200% Modulus vs. Dose. BR	63
5-21.	Elongation % vs. Dose. BR	64
5-22.	Hot Tear Strength vs. Dose. BR	65
5-23.	Tensile Strength vs. RB-820 Concentration. BR	69

LIST OF ILLUSTRATIONS (Continued)

Figure	Title	Page
5-24.	200% Modulus vs. RB-820 Concentration. BR	70
5-25.	Elongation % vs. RB-820 Concentration. BR	71
5-26.	Hot Tear Strength vs. RB-820 Concentration. BR	72
5-27.	Tensile Strength vs. 200% Modulus. BR	73
5-28.	Hot Tear Strength vs. 200% Modulus. BR	74
5-29.	Stress-Strain Comparison of RBR-20-B to BR-150	76
5-30.	Tensile Strength vs. RB-820 Conc. BR (Heat Treatment)	78
5-31.	200% Modulus vs. RB-820 Conc. BR (Heat Treatment)	79
5-32.	Elongation % vs. RB-820 Conc. BR (Heat Treatment)	80
5-33.	Change in IR Spectrum of Irradiated Syndio-1,2-PBD by Heat Treatment	81
5-34.	X-Ray Diffraction Patterns	83
5-35.	Tank Pad and Model Compound - Tensile Strength	87
5-36.	Tank Pad and Model Compound - 200% Modulus	88
5-37.	Tank Pad and Model Compound - Ultimate Elongation	89
5-38.	Tank Pad and Model Compound - Hot Tear Strength	90

LIST OF TABLES

Table	Title	Page
5-1.	Activation Measurements of Irradiated Tank Pads . .	15
5-2.	Temperature Measurements of Irradiated Tank Pads . .	20
5-3.	Mechanical Property Test Results: Delivered Tank Pads	25
5-4.	Properties Comparison of Natural and Synthetic Rubbers and Natural Rubbers	27
5-5.	SBR Formulations	28
5-6.	Mechanical Properties - Series A-F, SBR	29
5-7.	Mechanical Properties - Series G'-K, SBR	30
5-8.	Mechanical Properties - Series GB, LB, SBR	31
5-9.	Oligomer Sensitizing Agents.	45
5-10.	Gel Fraction Tests for Radiation Sensitizers - SBR .	46
5-11.	NR, BR, and SBR Formulations	49
5-12.	Identification of NR BR and SBR Sample Sheets . . .	50
5-13.	Mechanical Properties: NR, BR, and SBR	51
5-14.	Gel Fraction Tests: BR plus TMPTMA	51
5-15.	BR Formulations	55
5-16.	Carbon Gel Results of RBR Series	56
5-17.	Mechanical Properties of RBR Series	61
5-18.	Sulfur-cured Polybutadiene Data from BRDC	66
5-19.	Mechanical Properties of S-Cured Series, BR	68
5-20.	Mechanical Properties of RBR-HT Series	77
5-21.	Mechanical Properties - Partial Sulfur Cure Only . .	86
5-22.	26-3 Plus Radiation Cure	86

LIST OF TABLES

Table	Title	Page
5-23.	Tank Pads Plus Gamma Rays	86
5-24.	Tank Pads Plus Electron Beam	91

1.0. INTRODUCTION

This report describes the production of 200 T-142 tank-pads cured with high energy electron beams and the results of a large array of experimental studies to optimize the rubber formulation and irradiation conditions for these pads. This work confirms that the high energy electron beam curing method is a feasible and available technology.

This work was performed under Army contract DAAE07-84C-R086 by the University of Maryland's Laboratory for Radiation and Polymer Science.

2.0. OBJECTIVE

This study is designed to improve the performance of elastomer pads used on track vehicles. The approach is to determine a formulation that can be cured by high energy electron beams under conditions which are practical, economical and safe. Among the parameters to be optimized to achieve this objective are a base elastomer, a crosslink sensitizer, and electron beam energy.

3.0. CONCLUSIONS

3.1. Electron Beam Pad Processing Feasibility

As demonstrated by the production of 200 T-142 tank-pads under this contract and by the discussion in par. 5.2, radiation curing of tank-pads by electron beam processing is feasible and the technology is commercially available.

3.2. Residual Activity

As measured experimentally and demonstrated theoretically, there is absolutely no significant residual activity of the pad or pad assembly from electron beam curing.

3.3. Quality of Radiation Cured Tank-Pads

At this writing, field testing of the 200 T-142 pads has yet to be performed. The pads are divided into two groups: 100 have a front-surface dose of 10 megarad (Mrad) and the remaining received a dose of 15 Mrad.

Mechanical property tests do not generally correlate well with field service. Nevertheless it is noteworthy that results obtained by others on the sulfur-cured pads are comparable to those we obtained on the radiation-cured pads we prepared in

nearly all tests and that our radiation-cured pads of similar composition are superior to the sulfur-cured pads in several significant tests (See pars. 3 & 5). The following general results have been observed.

- Hot tear strength, a test thought to correlate with the major failure mode of tank-pads, is better than the best sulfur cured formulations.
- Crack initiation and crack growth test results are excellent.
- Ozone resistance of the pads is excellent.

On the other hand, heat buildup is an area of concern. We believe this shortcoming would be overcome in the electron-cured butadiene rubber (BR) we have discovered but have not had sufficient opportunity to develop.

3.4. Potential for Improvement of Radiation Cured Formulations

Evidence presented in a patent disclosure we have filed on our discovery of crystallinity in a stretch-oriented radiation-cured blend of BR with syndiotactic-1,2-polybutadiene (R) (see APPENDIX A) suggests there is a great potential for pad application. These observations were made too late to allow us to investigate adequately the possible use of such formulations in the preparation of the 200 T-142 pads specified for delivery in accordance with this contract (see par 4.0.).

4.0. RECOMMENDATIONS

Laboratory tests as discussed in this report justify a more detailed and extended development program of suitable electron beam cured elastomeric formulations. We have particular faith in the prospects relating to our patent disclosure on the discovery of crystallinity in a stretch oriented blend of BR with R. Butadiene rubber as usually made has excellent abrasion resistance and heat dissipation properties which make it attractive for pad application. However, its poor tensile properties have limited its application. Our discovery of a blend of BR with R which induces crystallinity upon stretching when it is radiation-cured with modest doses (and not upon sulfur-curing) greatly improves these mechanical properties.

While the BR-R blend is of special interest, there is also substantial promise in sensitized styrene-butadiene rubber (SBR) formulations. The apparent failure of the polyfunctional additives to reduced dose requirements substantially can most likely be overcome by changes in the conditions and order of

blending operations. We recommend such a development program be pursued.

5.0. DISCUSSION

This section begins with background information and a survey of literature reporting the mechanical properties of radiation-cured elastomers. This is followed by a detailed discussion of the tank-pad electron beam curing process. Next is the important section describing the final deliverables of this contract. The final section discusses the extensive laboratory studies performed to optimize dose and formulation for the electron-cured pad.

5.1. Background

When rubber track is examined microscopically, pockets of the rubber's individual components are observed. This inhomogeneous mix of vulcanized agents can give rise to spatial crosslink distributions which cause the track's failure in the field. A more even crosslink distribution or one tailored to overcome specific failure modes may prove to be especially important when the tank's entire 60-ton weight sits on a few tracks. Under these conditions, uneven crosslink distribution would certainly tend to induce their failure.

Ionizing radiation provides a method for curing plastics and rubber in the absence of chemical curing agents and produces a spatially-uniform crosslink distribution. Although gammas from cobalt-60 could provide the penetration required to cure treads one-two inches thick, its dose rate is too low to maintain reasonable processing rates or compete effectively with oxidative degradation. Most electron devices (1-4 million electron volts [MeV]), on the other hand, are unable to penetrate the tread's entire thickness. A possible solution is high-energy electrons (10 MeV) from a linear accelerator. These electrons could provide the penetration at a dose rate consistent with processing considerations.

5.1.1. Mechanical Properties of Radiation-Cured Elastomers. The motivation to apply high electron beam processing technology to tank-pad production is more fully understood after examining the mechanical properties of radiation-cured elastomers and the advantages of radiation cure over sulfur cure. To date, tank-pads are made with an SBR base and are crosslinked by traditional sulfur vulcanization. Sulfur, sulfur activators and accelerators, and the other additives are compounded into the uncured SBR and formed by heat under high pressure in the mold to form a network of sulfide and polysulfide crosslinks. Ionizing radiation, alternatively, produces chemically active

radicals, ions, and excited molecules directly on the polymer chains, and on the crosslink promoters if present, which then react to form the rubber network. The literature data available on the mechanical properties of radiation cured systems is relatively sparse.

Early data from the 1950's and 1960's showed that the tensile strength of sulfur-cured rubbers was markedly higher than that of radiation-cured samples. Recent data primarily on SBR, however, demonstrate that tensile strength and energy at break of radiation-cured samples are only a few percent lower than those of sulfur-cured samples, while the flex life measurements of radiation-cured samples are superior by a factor of two. Bohm has recently reviewed all of the small amount of data available on the mechanical properties of irradiated rubbers. He has analyzed both the large discrepancies between early and more recent data, as well as the small differences in properties reported in recent data between sulfur- and radiation-cured samples, and has concluded that radiation-cured rubber has mechanical properties nearly equal to those of sulfur-cured rubber.

Both of the issues analyzed by Bohm have been difficult to explain theoretically. Well developed rubber elasticity theory predicts the modulus of unfilled rubber systems and some filled systems. Tensile theory accurately relates energy at break to hysteresis, and both of the theories apply to radiation-cured rubbers. However, neither is sufficient to explain the differences in radiation and sulfur-cured physical property data. Hence, most discussion of these data is speculation about the influence of various factors which affect the mechanical properties of rubbers.

Six general factors affecting the mechanical properties of rubbers and associated interpretation of observed mechanical property data are summarized below.

- The size, shape, and activity of fillers and the blending procedure.
- Polymer backbone modification during the crosslinking process. An example is the 4°C rise in glass transition temperature (T_g) of SBR after sulfur vulcanization because of the sulfur graft to the polymer chains. Also, this factor is suggested as a major reason for the large discrepancy in early data showing radiation cured sample tensile strength much inferior to that of sulfur cured samples. High doses and low dose rates, typical of gamma ray source irradiations of early investigators, are thought to have caused polymer backbone degradation and corresponding inferior

properties.

- Intermolecular forces among polymer chains.
- Concentration of network crosslinks. This is possibly the most important characterization of an elastomeric network. Mechanical property data are commonly plotted against crosslink density. 200 percent and 300 percent modulus are frequently used indicators of relative crosslink density. Radiation and sulfur-cured elastomers should, in general, be compared at the same crosslink density.
- Chemical nature of the crosslinks. This was a popular explanation evoked to explain the early data that sulfur-cure tensile strength is much higher than that of radiation-cure. Bateman argued that the lower thermodynamic strength of S-S versus C-C bonds results in S-S bond slippage under stress to relieve localized stress and avoid failure modes. However, Tobolsky and Lyons reported relaxation of stress data at constant elongation which indicate that S-S is no more labile than C-C at room temperature, although it is more labile at elevated temperatures. Lal more directly refutes Bateman by converting S-S_n-S crosslinks to S-S links with no resulting change in physical properties. Also, Bohm polymerized ethylene-propylene-diene monomer rubber (EPDM) with a polyfunctional monomer which is very reactive to both sulfur cure and radiation cure, hence specifying the crosslink distribution in both systems. In these systems, where the type of crosslink should be the only variable affecting mechanical properties, the tensile strength in the radiation samples is within 7 percent of the sulfur-cured system.
- Spatial distribution of crosslink density. To explain the earlier data showing large superiority in strength of sulfur cure, a disparity of crosslink density distribution uniformity on the molecular level was proposed. Gehman proposed a random, uniform crosslink distribution for the radiation system and a nonuniform distribution for the sulfur system due to a tendency to form vicinal crosslinks. An analysis of these crosslink distributions indicates that the sulfur system results in a more uniform distribution of chain length between links, M_c , which leads to a less stressed, stronger network.

To explain small discrepancies in recent property data of radiation- and sulfur-cured samples, a disparity of crosslink

density distribution on the molecular level was again proposed. However, Bohm proposed that the sulfur system has a uniform crosslink density distribution while the radiation sample has an increased crosslink density near carbon black particles due to an increase in energy dissipation surrounding the relatively high density particles. Increased crosslink density resulting from increased energy dissipation around more dense fillers in polyethylene (PE) systems has been reported before, but replicate experiments at other laboratories fail to confirm such a phenomenon.

5.1.2 Radiation Cure Advantages. Radiation curing has many potentially attractive features, such as cold cure, cure without chemical additives, and in some cases energy, space, time and cost savings. However, a particularly attractive feature with respect to pad production may be radiation's ability to readily adjust the spatial distribution of crosslink density. A patent by Bohm provides an outstanding illustration in which different layers of a composite are cured to vastly differing crosslink densities using ionizing radiation. This feature can undoubtedly help overcome specific elastomeric failure modes in a given application, and hence improve the mechanical properties for that application.

Speculation concerning how radiation can improve mechanical properties for tank-pad applications can be understood in light of tank-pad failure modes. For off-road and gravel surfaces, "cutting and chunking" are reported to be the principal failures. Cutting is caused when the pad hits a "road hazard," a rock or other sharp obstacle able to produce high point stress, with enough force to penetrate or cut the surface. Chunking can then follow by "scrubbing" the pad over rough or sharp objects, or it can also occur as a first step. It should also be noted that pad operating temperatures are high due to hysteretic heat production. Under such failure conditions, a network with high point tear strength at elevated temperature (as measured by the hot tear test), high elongation and high energy at break has been speculated to have optimum performance. The optimization of these properties is balanced by the fact that a network with very high energy at break leads to high hysteretic temperature increases and another failure mode, blowout.

A rubber with high point tear strength might be expected to form a uniform crosslink density spatial distribution of bonds of high strength at elevated temperatures. It is clear that the crosslink density distribution of sulfur crosslinked systems is dependent on the microscopic dispersion level of sulfur in the complex rubber formulation, and by any measure, dispersion is not perfectly uniform. Also, the high temperature lability of S-S bonds is inferior to C-C bonds, as

reported by Tobolsky and Lyons. A radiation-cured system, on the other hand, is expected to have a crosslink density spatial distribution of C-C bonds that closely follows the spatial distribution of the dose. This is one potentially advantageous property of radiation which offers promise for overcoming tank-pad failures and hence improving the mechanical properties. Another is that radiation curing can be used to provide a wide range of specified spatial distributions of crosslinking density designed to overcome failure modes. Development studies are required to determine such desirable distributions.

5.2. Pad Production by Electron Beam

The technology for electron beam curing of tank-pads on a production basis is feasible and currently available. The techniques and results from electron beam curing employed to produce the 200 T-142 pads of this contract are outlined in this section.

5.2.1. Radioactivity. The best evidence that radioactivity is not a problem is the fact that an industrial electron accelerator operating at 12 MeV has been processing materials for consumer markets for years; neither the radiation facility nor the products became radioactive. This is the facility at which our pads were electron-cured. The radioactivity level in the electron-cured pads is less than that found in un-irradiated meat. The measured activity of the pads after electron beam irradiation is reported in Table 5-1. It should be noted that the maximum recorded activation level corresponds to less than 20 picocuries in a pad that weighs 3,000 grams. Calculated activation per pad, using conservative numbers, was 80 picocuries per pad (See APPENDIX B). This is to be compared with the radioactivity of natural potassium which is 750 picocuries (30 decays per second) in a single gram.

5.2.2. Dose Depth Profiles. Dose depth profiles were both theoretically calculated and measured. The experiment involved slicing an actual T-142 pad at five locations parallel to the metal backing plate. Six dosimeter packages were identically positioned (See APPENDIX C) at each level. Each dosimeter package contained three Far West dosimeter films calibrated at the National Bureau of Standards traceable University of Maryland cobalt-60 gamma source. The pads were reassembled with dosimeters in place and irradiated at IRT Corporation to a dose of 2.5 Mrads per side. The results are shown in Figure 5-1. (See also APPENDIX C). A quite flat profile is seen, with a $D_{\max}/D_{\min} < 1.3$ in most positions. There is an anticipated area of low cure directly behind the steel bolt (position 3).

Theoretical dose depth curves for two-sided irradiations using

Table 5-1. Activation Measurements of Irradiated Tank Pads

<u>Time</u>	<u># of Completed Passes</u>	<u>counts/min</u>		
		<u>Background</u>	<u>Total</u>	<u>Pad Activity</u>
12:20	3	60	80	20
2:03	4	60	90	30
3:30	5	60	90	30
5:15	6	60	100	40
6:30	8	60	100	40

NOTE: Measurements were done during pad irradiations with $\frac{1}{4}$ " plywood on steel side, $\frac{1}{4}$ " plywood on rubber side, and rubber stoppers on the bolts.

NOTE: $40 \text{ counts/min} = (40 \text{ cnts/min}) (1 \text{ min}/60 \text{ sec}) (1 \text{ Curie}/3.7 \cdot 10^{10} \text{ cnts/sec}) (10^{12} \text{ pC/Curie}) = 18 \text{ picocuries/pad}.$

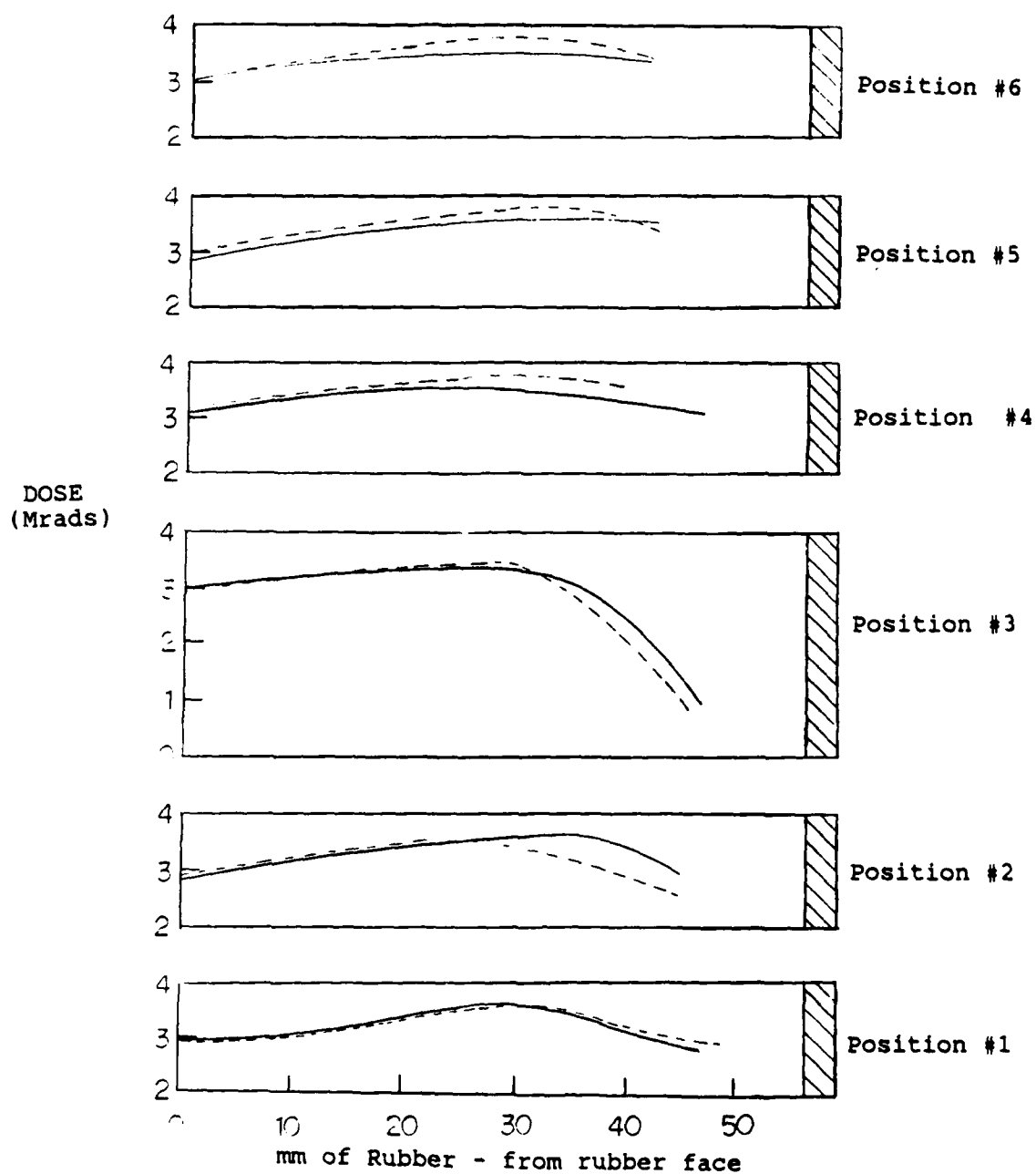


Figure 5-1. Measured Dose Depth Profiles

- Pad No. 1 - $\frac{1}{4}$ " plywood on each side of the pad
- Pad No. 2 - $\frac{1}{4}$ " plywood on rubber face; $\frac{3}{4}$ " plywood on steel face

10.0, 10.25, 10.5, 10.75 MeV are given in APPENDIX D. The high dose maxima expected from theoretical considerations was not observed, probably because of our failure to place any dosimeters at points where the maxima should be observed.

The beam energy penetrating the pad can be manipulated in two ways. The first is to vary the machine beam energy. This is practical for a long production run of a pad of a specified thickness. However, for a smaller number of pads, it is more efficient to run the accelerator at its preset energy and to degrade the beam energy before it strikes the pad. This was done in the present work using $\frac{1}{4}$ -inch plywood sheets. The dose depth profiles, theoretical and corresponding experimental data points, for the electron beam attenuation scheme used for the pad irradiations is given in Figure 5-2.

It should be noted that a more consistently flat dose profile may be achieved via a one-sided irradiation at an energy sufficient to penetrate the entire pad (17.5 MeV - see Figure 5-3). However, at this energy residual activities begin to be a concern, and the only accelerator at which we could perform the tests (Armed Forces Radiobiological Institute, Bethesda, MD) was shut down.

5.2.3. Temperature Profiles. The relatively brief period available for selection of a combination of styrene-butadiene rubber formulation, partial cure level, and appropriate cure dose indicates that our best results are in the range of a 10-15 Mrad dose. This leads to an absorption of 25-75 calories per gram (cal/g). The temperature rise in an adiabatic environment, such as would arise from an intense electron beam delivering such a dose, would be intolerable if it were delivered in a single irradiation.

Numerical solution of the time dependent equations for cooling show that an optimum for production processing of pads is reached with 6-7 Mrad per pass and a 15-minute cooling period between passes in ice water. These results are derived using the most conservative values for the dose depth profile and thermal diffusivity.

For the production of the 200 T-142 pads of the contract, 2.5-Mrad dose increments were used with at least 60 minutes between passes [at room temperature]. From Table 5-2 it is clear that heat build-up is not a concern under these circumstances.

5.2.4. Process Specifications. The process specifications from molding through electron beam curing are discussed in the following paragraphs.

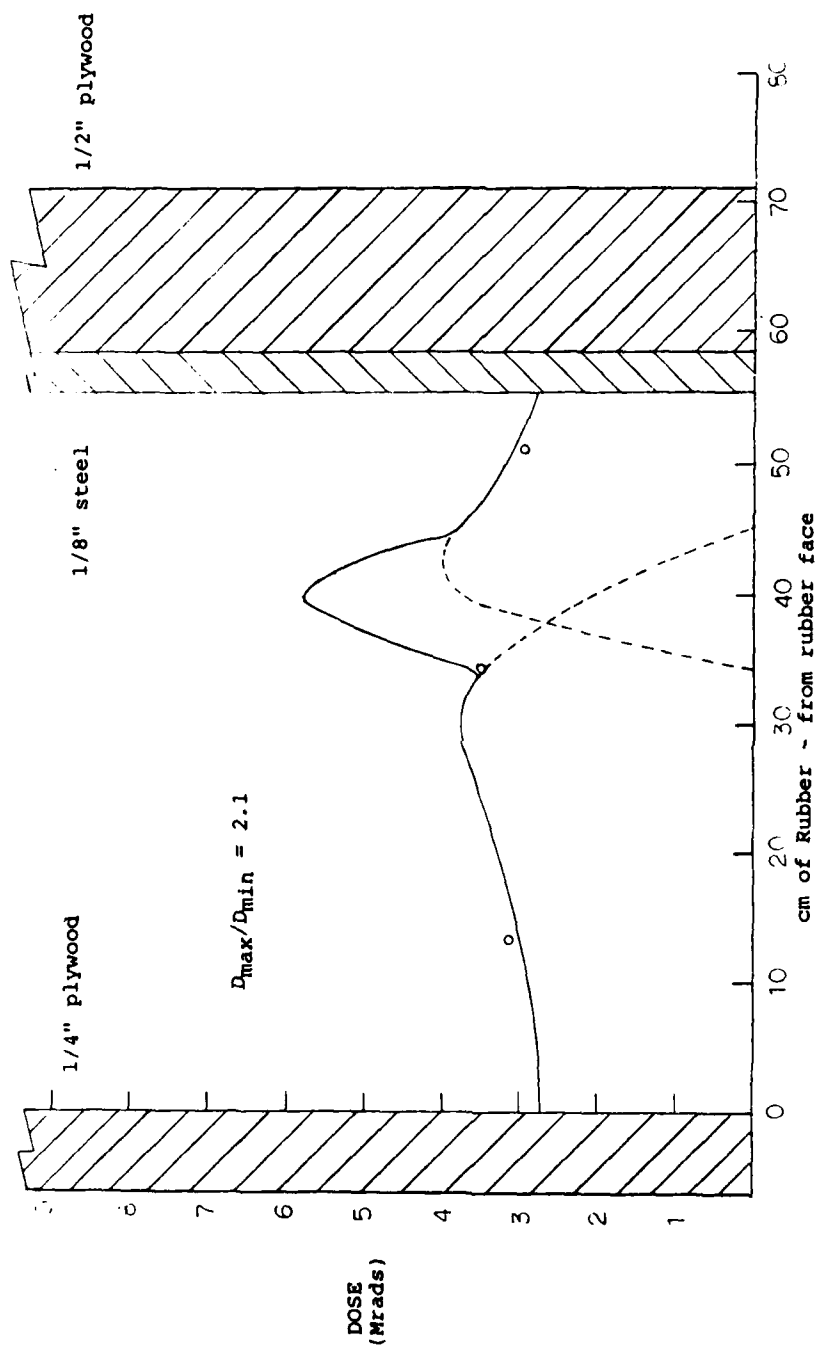


Figure 5-2. Theoretical Dose Depth Profiles for irradiation scheme. 0 - Expt'l data points. Electron Energy = 12 MeV.

Figure 5-3. One-Sided Irradiation Dose Depth Profiles

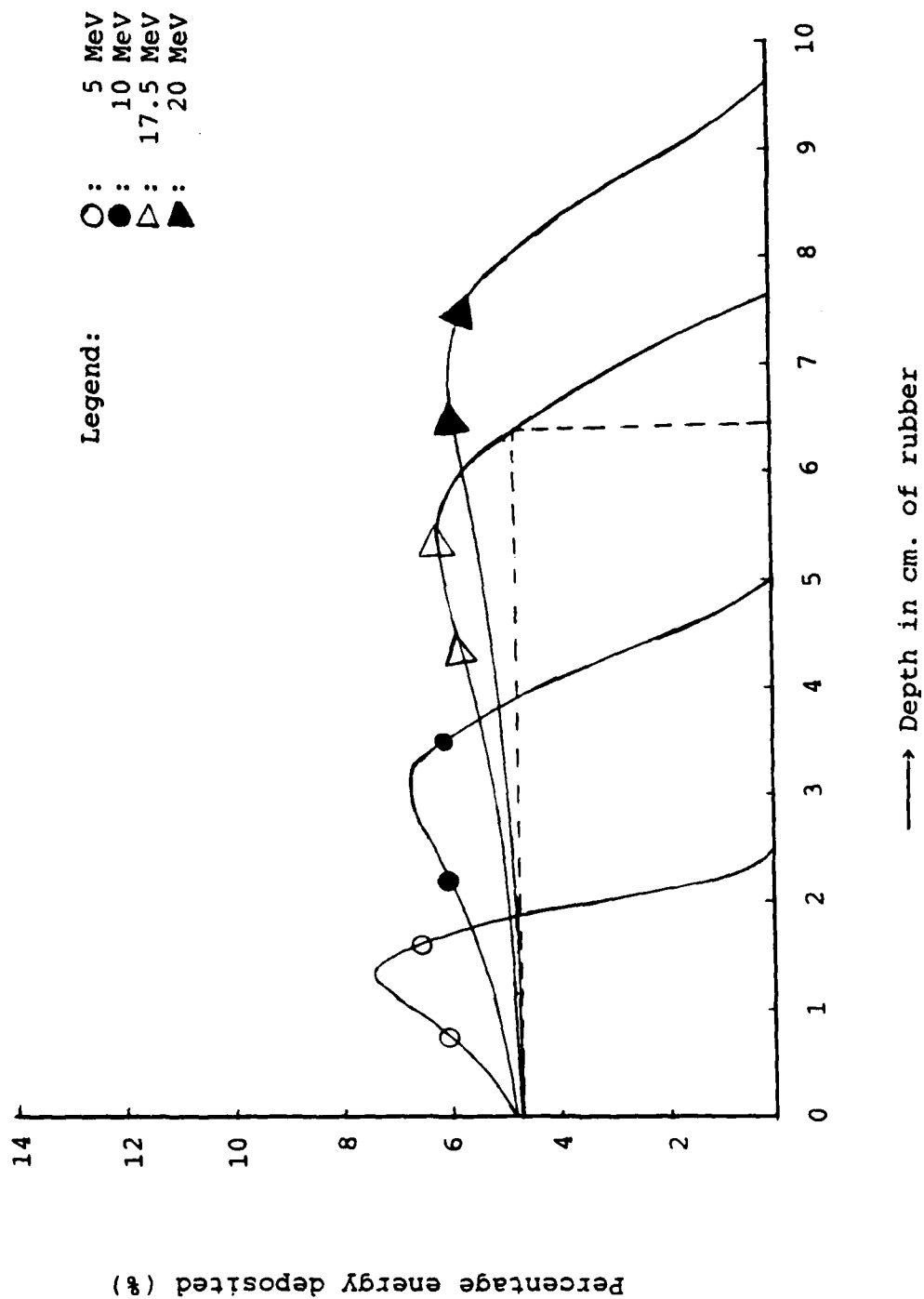


Table 5-2. Temperature Measurements of Irradiated Tank Pads

Completed Passes	*Time(min)	Thermocouple (°C)					Thermistor(°C) Air Surface	
		1	2	3	4	5	1	2
Pass #1	76	29	27	26	25	25	20	--
	86	27	24	24	23	25	--	26
	98	25	23	23	23	23	--	26
Pass #2	187	28	27	28	29	30	--	28
	197	28	27	28	28	29	21	27
	217	29	29	30	30	30	--	--
Pass #4	370	30	30	32	34	35	22	29
	380	30	30	30	32	33	--	28
	393	29	28	28	29	30	--	28
Pass #6 (large t_o)	514	33	32	33	33	33	22	31
	524	33	30	32	32	32	--	30
	538	30	29	30	30	30	--	29
Pass #8 (large t_o)	684	30	29	30	32	33	20	26
	694	29	28	28	29	32	--	25
	710	28	25	25	27	29	--	--
	730	25	24	24	25	25	--	23

*Time = 0.0 at beginning of irradiations

NOTES: T.C. #1 → 1.5 cm from rubber face of pad
 #2 → 2.5 cm from rubber face of pad
 #3 → 3.5 cm from rubber face of pad
 #4 → 4.5 cm from rubber face of pad
 #5 → 5.5 cm from rubber face of pad

Thermistor #1 → air temperature
 #2 → surface temperature; at end of pad, 2cm
 from rubber face of pad

t_o = [30 min + down time]
 = time between irradiation and measurement of T.

5.2.4.1. Molding. The 200 T-142 pads were molded at Firestone Tire and Rubber Company under the supervision of Steve Brunner. A crosslinking agent, shown to be mildly effective at low concentrations (0.1 parts per hundred rubber (pphr) of 3, 9-divinyl -2, 4, 8, 10 tetraoxaspiro [5,5] undecane (DTUD), and one-third of a typical sulfur loading were used in the formulation (see APPENDIX E). The partial sulfur cure insures processability and proper form of the pads coming out of the mold. When pads were formed without sulfur, they could not be released from the molds without distortion.

The molding procedure went according to the following procedure. The bolt and backing plate were degreased and cleaned. The bolt head and backing plate were coated with adhesive Chemlock 205, air-cooled, coated with Chemlock 233, and then assembled and put into the mold. The SBR was mixed in a Banbury mixer and hot-extruded into strips, followed by hot-extrusion into 6 in. by 6 in. by 8 in. blocks. The blocks were water cooled and placed in the molds. The mold top plate was at 300°F and the backing plate face at 290°F. They were bumped three times to remove air pockets, cured for 70 minutes (see APPENDIX E), cooled in the mold for 5 minutes, and removed. The specific gravity was measured at 1.15. Trimming was the only other treatment performed.

5.2.4.2. Adhesion. We had considerable concern over the bonding of completely uncured pads to the backing plates and devoted substantial efforts to solution of the problem. However, with the partial sulfur cure described above, a standard adhesion application procedure was followed with commercial adhesives. The adhesion of the rubber to the backing plate was excellent. It was as high as 270 lb/in and was always greater than 150 lb/in.

5.2.4.3. Material Transport. The conveyor system at IRT which transports the pads underneath the electron beam is automated to correlate the conveyor speed with the beam current. This keeps the surface dose to the pads constant. For commercial production of pads, the conveyor or attachable conveyor compartments could be designed to hold the pads perpendicular to the electron beam.

For the irradiation of the 200 T-142 pads, we designed wood pad carriers to place on the conveyor system (See Figure 5-4). The carriers kept the pads perpendicular to the beam as well as providing the necessary beam attenuation.

5.2.4.4. Electron Beam Dose Uniformity. As mentioned earlier, the automated conveyor system allowed for uniform doses in the direction of conveyor travel. Figure 5-5 also shows that side-to-side dose variations are also minimal (~5 percent).

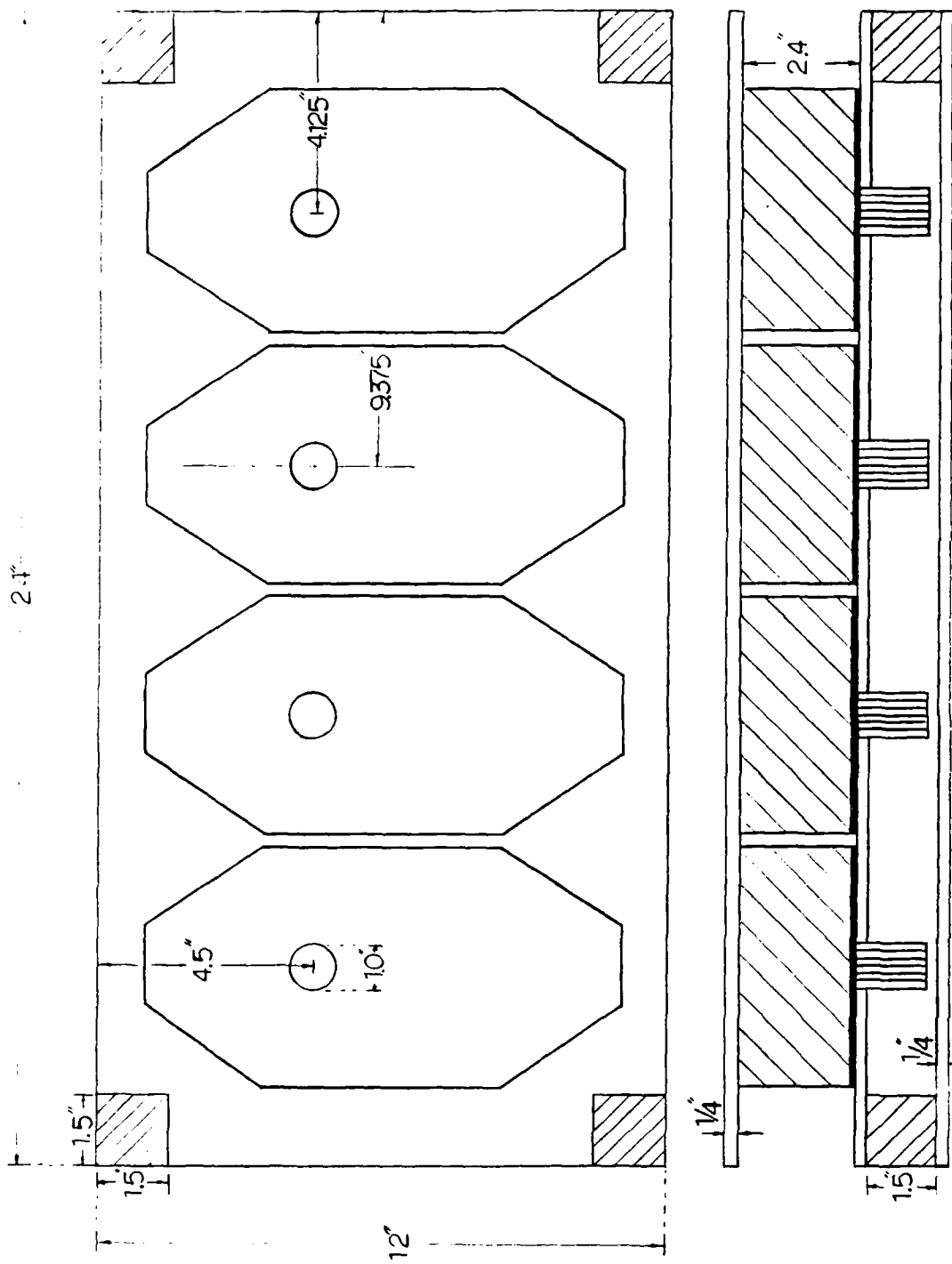


Figure 5-4. Pad Carrier Design

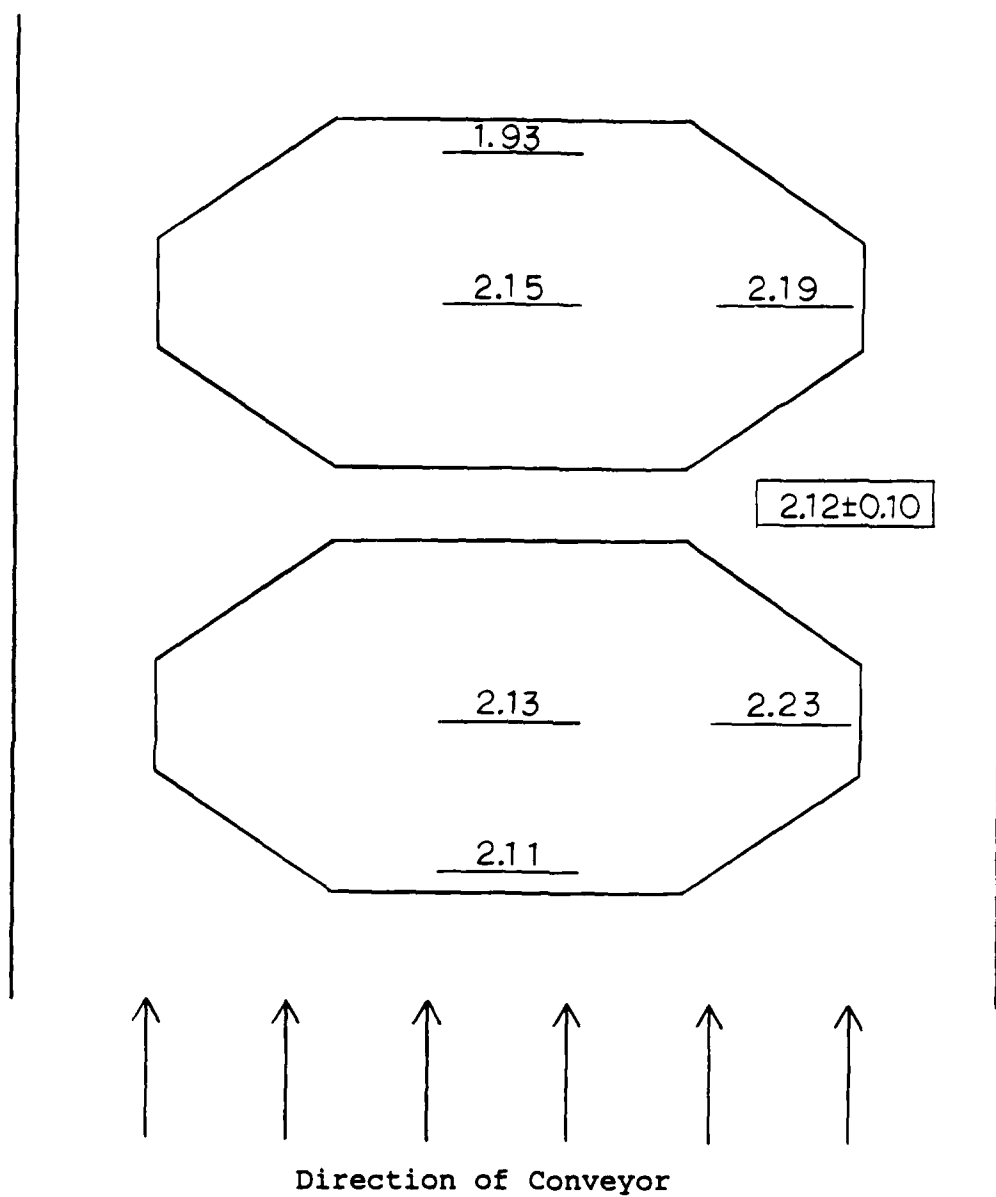


Figure 5-5. Electron Beam Horizontal Dosimetry

5.2.4.5. Accelerator Specifications. The electron accelerator at IRT has an electron energy range of 6-16 MeV, with maximum power at 12 MeV, the energy used for our irradiations. The average beam current was 275 microamperes. The conveyor speed was 1.5-2.0 ft/min. Maximum power is 8.5 kilowatt (kW). The beam width is 1.5 inches and scan width is 12-16 inches.

5.3. Contract Deliverables

One hundred T-142 tank-pads irradiated to a surface dose of 10 Mrads and 100 T-142 tank-pads irradiated to 15 Mrads have been delivered to Yuma Proving Grounds and await field testing.

The mechanical property tests of the delivered pads, as specified under this contract, are listed in Table 5-3. It should be noted that multitudinous additional mechanical property test results are reported in par. 5.4. Many of the mechanical tests were performed to our specifications at Fort Belvoir Research and Development Center with the participation of university research assistants.

From the formulation studies performed and from the data available to date on the actual electron beam-cured pads, the following general results are observed.

- Hot tear strength is high.
- Resistance to crack, initiation, and growth are high.
- Ozone resistance is high.
- Heat build up may be troublesome.

We believe the shortcomings in heat build-up would be overcome in the electron-cured butadiene rubber (BR) we have discovered but have not had sufficient opportunity to develop.

5.4. Optimization Studies: Formulation and Dose Requirements

A wide variety of mechanical property optimization tests were performed. The main thrust was to find a radiation sensitizer to lower the dose requirements for SBR and/or to improve mechanical properties of otherwise promising BR. Due to the relatively short period of time for these studies, we were unable to incorporate the most significant advances in the formulations of the 200 T-142 pads for this contract. The motivation for finding a radiation sensitizing agent, the studies performed, the advances made, and the areas warranting continued investigation are outlined in this section.

5.4.1. Motivation for Radiation Sensitization. The first reason to seek after an effective radiation sensitizing agent is to lower the required cure dose. It has been reported that high-radiation doses are required to cure SBR to the same crosslink density as typical sulfur-cured systems when no radiation crosslink promoters are present. A radiation crosslink promoter lowers the dose requirements and the cost of electron beam processing. Also, from a processing point of view, lower dose requirements facilitate the process design considerably. The adiabatic temperature increase of a 10 Mrad dose to raw SBR is greater than 50°C. So, if the cure dose requirement is high, several passes through the electron beam with extended cooling periods in between passes are necessary in order to prevent overheating of the pads. The complication of cooling baths and/or hold-up space and time could be avoided if dose requirements were less than 15 Mrad. And finally, lower dose requirements lower the degradative effects of radiation which may occur at high doses. This may broaden the declining edge of the hot tear strength versus dose curve to allow a reasonably broad range of cure doses with acceptable hot tear strength. Again, processing would be facilitated due to a less stringent dose requirement.

Another motivation for finding a sensitization agent is in order to overcome some of the strength shortcomings of BR, a rubber in many other ways ideal for radiation-cured tank-pad application. Stereospecifically polymerized polybutadiene rubber (BR) has the highest rubber elasticity, the best abrasion resistance, and the lowest heat generation when compared with the other main synthetic rubbers and natural rubber from Table 5-4. Besides, BR has unsaturated double bonds which can be crosslinked by high energy sources such as gamma-rays, electron beams, etc. The radiation yields of crosslinking (G(x) values) of natural rubber (NR), BR, and SBR are reported to be 2.0, 1.3 and 1.6 bonds per 100 electron volt (eV) absorbed, respectively. Emulsion polymerized elastomers such as SBR-1500 may contain up to 10 percent impurities (catalyst fragments, emulsifiers, antioxidants, etc.,) which often interfere with the radiation chemistry of the elastomers. Also, a higher styrene-to-butadiene ratio leads to a reduction in the yield of crosslinks under irradiation. So polybutadiene is a prime candidate material for tank-pad base rubber provided its disadvantages can be overcome by suitable additives.

5.4.2. Mechanical Property Tests - SBR. Tables 5-5 through 5-8 contain the formulations and mechanical property test results of some SBR radiation-cured samples as well as the mechanical property data from Belvoir Research and Development Center on the sulfur-cured analogs. Hot tear data are plotted against cure dose for series A-F and G'-K in Figures 5-6 and

Table 5-4. Properties Comparison of Natural and Synthetic Rubbers

Items	Rubbers	NR	IR	BR	NBR	EPDM	IIR	CR	SBR
Specific Gravity		0.92	0.91	0.91	0.98	0.86	0.92	1.23	0.94
Curing Rate		quick	quick-med.	medium	medium	slow	slow	medium	medium
Uncured Strength		std.=♦	▲-X	X	▲	▲-X	▲-X	♦-X	▲-X
Tensile Strength		" ♦	♦	▲	♦	▲	▲-X	▲	♦
Resilience		" ♦	♦	O	▲-X	▲	X	▲-X	▲
Heat Build-up		" ♦	♦	O	▲-X	▲	X	▲-X	▲
Compression Set		" ♦	♦	■	♦-O	▲	▲-X	♦-▲	O
Abrasion		" ♦	♦	■	♦	♦	▲	♦	O
Anti-heat		" ♦	♦	♦	O	■	■	O-■	O
Anti-cold		" ♦	♦	■	▲-X	O	▲	▲-X	▲
Anti-ozonant		" ♦	♦	♦-▲	♦	■	■	O	♦
Electricity		" ♦	♦	♦	▲-X	O	O	▲	♦
Gas Penetration		" ♦	♦	♦	O	♦	■	O	♦
Anti-flame		" ♦	♦	♦	♦	♦	♦	O	♦
Anti-oil		" ♦	♦	♦	■	♦	♦	O	♦
Anti-acid { H ₂ SO ₄ HCl		" ♦	♦	♦-▲	♦-O	♦-O	♦-O	♦-O	♦-▲
		" ♦	♦	♦	▲	O	O	▲	♦
Anti-caustic { NaOH NH ₄ OH		" ♦	♦	♦-O	♦	♦-O	♦-O	♦	♦-O
		" ♦	♦	♦	♦	O	O	♦	♦

Note: (■) much better; (O) better; (♦) same; (▲) worse. (X) much worse;

Table 5-5. SBR Formulations

(a)	(b)		Radiation Systems												
	Sulfur Systems														
Ingredients (pphr)	S-FRS	S-COPO	S-PLIO	A	B	C	D	E	F	G'	H	I	J	K	A GB LB
FRS - 1500	100	----	----	100	100	100	100	100	100	100	----	----	----	----	100 ----
COPO - 1500	---	100	----	----	----	----	----	----	----	100	100	100	100	100	100 ----
PLIO - 1500	---	----	100	----	----	----	----	----	----	----	----	----	----	----	100 ----
Sulfur Vulcanization Agents	3.5-6.5	3.5	3.5	----	----	----	----	----	----	----	----	----	----	----	----
Antioxidant, Agerite Resin D	0.5	0.5	0.5	0.5	0.5	0.5	0.5	0.5	0.5	0.5	1.0	2.5	5	10	0.5 0.5 0.5
DTUD	---	---	---	0	0.1	0.5	1	2.0	5.0	----	----	----	----	----	----
1,5-cyclo-octadiene	---	---	---	----	----	----	----	----	----	1.0	1.0	1.0	1.0	1.0	1.0 ----

(a) The following additives are common in all formulations:

Additive	pphr
carbon black	45.0
zinc-oxide	4.0
stearic acid	2.0
antiozonant	3.0
antioxidant	0.5
(Agerite, white)	54.5

(b) Prepared by BRDC Tank Pad Group

Table 5-6. Mechanical Properties - Series A-F, SBR

Mechanical Properties	Analog Sulfur Formulations	Radiation Formulations														
		A-7	A-14	A-22	A-36	A-50	B-7	B-14	B-22	B-36	B-50	C-7	C-14	C-22	C-36	C-50
Hot Tear Strength 10min @ 250°F (lb/in)	104-165	24	54	155	210	71	27	112	183	187	55	35	64	198	183	76
				(1)				±16	±16					(4)	±22	±8
200% Modulus (psi)	740-1911	93	159	277	516	1266	80	180	322	580	1017	80	158	307	460	930
				(1)	±29						±56				±19	
Tensile Strength (psi)	2498-3911	415	1455	2549		3040	260	1740	2660	3450	3440	456	1530		2980	2340
		±27				±310	±18	±170	±240						±200	±470
Ultimate Elongation (%)	233-687	>1100	940	825		515	>1100	810	730	620	460	>1100	955		660	400
							(1)	±95	±45							±40
Mechanical Properties		D-7	D-14	D-22	D-36	D-50	E-7	E-14	E-22	E-36	E-50	F-7	F-14	F-22	F-36	F-50
Hot Tear Strength 10min @ 250°F (lb/in)		22	54	161	112	63	22	59	179	172	57	19	48	103	109	55
		±8			±33						±5			±16	±43	
200% Modulus (psi)		71	115	209	383	1014	87	132	212	393	694	(1)	51	102	168	693
					±26					±85	±42					±68
Tensile Strength (psi)		289	1260	2210	1960	2340	517	1512	1900	2490	2540	170	1075	1360	2020	2140
				±130	±270	±380			±360	±260	±270	±28	±64		±290	±370
Ultimate Elongation (%)		>1100	1040	775	540	370	>1100	1020	765	670	400	>1100	980	715	550	440
				±110	±70	±80		±60	±80	±50	±35					

Notes: 1) "A-7" means series A at cure dose of about 7 Mrads as reported by CRC.
 2) 2 or 3 samples at each data point unless otherwise indicated by a superscript number in parentheses.
 3) Standard deviation is within ±5% unless otherwise indicated.

Table 5-7. Mechanical Properties - Series G'-K, SBR

Analog Sulfur Formulations		Radiation Formulations												
Mechanical Properties	S-COPO	G'-16	G'-20	G'-24	G'-28	G'-32	H-12	H-16	H-20	H-24	H-28	H-32	H-48	
Hot Tear Strength 10min @ 250°F (16in)	132-167	175	197 ±14	178	186	190 ±12	78	158 ±14	193 ±27	218 ±26	170 ±28	153 ±37	(1) 58	
200% Modulus (psi)	734-1014	255	329	456	510	615	190 ±84	255	297 ±76	460 ±52	453	537	880 ±66	
Tensile Strength (psi)	3649-3878	1800 ±300	2370	2880	2840	3220				2810 ±220				
Ultimate Elongation (%)	463-553	780 ±110	760 ±110	775	713	738				770				
Mechanical Properties		I-12	I-16	I-20	I-24	I-28	I-32	J-20	J-48	K-20	K-48			
Hot Tear Strength 10min @ 250°F(16in)		53 ±4	107 ±17	181 ±17	(4) 178 ±16	204 ±17	180	118 ±9	125 ±17	49 ±3	73			
200% Modulus (psi)		226	234	(6) 292 ±19	316 ±59	422	467	249		189 ±25				
Tensile Strength (psi)														
Ultimate Elongation (%)														

Notes: 1) G'-16 means formulation G' at cure dose of about 16 Mrads as reported by CRC.
 2) 2 or 3 samples at each data point unless otherwise indicated by a superscript number in parentheses.
 3) Standard deviation is within ±5% unless otherwise indicated.

Table 5-8. Mechanical Properties - Series GB, LB, SBR

Mechanical Properties	Analog Sulfur Formulations		Radiation Formulations					
	S-COPO	S-PLIO	GB-20	GB-24.1	GB-24.2	GB-28.1	GB-28.2	LB-16 LB-20 LB-24
Hot Tear Strength 10min @ 250°F (16in)	132-167	131	(7) 172 ±16	(4) 135 ±8	180	162	65	(8) 190 250 ±56
200% Modulus (psi)	734-1014	937	(4) 421	291	528 ±32	529	1040	269 340 ±16
Tensile Strength (psi)	3649-3878	3297	(4) 2640 ±400	2210	2400 ±350	3260	3260 ±250	
Ultimate Elongation (%)	463-553	437	(4) 730 ±45	815	640	765	590	

Notes: 1) "GB-20" means formulation GB at cure dose of about 20 Mrads as reported by CRC.
 2) 2 or 3 samples at each data point unless otherwise indicated by a superscript number in parentheses.
 3) Standard deviation is within ±5% unless otherwise indicated.

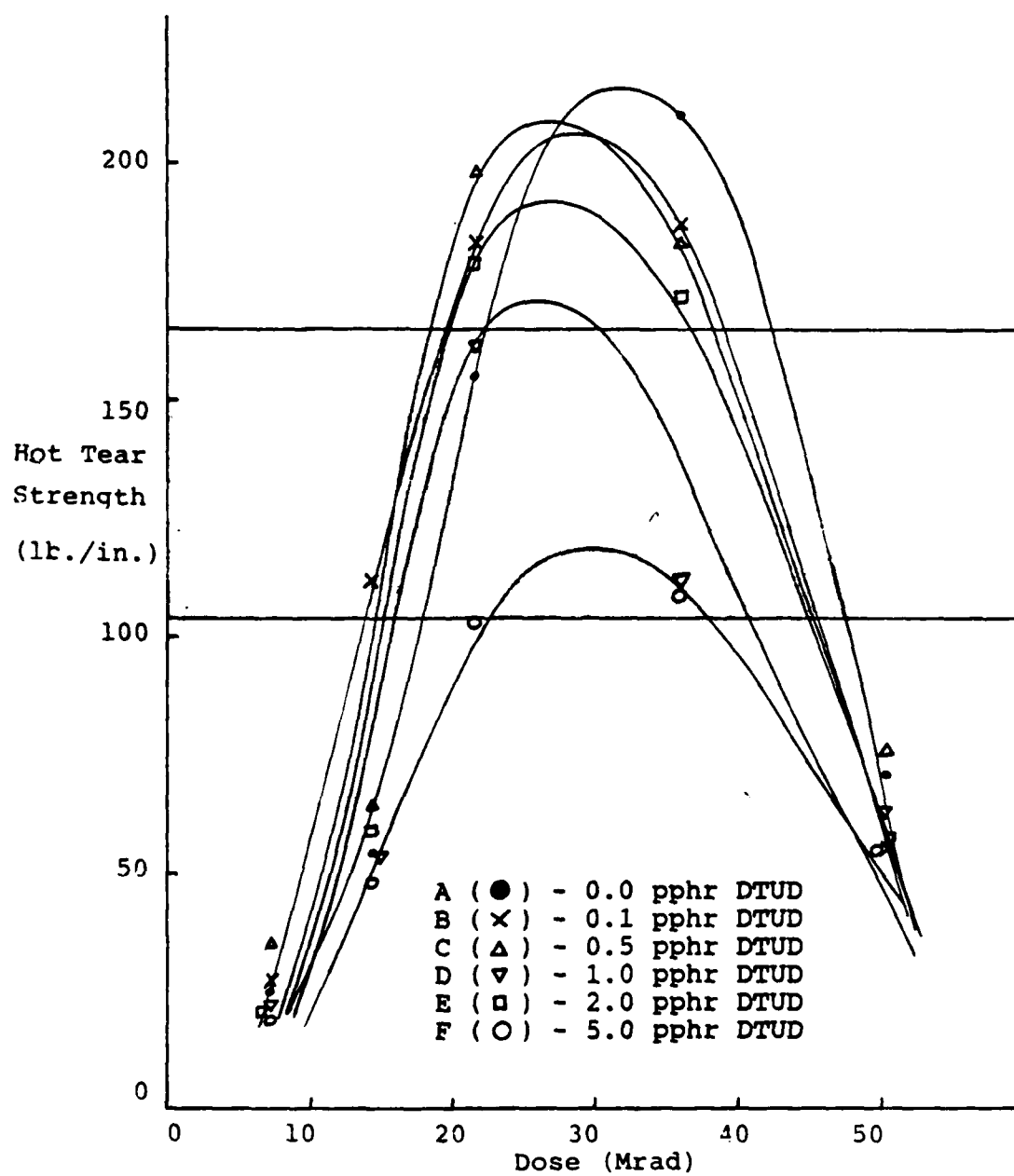


Figure 5-6. Hot Tear Strength vs. Dose. SBR (A-F)

5-7, respectively. The shaded area gives the range of hot tear values obtained by BRDC for the analog sulfur-cured samples. The first outstanding observation is that radiation-cured systems can significantly increase an elastomer's high temperature point tear strength. The radiation-cured samples are superior to the best sulfur-cured samples in hot tear strength by more than 25 percent. These data are an initial experimental indication that radiation-cured elastomers may be able to overcome tank-pad failure modes and improve pad service life.

Before looking more closely at the effect of the variable parameters on the radiation-cured system, one more general observation can be made. The data are characteristic of a system receiving higher and higher crosslink density as dose increases. For instance, in Series B, as dose increases from 7 to 50 Mrad, 200 percent modulus increases from 80 to 1017 pounds per square inch (psi) while ultimate elongation decreases from >1100 to 460 percent elongation.

5.4.2.1. Sensitization Agent. The first radiation sensitizer to be tested was 3,9 divinyl-2, 4, 8, 10 - tetraoxaspiro [5,5] undecane (DTUD). The effectiveness of DTUD as a crosslink promoter can be seen in Figure 5-8, a plot of 200 percent modulus against cure dose for a series of DTUD concentrations ranging from 0.1 to 5.0 pphr. In the middle dose range, Series B (0.1 pphr) affords a small increase in crosslink density at a given dose over Series A (0.0 pphr). However, as DTUD concentration increases above 0.1 pphr, the crosslink density decreases at any given dose (Series C-F). This indicates that above very low concentrations, DTUD is not promoting crosslinks, but actually acting as a mild crosslink inhibitor. This can be visualized more clearly in Figure 5-9, a plot of 200 percent modulus against pphr DTUD at constant dose.

The effect of DTUD on hot tear strength can be seen in Figure 5-10, a plot of hot tear strength against 200 percent modulus. Since 200 percent modulus is a direct measure of crosslink density, this allows comparison of hot tear strength with different DTUD concentrations normalized with respect to crosslink density. This figure shows a general trend that maximum hot tear strength is decreasing as DTUD concentration increases, and that this maximum is shifting to lower crosslink density.

Further insight can be gained by plotting hot tear strength against pphr DTUD at constant crosslink density, as shown in Figure 5-11. At low crosslink density (200 psi), the highest hot tear strength is achieved in the samples with 2 pphr DTUD. This maximum increases, as noted earlier, and shifts to lower DTUD levels as crosslink density increases up to 400 psi.

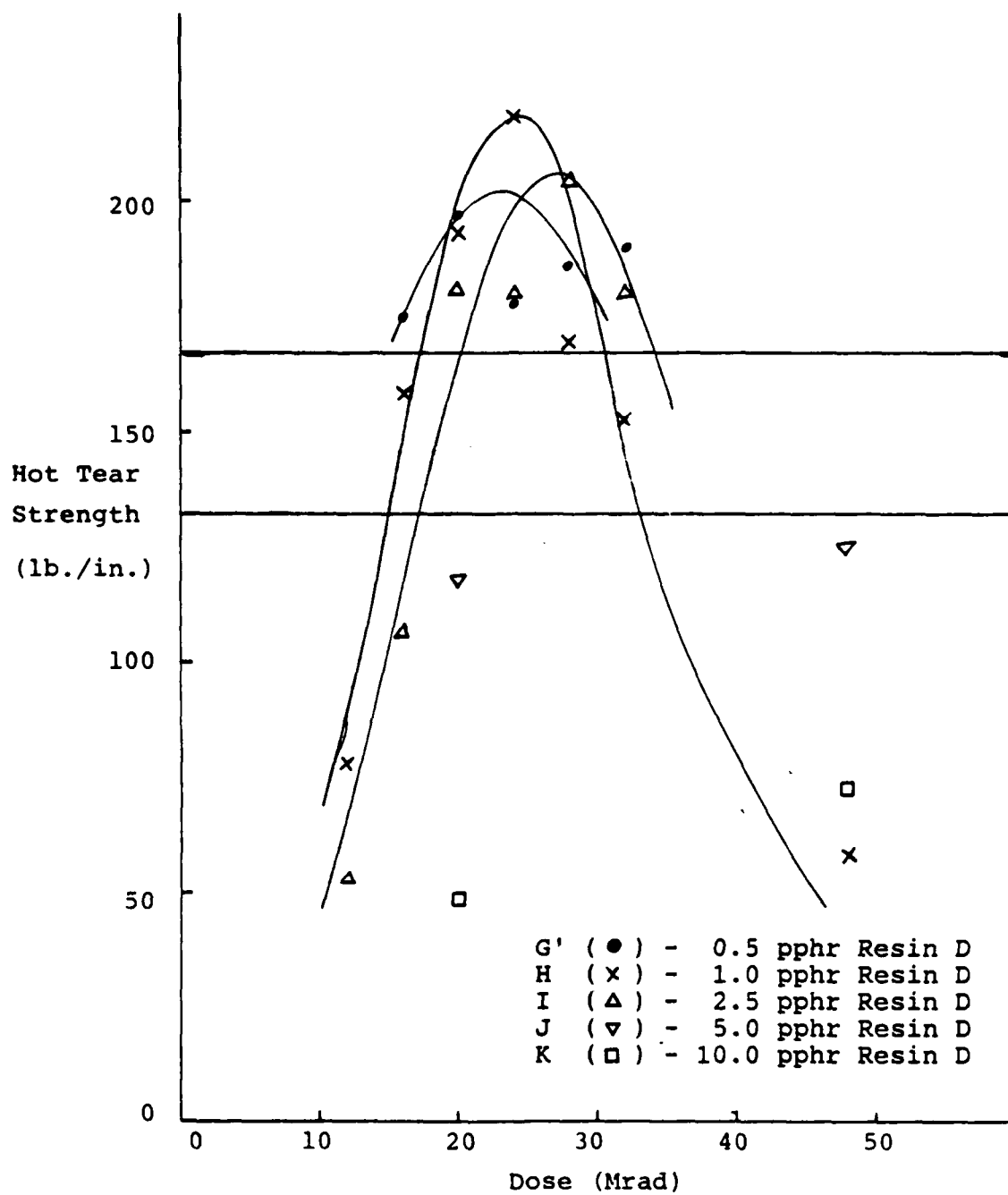


Figure 5-7. Hot Tear Strength vs. Dose. SBR (G'-K)

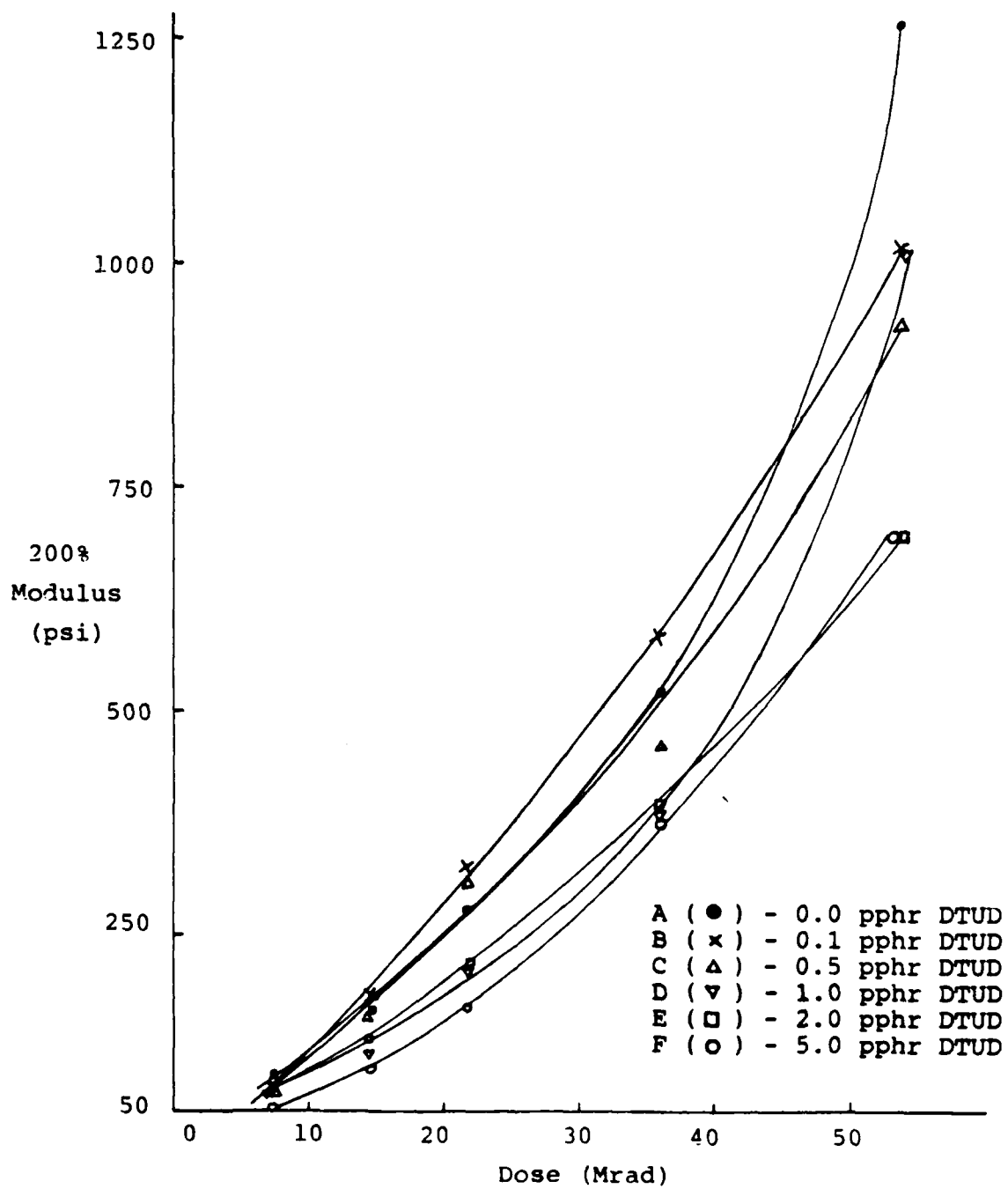


Figure 5-8. 200% Modulus vs. Dose. SBR (A-F)

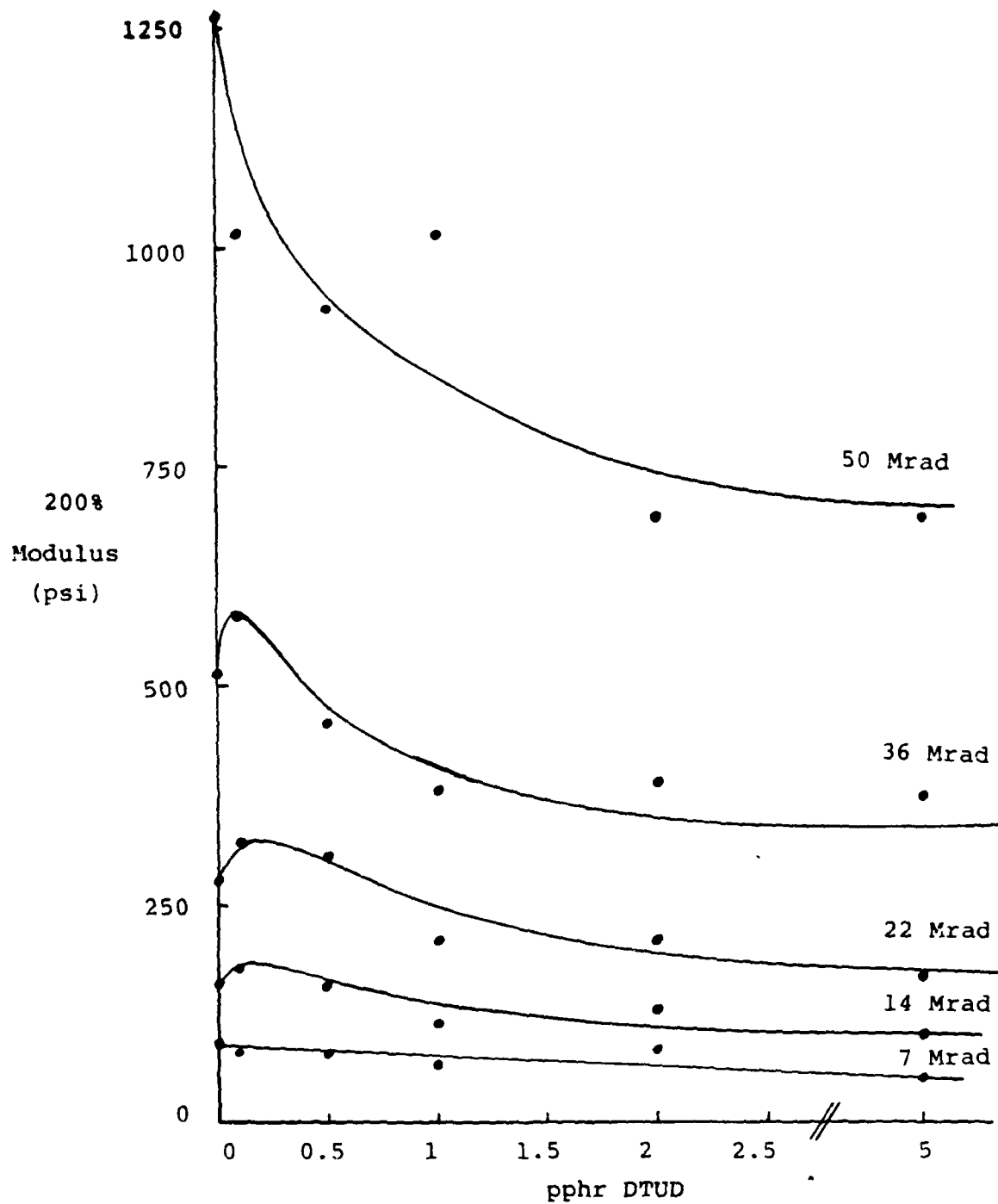


Figure 5-9. 200% Modulus vs. pp/hr DTUD. SBR (A-F)

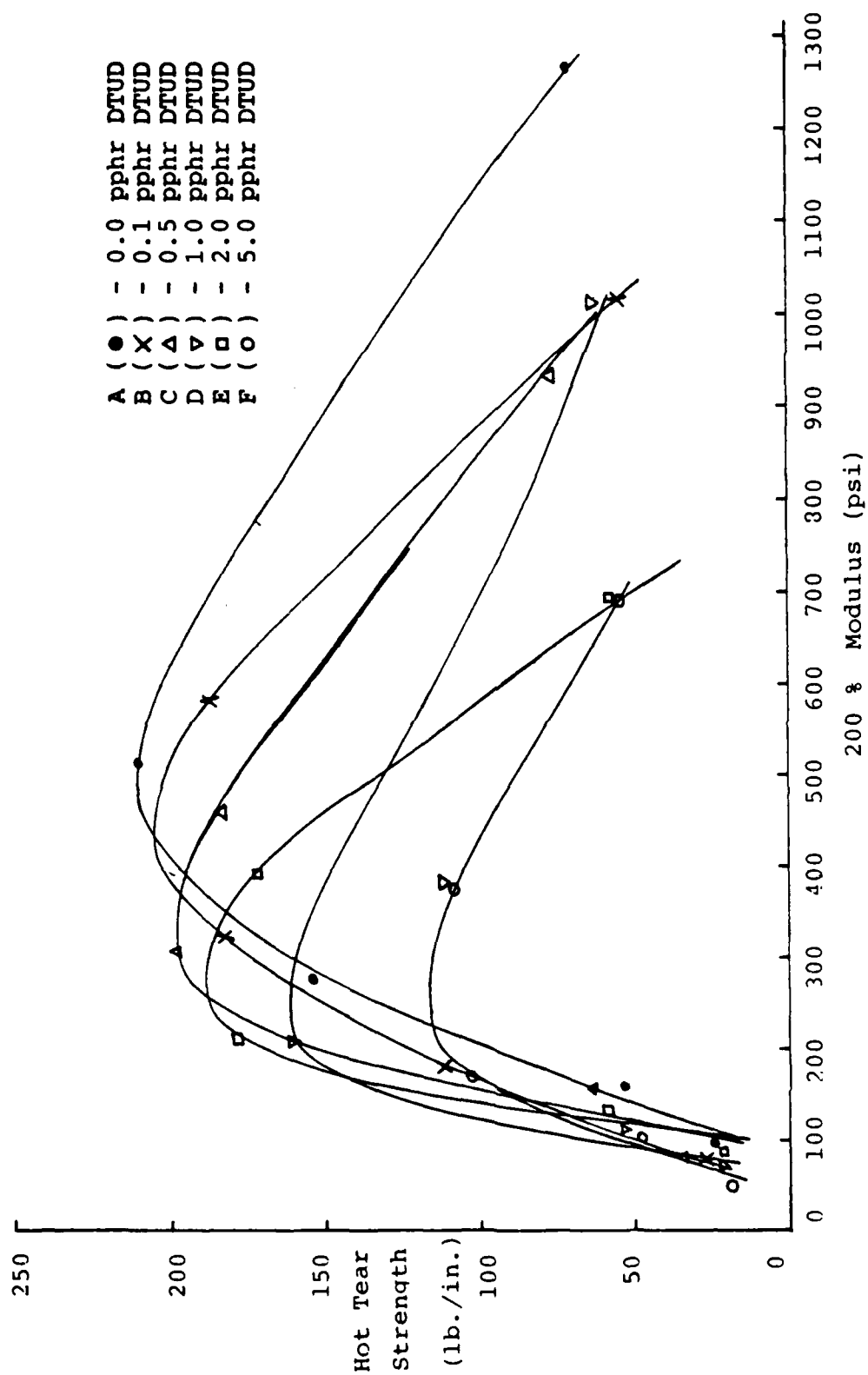


Figure 5-10. Hot Tear Strength vs. 200% Modulus. SBR (A-F)

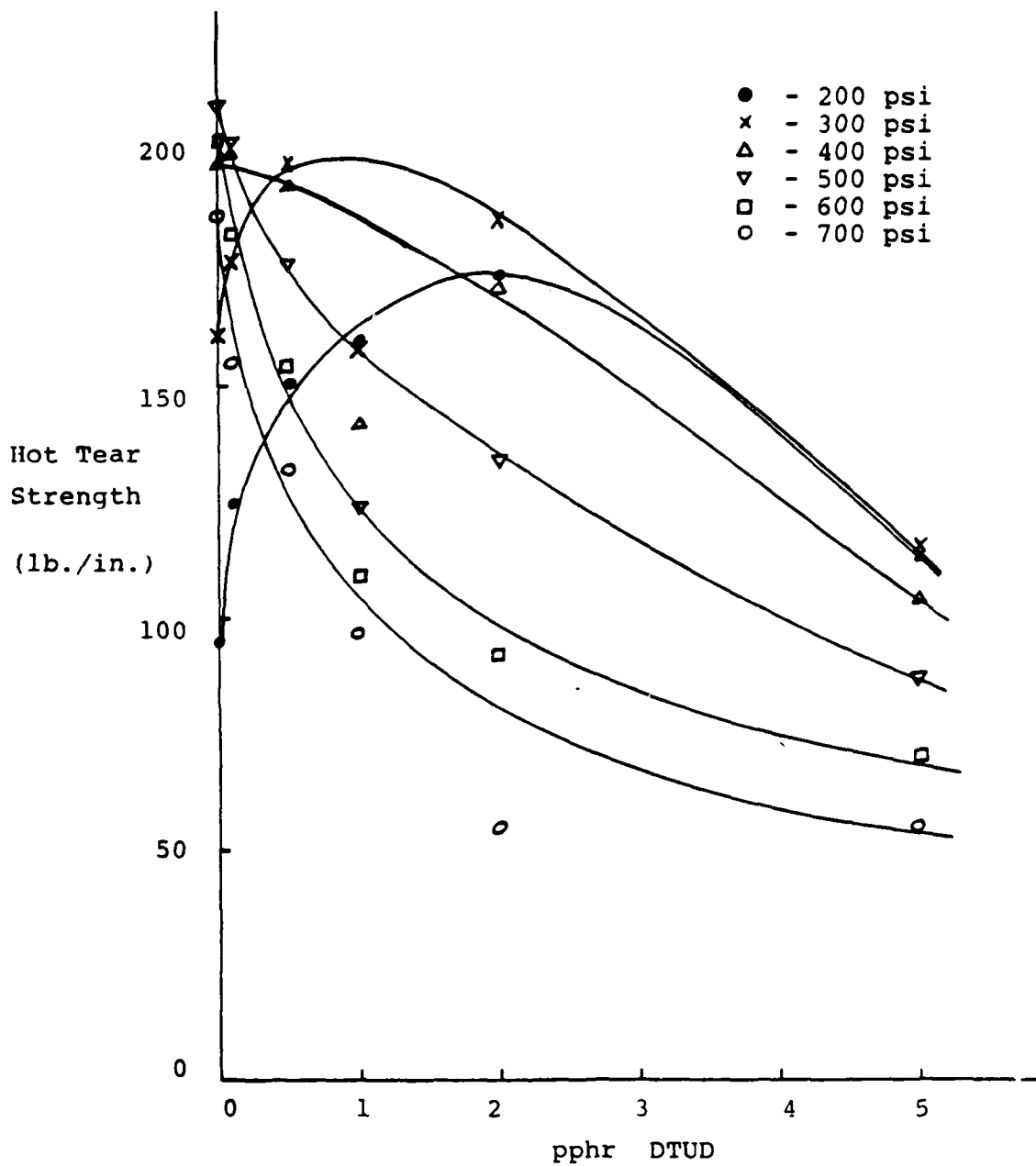
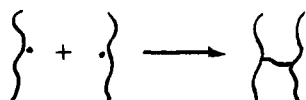


Figure 5-11. Hot Tear Strength vs. pphr DTUD. SBR (A-F)

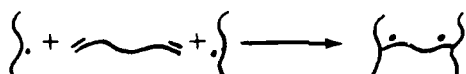
Above 400 psi, hot tear strength continuously decreases at an increasing rate as crosslink density increases.

The effect of DTUD on tensile strength can be seen in Figure 5-12, a plot of tensile strength against 200 percent modulus for the Series A-F. A similar general trend is observed in that tensile strength decreases as DTUD concentration increases at a given crosslink density. One additional noteworthy observation is that the maximum radiation cured sample falls only 10 percent lower than the maximum sulfur cured sample tensile strength. This is in agreement with data reported by Bohm.

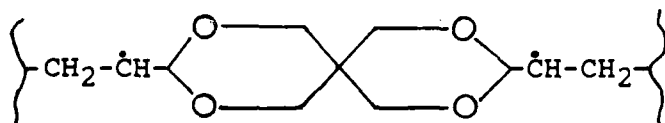
The first of two possible explanations of the poor performance of DTUD as a crosslink promoter arises from looking at the nature of divinyl-type crosslink. A crosslink reaction without promoter results in the consumption of two radicals to produce one crosslink:



A divinyl promoter may crosslink the radicals by two Y-links:



In this case, a crosslink has been formed and yet still two radicals exist to form further crosslinks. One argument, however, is that the radicals may be too sterically hindered to react with another promoter molecule before they migrate to each other and "die" by forming double bond. In the case of DTUD, the crosslink looks like the following:



The rings make each half of this link nearly planar. Hence the steric hindrance would be small. Another problem with this argument is that it does not account for the increase in crosslink density at very low DTUD concentrations, and it does not explain the effect of DTUD on the SBR physical properties.

The second possible argument which does explain the rest of the DTUD data mentioned above is that DTUD fails to meet the major requirement of a tank-pad radiation crosslink promoter. This requirement is that the promoter be homogeneously dispersed in the elastomer. If this requirement is not met, one advantage of radiation cure over sulfur cure, the ability to create a uniform crosslink spatial distribution, is negated. In this case, the DTUD will tend to aggregate and homopolymerize upon

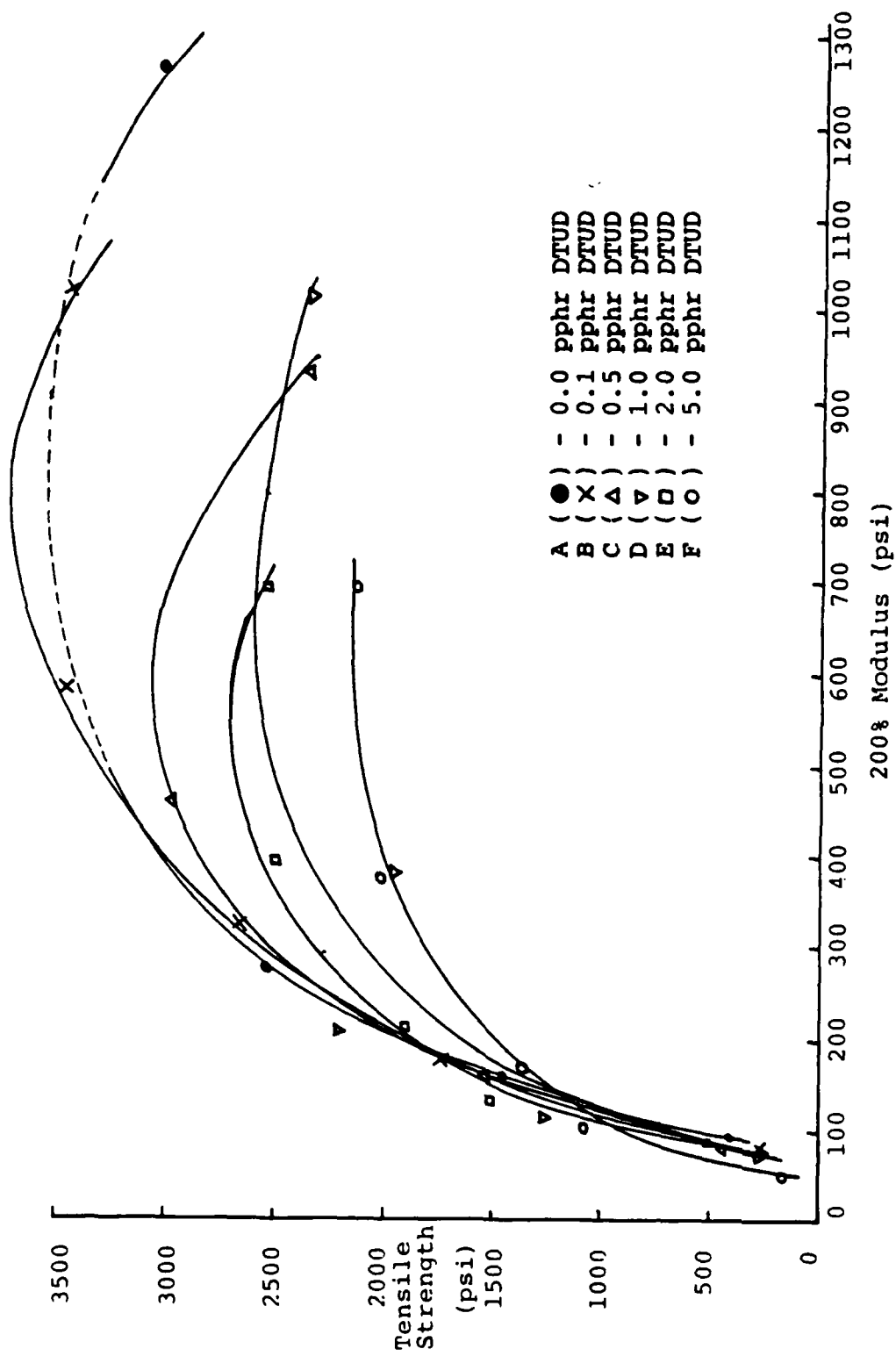


Figure 5-12. Tensile Strength vs. 200% Modulus. SBR (A-F)

irradiation, hence failing to act as a crosslink promoter as Figures 5-8 and 5-9 indicate. However, at very low DTUD concentration, as in series B where a small crosslink enhancement was observed, the DTUD may be so diluted in the rubber network that it can not effectively aggregate and, therefore, is able to promote crosslinking a small amount.

Aggregation of DTUD also explains the hot tear data reported here. Odian reported that divinyl-type crosslink promoters homopolymerize at a fast rate as compared to the rate at which the elastomer itself crosslinks. Therefore, at low doses and lower crosslink density, aggregations of DTUD would be already homopolymerized. Such a system might conceivably have a higher tear strength, due to the filler effect of these homopolymerized aggregates, than the grossly undercured system without DTUD. This corresponds with the data in Figure 5-11 indicating maximum hot tear strength at 1-2 pphr DTUD at low system crosslink density (200,300 psi).

At higher system crosslink density, the same line of reasoning discussed in par. 5.1.2. may be applied. The sulfur-cured systems were predicted to have a lower high-temperature tear strength than the radiation-cured systems because of the crosslink density nonuniformities resulting from sulfur dispersion imperfections. Likewise, radiation-cured samples with crosslink density nonuniformities due to homopolymerized DTUD aggregates are expected to decrease in hot tear strength as aggregate concentration increases. And indeed, at 200 percent modulus greater than 400 psi, Figures 5-10 and 5-11 show that hot tear strength continuously decreases as DTUD concentration increases.

Factors contributing to the aggregation of DTUD within the SBR are its melting temperature ($T_m = 40-45^\circ\text{C}$) and its dielectric constant relative to SBR. Since the melting temperature is above room temperature, DTUD will tend to aggregate in order to crystallize. The ether links in DTUD are one source of the difference in dielectric constant with respect to SBR. It is not clear which of these factors has the dominant effect, but the data indicate that their combination results in a crosslink promoter which is not homogeneously dispersed.

5.4.2.2. Antioxidant. The optimum antioxidant loading was also investigated in this series of experiments. Grossman warns that amine-type antioxidants are of "dubious value" in Hypalon rubber systems. Also, he suggests that quinoline-type antioxidants are consumed during irradiation and hence the high temperature mechanical properties decrease once the antioxidant is gone. This is the motivation for increasing the Agerite Resin D concentration, the quinoline-type antioxidant, in order to see if the high temperature physical properties also

increase.

The results of the hot tear test for Series G'-K are given in Figure 5-13 plotted against 200 percent modulus. There is no significant increase in hot tear strength as Resin D concentration is increased. However, since raising Resin D concentration to 1.0 - 2.5 pphr has no apparent detrimental effect, and since pads undergo prolonged high temperature service, it appears advantageous to increase the Resin D level to 1.0 - 2.5 pphr.

5.4.2.3. Base Rubber. The final parameter varied in this series of experiments was SBR-base rubber. As seen by gel permeation chromatography (GPC) analysis, the three base SBR rubbers employed are nearly identical in molecular weight distribution. However, there are undoubtedly marked differences in their heat histories, impurity level, etc., since they were produced by different manufacturers. The objective in comparing these rubbers is to see the effect of these factors on hot tear strength.

Figure 5-14 is a plot of the hot tear results of each rubber versus 200 percent modulus. It is clear that even nominally identical base rubbers have different physical properties. This opens a vast array of parameters to speculation when one considers varying molecular weight as well as base rubber composition itself (i.e., natural rubber, butyl rubber, blends, etc.). It seems this result merely encourages further study instead of leading to a conclusion.

5.4.2.4. Additional Sensitization Agents. The second series of tests focused on determining an effective radiation cross-linking agent by measuring the gel fraction of SBR with the additive after irradiation. Trimethylolpropane trimethacrylate (TMPTMA) (Aldrich Chem. Co.) was tested because of its success seen in the literature as a radiation crosslink promoter of other polymers. Another promising aspect of TMPTMA with respect to the aggregation problems is that it is a liquid at room temperature with a very high boiling point. However, it is structurally quite dissimilar to SBR. The other cross-linking agents employed were SBR and BR oligomers (Rycon 181, 100, and 131 from Colorado Chem Co, see Table 5-9). These compounds have varying concentrations of 1,2-butadiene which provides pendant vinyl groups to act as crosslink promoters. It was hoped that controlling the concentration of pendant vinyls would allow preferential crosslinking over cyclization of the vinyls. Also, since the oligomers are structurally identical to SBR, it was hoped that the blending would be completely homogeneous with no tendency to aggregate.

The results are summarized in Table 5-10. For a reason

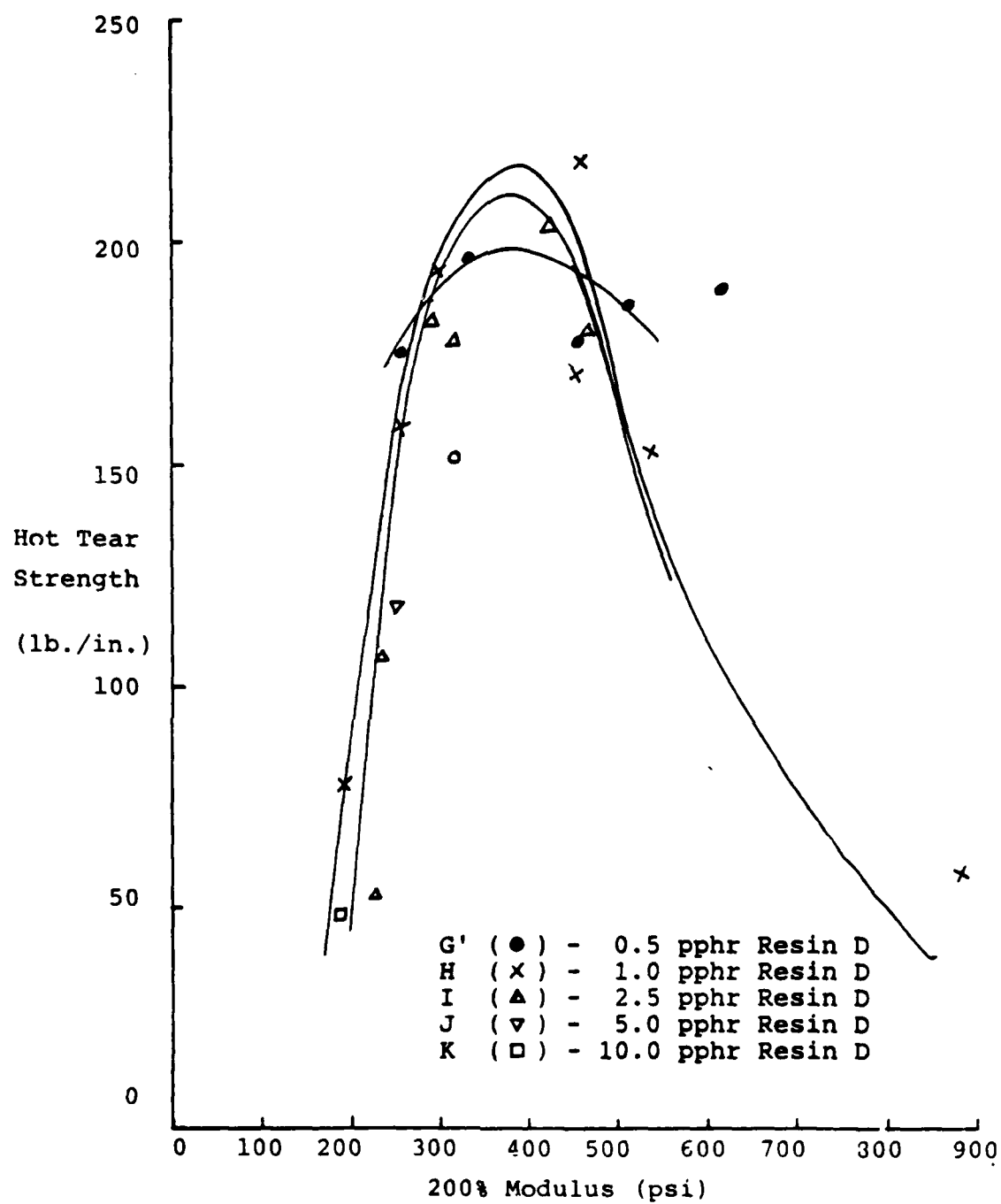


Figure 5-13. Hot Tear Strength vs. 200% Modulus. SBR (G'-K)

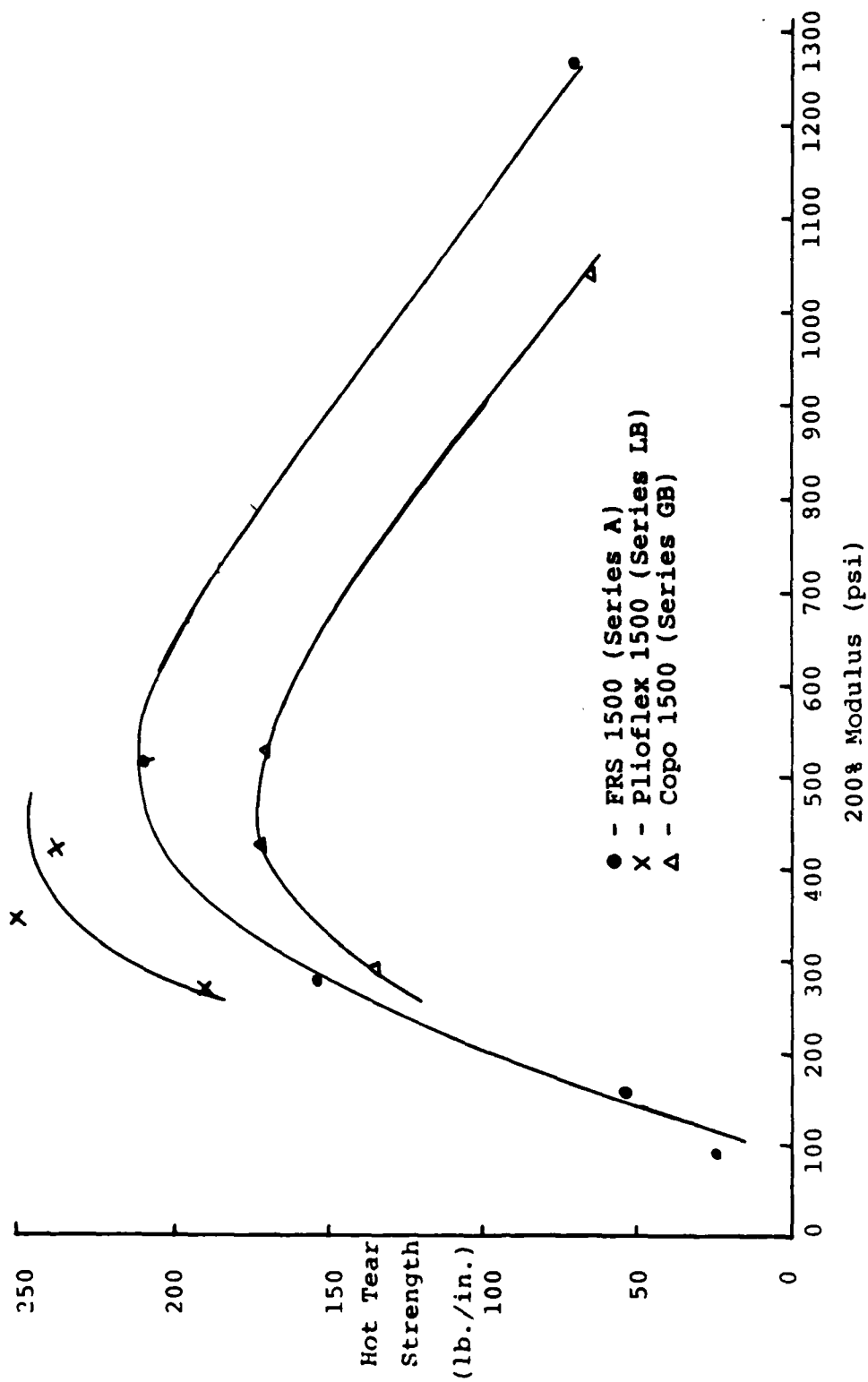


Figure 5-14. Hot Tear Strength vs. 200% Modulus. SBR (A, GB, LB)

Table 5-9. Oligomer Sensitizing Agents

Materials

Oligomers	% st	% vinyl	m.w.	viscosity (CP)	Note
Rycon-131	0	20	--	---	(BR)
Rycon-181	30	20	3000	360,000@ 45	(SBR)
Rycon-100	20	70	2400	380,000@ 45	(SBR)

Table 5-10. Gel Fraction Tests for Radiation Sensitizers - SBR

(1) Comparison of Pure SBR to SBR + TMPTMA 5 PHR

Dose Mrad Gel%	0	1	2	4	8	13
SBR	0	0	0	26.4%	71.3%	80.5%
SBT	0	56.96%	69.84%	78.9%	86.5%	91.43%

(2) Comparison of Pure SBR to SBR + 100 (5PHR), SBR +100 (5 PHR, Purified)

Dose Mrad Gel%	0	1	2	4	8	13
SBR	0	0	0	26.4%	71.3%	80.5%
SBR + 100	0	0	0	27.9%	67.3%	79.2%
SBR + 100P	0	---	0	26.6%	67.2%	78.3%

(3) SBR + TMPTMA

Dose Mrad Gel%	0	1	2	4	8	13.2
GEL %	0	57.0%	69.8%	78.9%	86.5%	91.4%
S %	1	43.0%	30.2%	21.1%	13.5%	8.6%
S $\frac{1}{2}$	1	0.656	0.550	0.459	0.367	0.29
S + S $\frac{1}{2}$	2	1.086	0.852	0.670	0.502	0.376
1/Dose	∞	1.000	0.500	0.250	0.125	0.076

Table 5-10. (CONTINUED) Gel Fraction Tests for Radiation Sensitizers - SBR

(4) For SBR

Dose Mrad Gel%	0	1	2	4	8	13.2
GEL %	0	0	0	0.264	0.713	0.805
S %	1	1	1	0.736	0.287	0.195
S ¹	1	1	1	0.858	0.536	0.44
S + S ¹	2	2	2	1.59	0.82	0.64
1/Dose	∞	1	0.5	0.25	0.125	0.076

(5) Comparison table of different crosslinking agent for SBR-1500

X.L. Agent	X.L.A. Conc. (PHR)	Gel % & Dose (Mrad) of						Effective	Note
		0	1	2	4	8	13		
--	0	0	0	0	26.4%	71.3%	80.5%	—	Pure SBR as Standard
Rycon-131	5	0	0	0	29.6%	66.6%	77.5%	No	
Rycon-181	5	0	0	0	11.4%	66.9%	74.7%	No	
Rycon-100	5	0	0	0	27.9%	67.3%	79.2%	No	
Rycon-100P	5	0	0	0	26.6%	67.2%	78.3%	No	Purified w/ NaOH
TMPTMA	5	0	56.96%	69.84%	78.9%	86.5%	91.43%	Yes	

yet unknown, but highly warranting investigation due to its great potential, the oligomers all failed to sensitize radiation crosslinking. However, the TMPTMA produced a significant crosslinking enhancement. The effect of TMPTMA on the rubber mechanical properties still was unknown, but would be revealed in the next series of mechanical property tests.

5.4.3. BR, NR, and SBR with TMPTMA. Because of the positive gel fraction results, TMPTMA was chosen as the crosslinking agent for tests on different base rubbers. The BR, NR, and SBR formulations used are given in Table 5-11. The nomenclature used is given in Table 5-12. All the samples were irradiated to approximately the same dose (~12 Mrads) by 2 passes under an electron beam at Columbia Research Corporation in Gaithersburg, MD.

The mechanical property test results are given in Table 5-13. The hot tear strength and tensile strength plotted against 200 percent modulus are shown in Figure 5-15. The hot tear strength results showing very low values for TMPTMA filled SBR discouraged the use of TMPTMA further as a crosslink promoter. The NR results also showed little promise. However, the high BR hot tear values, along with the other qualities of BR which are advantageous for tank-pad application (as discussed in par. 5.4.1.), motivated further study on this base elastomer.

The result of TMPTMA and BR gel tests are given in Table 5-14. An alternative crosslink promoter was located.

5.4.4. BR plus Syndiotactic-1,2-polybutadiene. To improve the mechanical properties of single phase high cis-polybutadiene rubber, RB-820, a syndiotactic-1,2-polybutadiene is chosen as a trace additive. The former is symbolized by BR, the latter by R. Not only could this polyfunctional agent enhance the crosslinking yield of high cis-1,4-polybutadiene but also it can form a crystalline domain that would increase the strength and toughness of the soft amorphous matrix.

RB-820 as developed by Japanese Synthetic Rubber containing 92 percent 1,2-vinyl unit, with an average molecular weight of more than 100,000 and a crystallinity of approximate 25 percent. RB-820 is comparatively reactive because of its structure; that is, it has a vinyl group and a hydrogen bonded to a tertiary carbon at the allyl position in each structural unit.

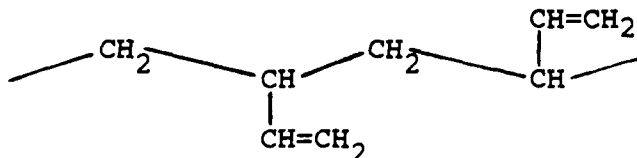


Table 5-11. NR, BR, and SBR Formulations

(14) For SBR and NR

Chemicals	PHR	1000g Batch
SBR-1500 /NR-	100	645.16%
ZnO	4	25.81
Stearic Acid	2	12.90
SAF, N110 Black	45	290.32
AO 1,2	0.5+0.5	3.23x2
Antozite 2	3	19.36
Total	155	1000.00

(15) For BR

Chemicals	PHR	1000g Batch
BR-1500 /NR-	100	621.12
ZNO	5	31.06
Stearic Acid	2	12.42
HAF	50	310.56
AO 1,2	0.5+0.5	6.21+6.21
Antozite 2	3	18.63
Total	161	1000.00

(16) For TMPTMA

TMPTMA (WT.) 1000 g batch TMPTMA (PHR)	SBR	BR	NR
0	0	0	0
1	6.45	6.21	6.45
2(BR/SBR), 4(NR)	12.9	12.42	25.8
5	32.26	31.05	---
8.4	54.2	----	---

Table 5-12. Identification of NR BR and SBR Sample Sheets

Base Rubber		NR	BR	SBR
X.L. Conc.				
A	0 (PHR)	NR-10A	BR-10A	SBR-10A
B	1	NR-10B	BR-10B	SBR-10B
C	2	NR-10C	BR-10C	SBR-10C
	4			
D	5		BR-10D	SBR-10D
E	8.4			SBR-10E

Table 5-13. Mechanical Properties: NR, BR, and SBR

Properties	SBR					BR					NR			
	0	1	2	5	8.4	0	1	2	5		0	1	4	
200% Modulus (psi)	210	145	210	300	340	573	380	440	600		324	313	417	
Tensile Strength (psi)	1750	1220	1620	2025	1925	1095	1460	1370	1090		675	520	1355	
Ultimate Elongation (%)	840	1000	980	800	780	330	455	405	380		320	285	395	
Tear Strength, Die C 10 min. @250°F	47	35	37	44	36	86	147	160	89		35	42	52	

Table 5-14. Gel Fraction Tests: BR plus TMPTMA

TMPTMA as crosslinking agent for BR-0150

X.L. Agent	X.L.A. Conc. (PHR)	Gel % & Dose (Mrad) of							Effective	Note
		0	1	2	4	8	13			
--	0	0	25.4%	54.3%	---	72.9%	91.2%			Pure BR
TMPTMA	5									

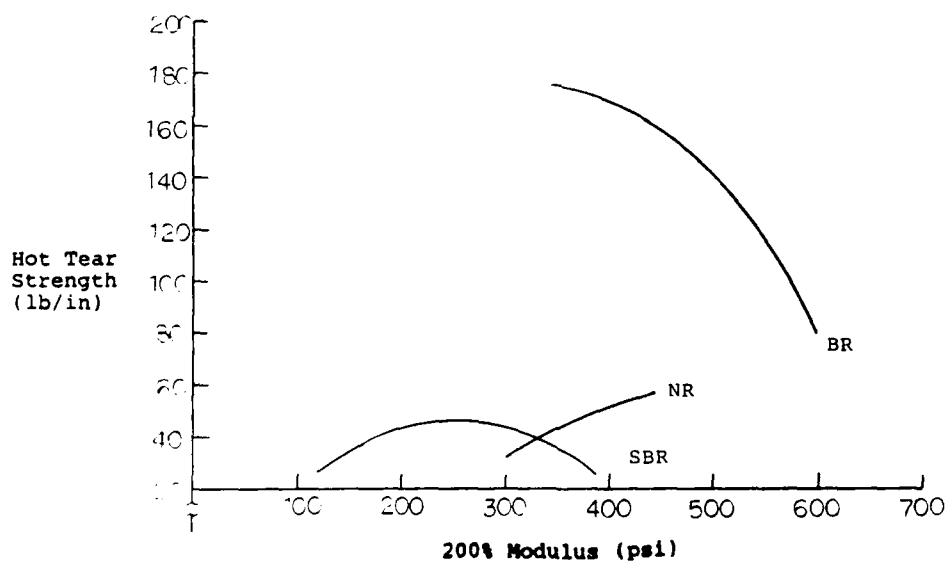
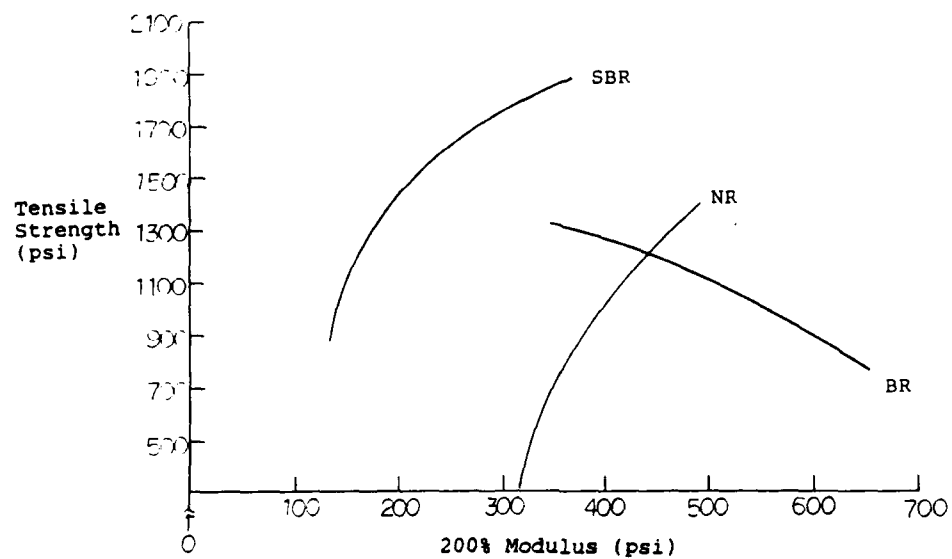


Figure 5-15. Mechanical Properties: NR, BR, and SBR

The syndiotactic arrangement not only favors crystallinity but also is less favorable than the isotactic form to cyclization or intramolecular linking of the vinyl groups. RB-820 has the characteristics of both rubber and plastic. Also, because of the polyfunctional vinyls, it can be crosslinked by high energy radiation. The crosslinked products show excellent thermal, weather, and ozone resistance. Finally, the melting point of RB-820 is only 80°C, so it is very easy to compound or process by ordinary rubber processing machines.

The plastic domain impedes growth of microcracks in the matrix because the tips of growing cracks undergo plastic deformation and dissipate the strain energy. Crystalline domains formed in a rubbery matrix by deformation are also effective in improving strength and toughness for the same reason. RB-820 with 25 percent crystallinity is dispersed in the BR as a crystalline domain to remedy the shortcomings of low tear strength and poor tensile strength of the BR.

Crystallinity in a polymer modifies the modulus curve of a amorphous polymer above its T_g by at least two mechanisms. First, the crystallites act as crosslinks by tying segments of many molecules together. Secondly, the crystallites have very high moduli compared to the amorphous parts, and behave as rigid fillers in an amorphous matrix. Thus, the modulus increases with the degree of crystallinity.

Most high cis-polybutadiene do not crystallize at room temperature. The reason is ascribed to the lower glass transition temperature (T_g) of BR (-102°C) compared with NR (-70°C). The higher segmental motion of BR molecules than that of NR molecules at the same temperature above T_g delays the strain-induced crystallization of BR until very high elongation. Fracture of BR takes place before arriving at the elongation where crystallization can proceed.

The properties of elastomers are much improved by strain-induced crystallization, which occurs only in polymers with high stereoregularity. BR and vinyl R are both highly stereoregular elastomers. We expect that R has a greater tendency to form strain-induced crystallinity than BR. X-ray diffraction patterns comparing BR and syndiotactic-1, 2-polybutadiene and butadiene rubber blend (RBR) samples at different extension rates were carried out to study this phenomenon.

During stretching, the elongational stress causes the deformation of crystalline domain, while the amorphous matrix molecules are relaxed and mobile enough to achieve epitaxial growth at the domain boundaries which act as a row nucleus for growing lamellar crystals. Lamellar crystals grow along the direction perpendicular to the stretching direction. This is

the so-called "shish-kebab" structure.

With more finely dispersed crystalline domains, more interfacial boundary area exists, which provides the stretched BR matrix with lots of nucleating sites for growth of lamellar crystals.

It is important to emphasize that the presence of crystallites is not the physical equivalent of some additional inert fillers. This is especially true when the crystallites are connected by primary chemical bonds to the amorphous matrix by means of a crosslinking reaction.

The RBR formulations used are given in Table 5-15. The irradiations were obtained at the University of Maryland cobalt-60 gamma source under continuous flow of N_2 . The results of these experiments and a discussion of the significant advances made in the morphological studies of radiation curing for tank-pad application are presented in the following pages.

5.4.4.1. Carbon Gel Test. The carbon gel content results are presented in Table 5-16. This is the percent of the R-plus-BR converted to a toluene-insoluble substance. Figure 5-16 shows the carbon gel percent vs. dose at various crosslink promoter concentrations. As dose increases, carbon gel increases. Carbon gel percent against RB-820 concentration at different doses is given in Figure 5-17 which depicts that increasing RB-820 pphr tends to increase the carbon gel percent, although the low dose data at 4 phr exhibit anomalous behavior. A Charlesby-Pinner plot of the BR-0150 and RBR-B series is presented in Figure 5-18. From these curves we find that the gel dose of BR-0150 and RBR-B is 1.25 and 1.0 respectively. From Charlesby's equation the following G (crosslink) values are obtained: 1.40 for BR-0150 and 1.75 for RBR-B. The G (crosslink) value of BR-0150 is slightly lower than the value reported by Bohm, et. al., probably due to the different microstructure and radiation atmosphere. Also, the calculation used in this work is based on the carbon gel percent instead of normal gel percent. In addition, the ratio of G (crosslink) values of RBR-B to BR-01500 shows that RBR-B can increase the crosslinking density of BR-0150 about 25 percent.

From the above, it is obvious that BR-0150 is crosslinked easily by ionizing radiation and that upon the addition of a few phr of the thermoplastic crosslinking agent RB-820, it is crosslinked even more readily. Indeed, the effective G (X) for the additive in this system is 10-15. A dose of only 5 Mrad will achieve carbon gel values up to 70 percent. This means less dose is necessary when compared with SBR or NR. One more interesting observation from the Charlesby Pinner plot is that the curve is convex upward. This suggests that some

Table 5-15. BR Formulations

Ingredients (phr)	(b) Sulfur System	Radiation System			
		RBR-A	RBR-B	RBR-C	RBR-D
(a) BR-0150	100	100	100	100	100
HAF black	60	50	50	50	50
Process Oil	10	---	---	---	---
Zinc Oxide	5	5	5	5	5
Stearic Acid	2	2	2	2	2
Antioxidant	1	1	1	1	1
Antiozonant	---	3	3	3	3
(c) RB-820	---	0	1	4	10
Sulfur	1.5	---	---	---	---
Accelerator	1.0	---	---	---	---
Total phr	180.5	161	162	165	171

Note: (a) High cis-1,4-polybutadiene, a solution polymerization product by Taiwan Synthetic Rubber Co.

(b) Prepared by T.S.R.C.

(c) A syndiotactic-1,2-polybutadiene by Japan Synthetic Rubber.

Table 5-16. Carbon Gel Results of RBR Series

Items \ (a) Dose	2	5	10	15	20
RBR - A	(b) 37%	74%	81%	94%	95%
RBR - B	39%	76%	90%	96%	97%
RBR - C	---	72%	88%	98%	99%
RBR - D	---	81%	97%	99%	100%

Note: (a) Irradiated by gamma-ray under nitrogen atmosphere at room temperature.

(b) By Soxhlet extraction apparatus.

(c) 94% carbon Gel fraction of BRS was measured under the same extraction condition.

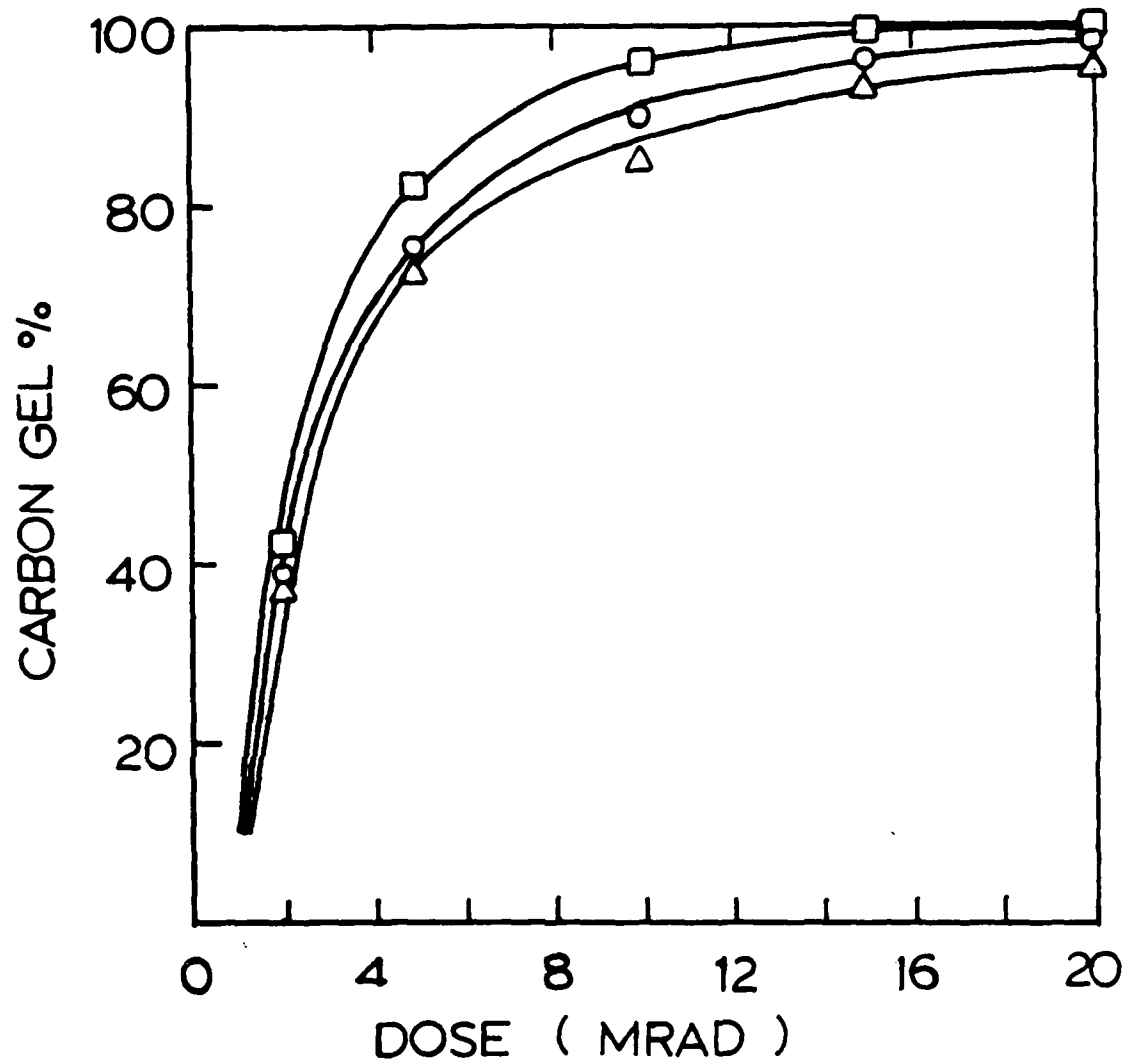


Figure 5-16. Carbon Gel% vs. Dose. BR

- (Δ) - 0 phr RB-820,
- (\circ) - 1 phr RB-820,
- (\square) - 10 phr RB-820.

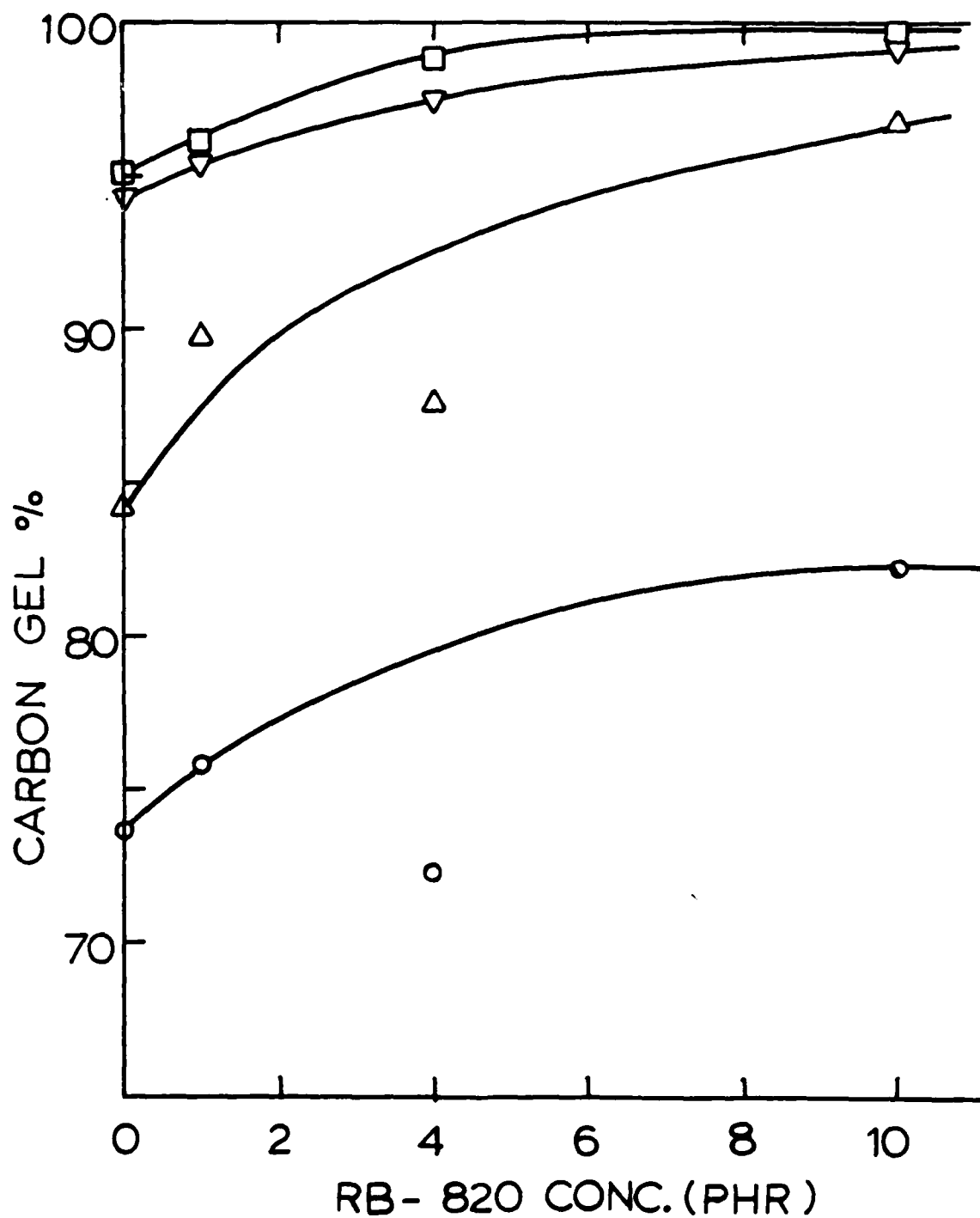


Figure 5-17 Carbon Gel% vs. RB-820 Concentration. BR
(O) - 5 Mrad,
(Δ) - 10 Mrad,
(▽) - 15 Mrad,
(□) - 20 Mrad.

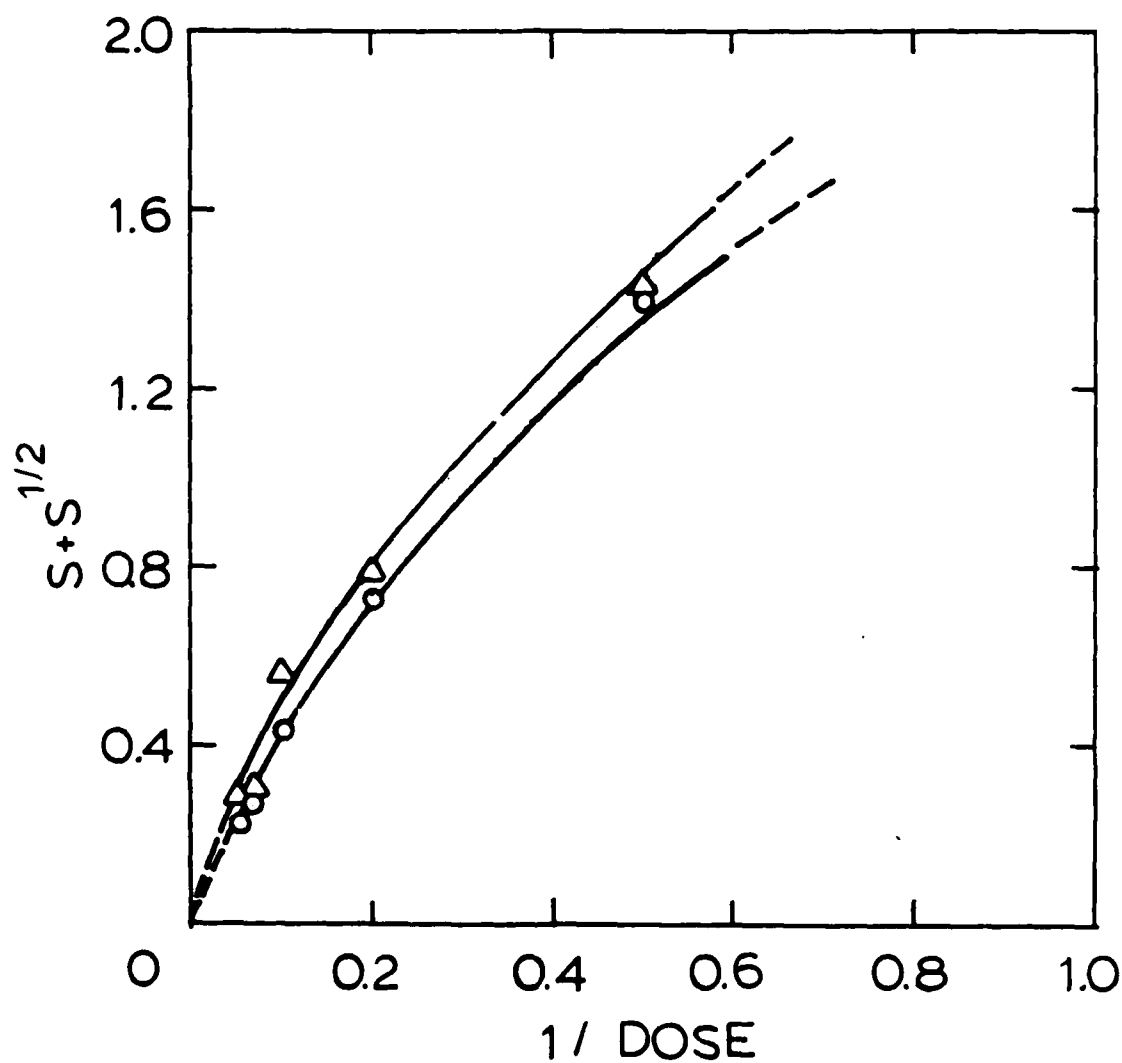


Figure 5-18. Charlesby-Pinner Plot for BR and RBR

(Δ) - 0 phr RB-820,
 (O) - 1 phr RB-820,

intramolecular crosslinking such as cyclization takes place simultaneously with the intermolecular crosslinking.

5.4.4.2. Mechanical Property Tests. Table 5-17 lists the mechanical properties of radiation-cured samples containing various RB-820 concentration levels. Figures 5-19, 5-20, 5-21 and 5-22 show the tensile strength, 200 percent modulus, elongation, and hot tear strength, respectively, against dose.

The mechanical property data of sulfur cured VCR-412 and Taktene-220 were reported by Belvoir Research & Development Center (BRDC) (Table 5-18). Sulfur-cured BR and RBR samples which were prepared in TSRC but were tested at the University of Maryland are also shown in Table 5-19.

The first outstanding observation is that RBR radiation cured systems have a greatly increased high temperature tear strength. The hot tear strength of the RBR series is much as 90 percent greater than that of the sulfur cured high cis-BR, and, astonishingly, 20 percent superior to VCR-12. Second, the tensile strength of RBR series also shows a remarkable improvement. For the RBR-B (Figure 5-19) series, the tensile strength at doses under 15-20 Mrad is 14 percent higher than that of BR and slightly higher than that of VCR-412. Figure 5-21 presents elongation versus dose. It also indicates the outstanding characteristics of the RBR radiation cured system which has an elongation greater than that of BR and VCR systems. Figure 5-20 shows that the 200 percent modulus increases almost linearly with increasing dose. Since the modulus is proportional to the combination of crosslinks, this indicates that the crosslink density is proportional to dose. The 20 Mrad samples have the same 200 percent modulus as the sulfur-cured samples of BR. But if we increase the dose, a higher value of 200 percent modulus is expected. These 200 percent modulus data are three to four times the values of SBR (Figure 5-8) at the same dose level. This means that the RBR system is much easier to crosslink by irradiation than the SBR system.

Figures 5-23 through 5-26 present the tensile strength, 200 percent modulus, elongation and hot tear strength versus RB-820 concentration. They show that the maximum tensile strength and hot tear strength is at RB-820 concentration of 1 phr and 4 pphr, respectively. From these results we can conclude that RB-820 improves the crosslinking density of BR to some extent, and also improves the mechanical properties. Further insight can be gained by plotting tensile strength and hot tear test against 200 percent modulus, i.e., crosslinking density, as shown in Figure 5-27 and 5-28. The highest tensile strength is achieved in samples with 1 phr RB-820. This maximum increases, as noted earlier, and shifts to lower RB-820 levels as the

Table 5-17. Mechanical Properties of RBR Series

Mechanical Properties	RBR A-5	RBR A-10	RBR A-15	RBR A-20	RBR B-5	RBR B-10	RBR B-15	RBR B-20	RBR C-5	RBR C-10	RBR C-15	RBR C-20	RBR D-5	RBR D-10	RBR D-15	RBR D-20
Hot Tear Strength 10 min @ 250°F (lb/in)	84	>192	213	174	77	>227 ±9%	226	180	122	>268	182 ±18%	157	85 ±13%	204	163 ±10%	151 ±36%
200% Modulus (psi)	243	407	651	847	211	406	624	847	251	416	647	773	273	464	654	832
Tensile Strength (psi)	1204 ±8%	1498 ±17%	2088	2128	1100	1663	2404	2451	1428	1817 ±12%	2095	1880	1495	1976	2185 ±8%	2245
Ultimate Elongation (%)	553	438 ±11%	457	397	530	467	510	438 ±8%	602	515	447	370	615	550	475	417

Note: (1) "A-5" means Series A at cure dose of 5 Mrads by gamma-ray source.

(2) 3 samples at each data point unless otherwise indicated by a superscript number in parentheses.

(3) Standard deviation is within ±7% unless otherwise indicated.

(4) "RBR" means RB-820 blended with Taipol BR-0150.

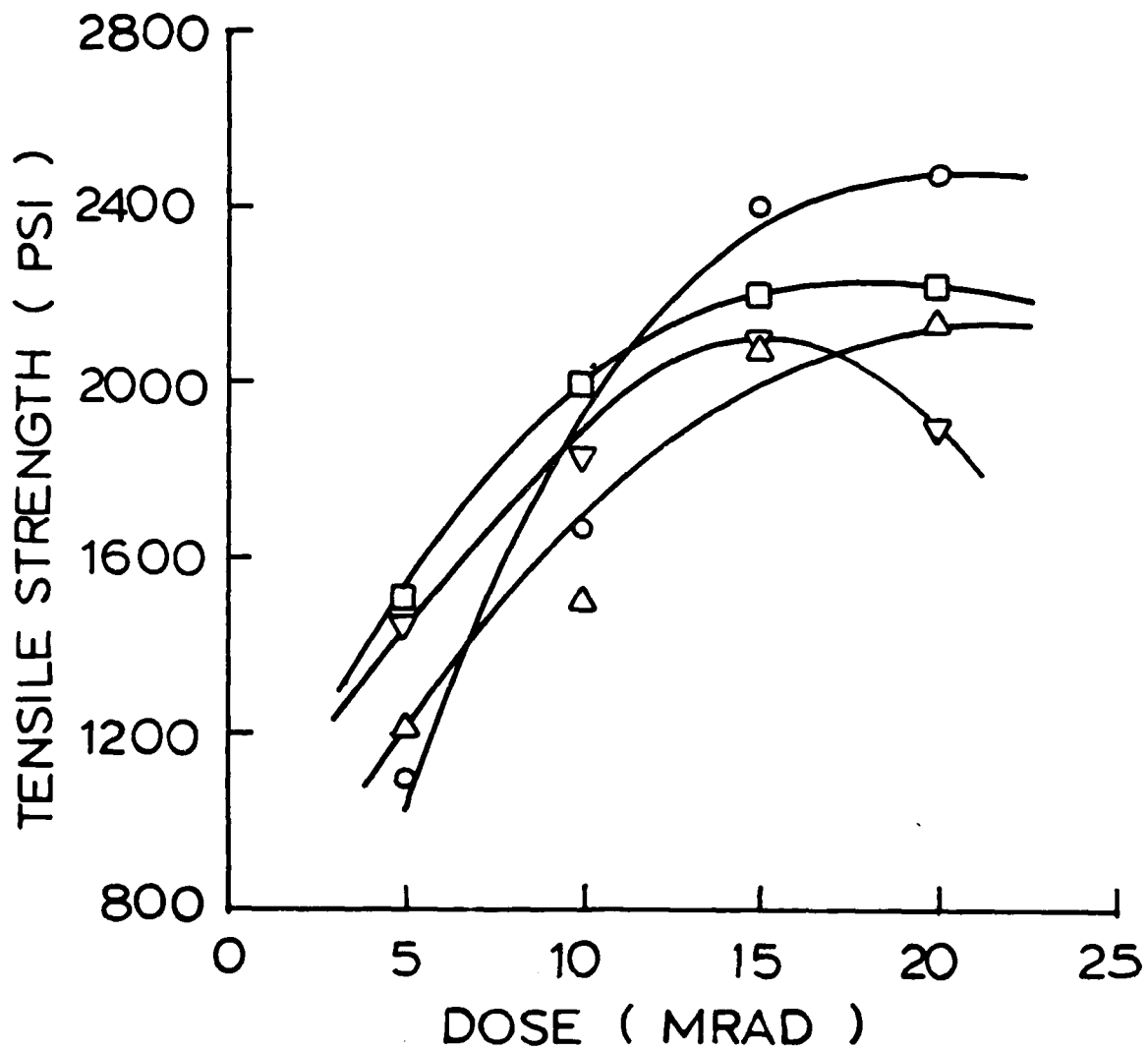


Figure 5-19. Tensile Strength vs. Dose. BR

- (Δ) - 0 phr RB-820,
- (\circ) - 1 phr RB-820,
- (∇) - 4 phr RB-820,
- (\square) - 10 phr RB-820.

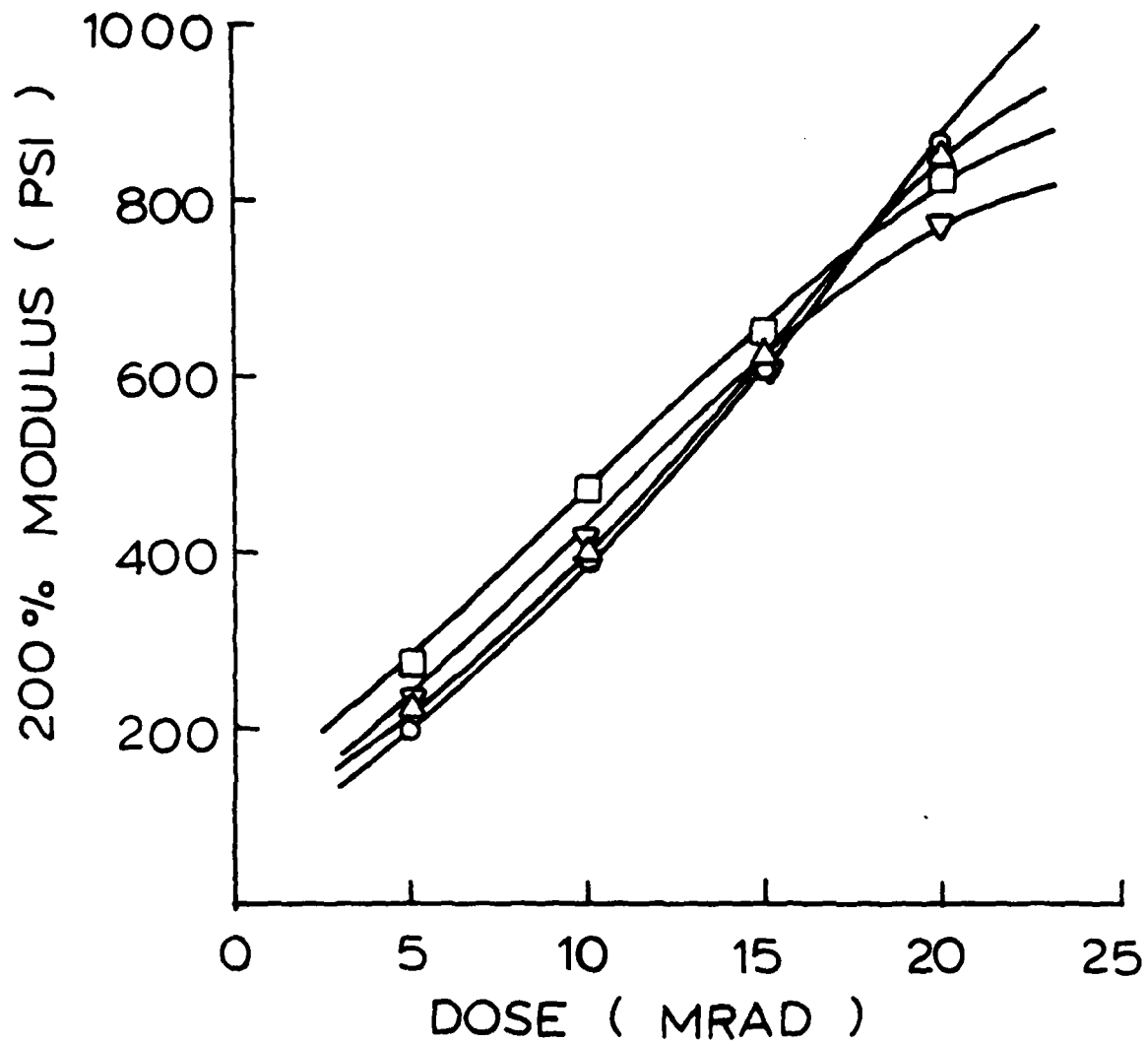


Figure 5-20. 200% Modulus vs. Dose. BR

- (Δ) - 0 phr RB-820,
- (\circ) - 1 phr RB-820,
- (∇) - 4 phr RB-820,
- (\square) - 10 phr RB-820

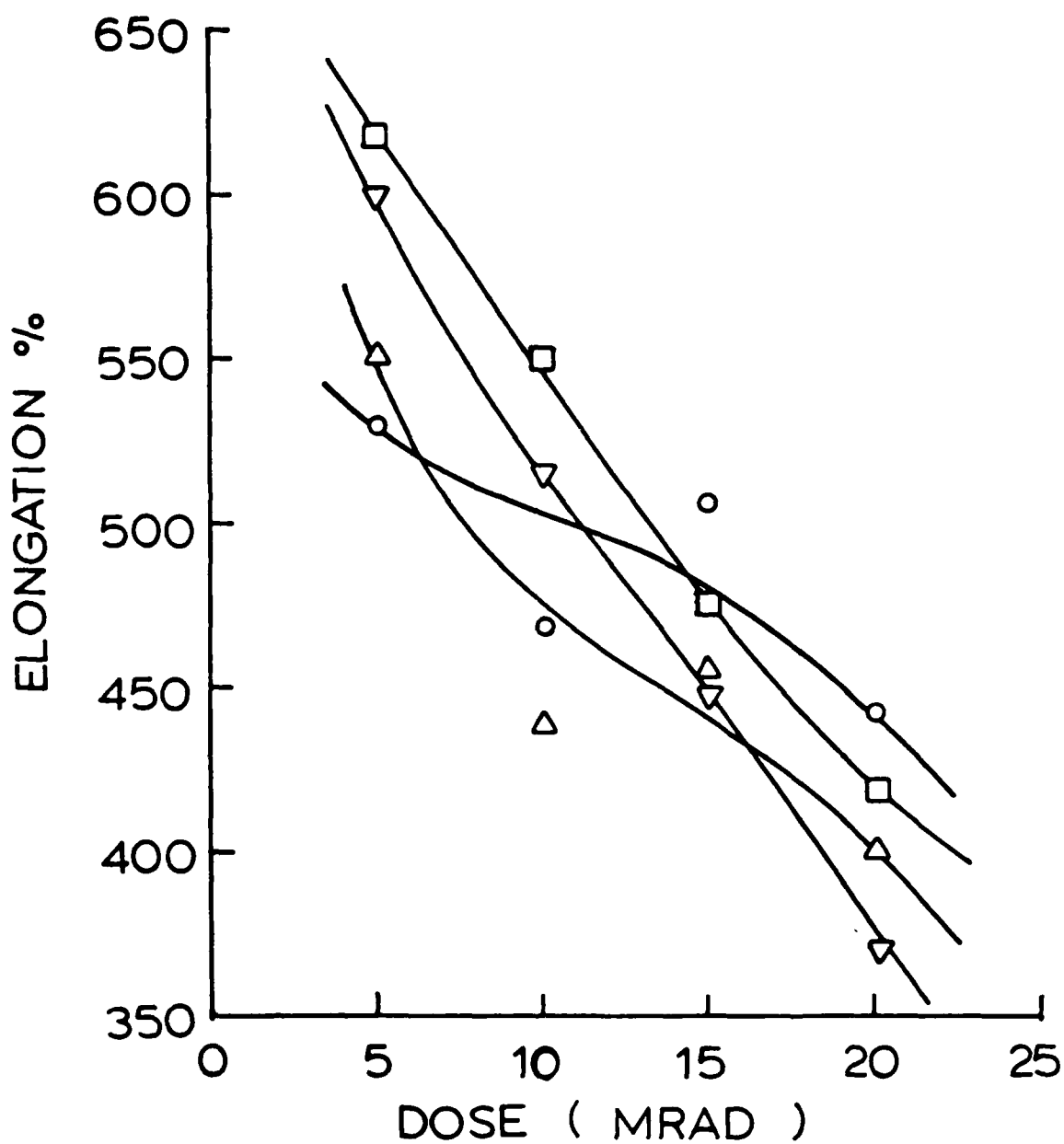


Figure 5-21. Elongation % vs. Dose. BR

(\triangle) - 0 phr RB-820,
 (\circ) - 1 phr RB-820,
 (∇) - 4 phr RB-820,
 (\square) - 10 phr RB-820.

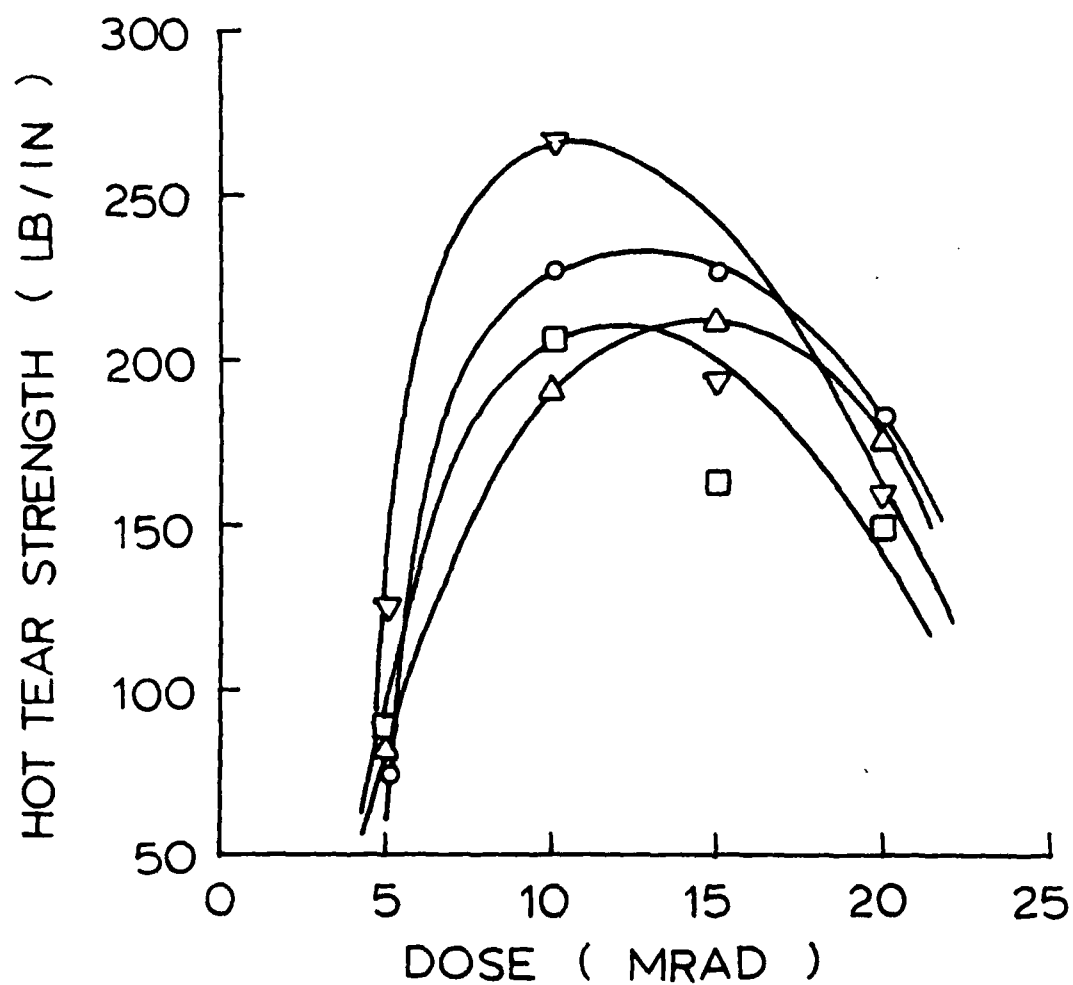


Figure 5-22. Hot Tear Strength vs. Dose. BR

- (△) - 0 phr RB-820,
- (○) - 1 phr RB-820,
- (▽) - 4 phr RB-820,
- (□) - 10 phr RB-820.

Table 5-18. Sulfur-cured Polybutadiene Data from BRDC

INGREDIENTS	PPHR			
	15 PBD 1	15 PBD 2	15 PBD 3	15 PBD 4
Natural RSS-1				
Polybutadiene Rubbers				
Cis 1, 4- 1203	100.0			
Diene 35 NF		100.0		
UBE Pol-VCR 412			100.0	
Taktene 220				100.0
Silicone Rubbers				
GE Tuf EL, SE 875				
Dow Corning, TR-70				
Nitrile Rubber				
Zetpol 2020				
Chloroprene Rubber				
Neoprene GW				
Zinc Oxide Kadox 15	4.0	4.0	4.0	4.0
Stearic Acid	2.0	2.0	2.0	2.0
SAF Black, N110	45.0	45.0	45.0	45.0
Red Ferric Oxide				
CA-2 Curing Agent				
Di Cup R				
Magnesium Oxide				
Vulcan 7H, N-234 Black				
Sundex 790				
Octamine				
Sulfur, Rubber Makers	2.0	2.0	2.0	2.0
Santocure	1.5	1.5	1.5	1.5
MBI				
YMTD, Metyl Tuada				
Antozite 2				3.0
Agorite Resin D				0.5
Agorite White				0.5
Santoflex 13				
Veron HII				
Cure Conditions				
minutes/Temp °F	20/300	15/300	15/300	15/300

Table 5-18. (CONTINUED) Sulfur-cured Polybutadiene Data from BRDC

PROPERTIES	15PBD	15PBD	15PBD	15PBD	PROPERTIES	15PBD	15PBD	15PBD	15PBD
	1	2	3	4		1	2	3	4
Original Properties					Flex Fatigue Properties				
Tensile Strength, Psi	831	1956	2385	2150	DeMattia Crack Growth				
200% Mod., Psi	545	475	1436	835	Unaged, mil/min	169	256	36.2	59.8
Elongation, %	280	443	320	360	70 Hrs @ 212°F, mil/min	1,213	1,540	740	295
Hardness, IRHD, Deg.	75	74	84	72	70 Hrs @ 250°F, mil/min	3,000	3,000	2,500	3,000
Bashore, Rebound, %	59	54	48	52	DeMattia Crack Initiation				
Specific Gravity	1.1030	1.0922	1.1036	1.0775	Unaged, cycle X 10 ³	10.0	4.0	20.5	8.0
Abrasion					Goodrich Flex @ 50°C				
Taber, gm/1000 cycl.	.0498	.0909	.0404	.0129	T, °C	29.5	34.3	42.2	20.8
Pico, Rating	167	146	225		Rate, °C/min	5.3	5.9	7.7	3.3
Tear Strength, Lb/In					Static Comp., %	11.3	13.0	7.3	13.2
ASTM Die C					Dynamic Comp., %	3.3	5.0	2.3	5.9
Unaged	317	261	344	173	Permanent Set, %	1.7	2.0	3.7	2.5
After 10 min @ 250°F	196	202	219	141	Blow Out Time				
After 4 Hr. @ 250°F	193	172	248	133	• 141.6 Psi, min	>120	>120	>120	52/115(3)
After 4 Hr. @ 300°F	76	78	94	89	• 265.4 Psi, min	11.8	9.1	4.3	
ASTM Die B					Compressibility				
Unaged	241	220	277	222	Unaged				
Mooney Viscometer					10%, Psi	150	137	246	128
M 1 + 4 (212°F)	100.5	74.6	85.7	60.5	20%, Psi	313	278	478	260
IS @ 250°F, min.	6.6	8.9	7.2	11.0	40%, Psi	807	682	1265	677
Puncture Resistance					After 70 Hrs @ 250°F				
Unaged, Lb	75	80	110	67	10%, Psi	174	130	177	97
10 min @ 250°F, Lb					20%, Psi	333	276	365	212
Heat Resistance					40%, Psi	761	664	889	510
f/fo = 70%, min.									
Dispersal Rating	127	97	187	163					
	6	6	7						

Notes: (A) Puncture could not be detected

(3) Four specimens tested, two sets of time produced

Table 5-19. Mechanical Properties of S-Cured Series, BR

Mechanical Properties	BRS _{<6>}	RBRS-B	RBRS-C
Hot Tear Strength 10 min @ 250°F (lb/in)	138±23%	128±14%	127±10%
200% Modulus (psi)	780	513	531
Tensile Strength (psi)	1747±16%	1686±9%	1797±13%
Ultimate Elongation (%)	350	423	457

- NOTE:
- (1) "BRS" means BR-0150 under sulfur curing, "RBRS" means RB-820 blended with BR-0150 under sulfur curing.
 - (2) Curing condition: 160°C, 6.7 minutes.
 - (3) Standard deviation is within ±7% unless otherwise indicated.
 - (4) 3 samples at each data point unless otherwise indicated by a superscript number in parenthesis.

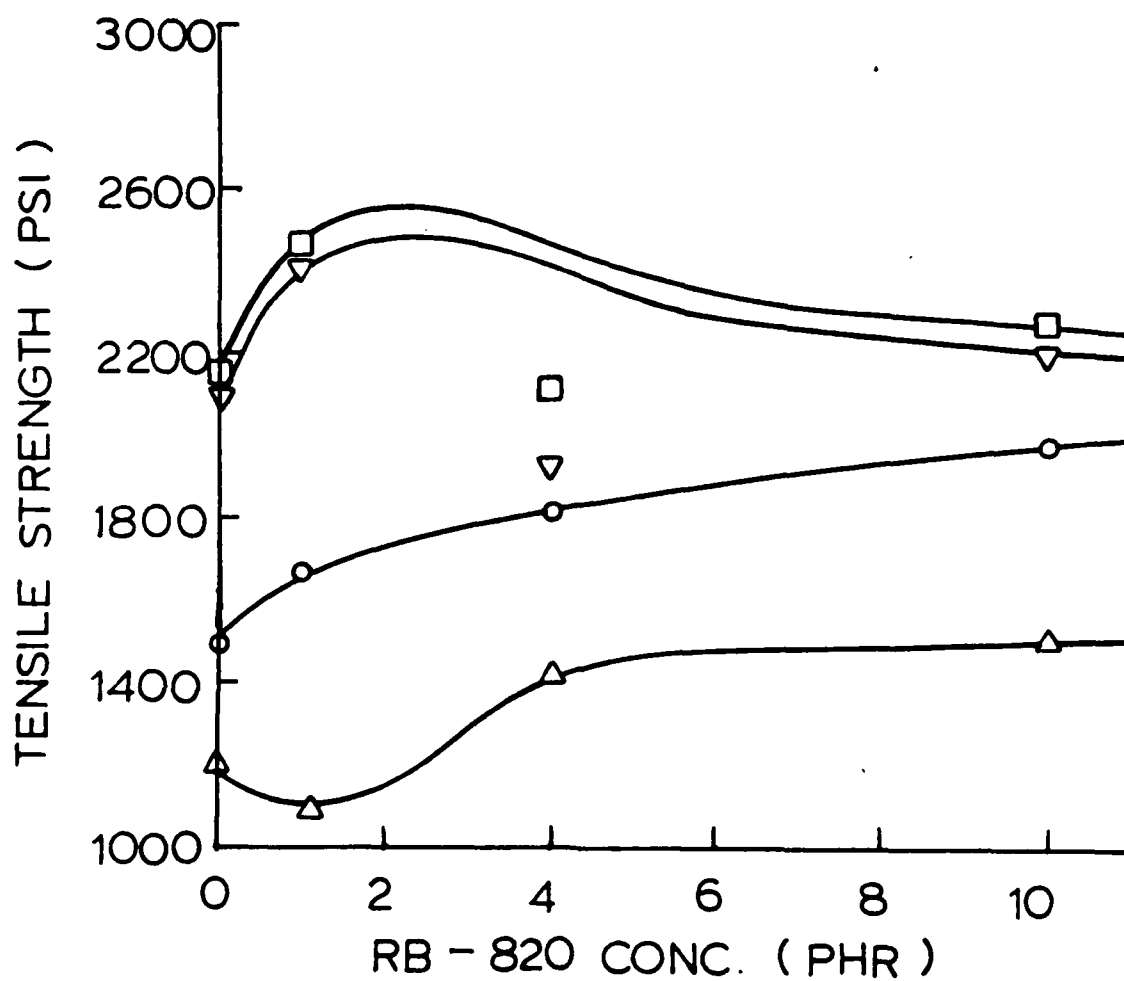


Figure 5-23. Tensile Strength vs. RB-820 Concentration. BR

(Δ) - 5 Mrad,
(\circ) - 10 Mrad,
(∇) - 15 Mrad,
(\square) - 20 Mrad.

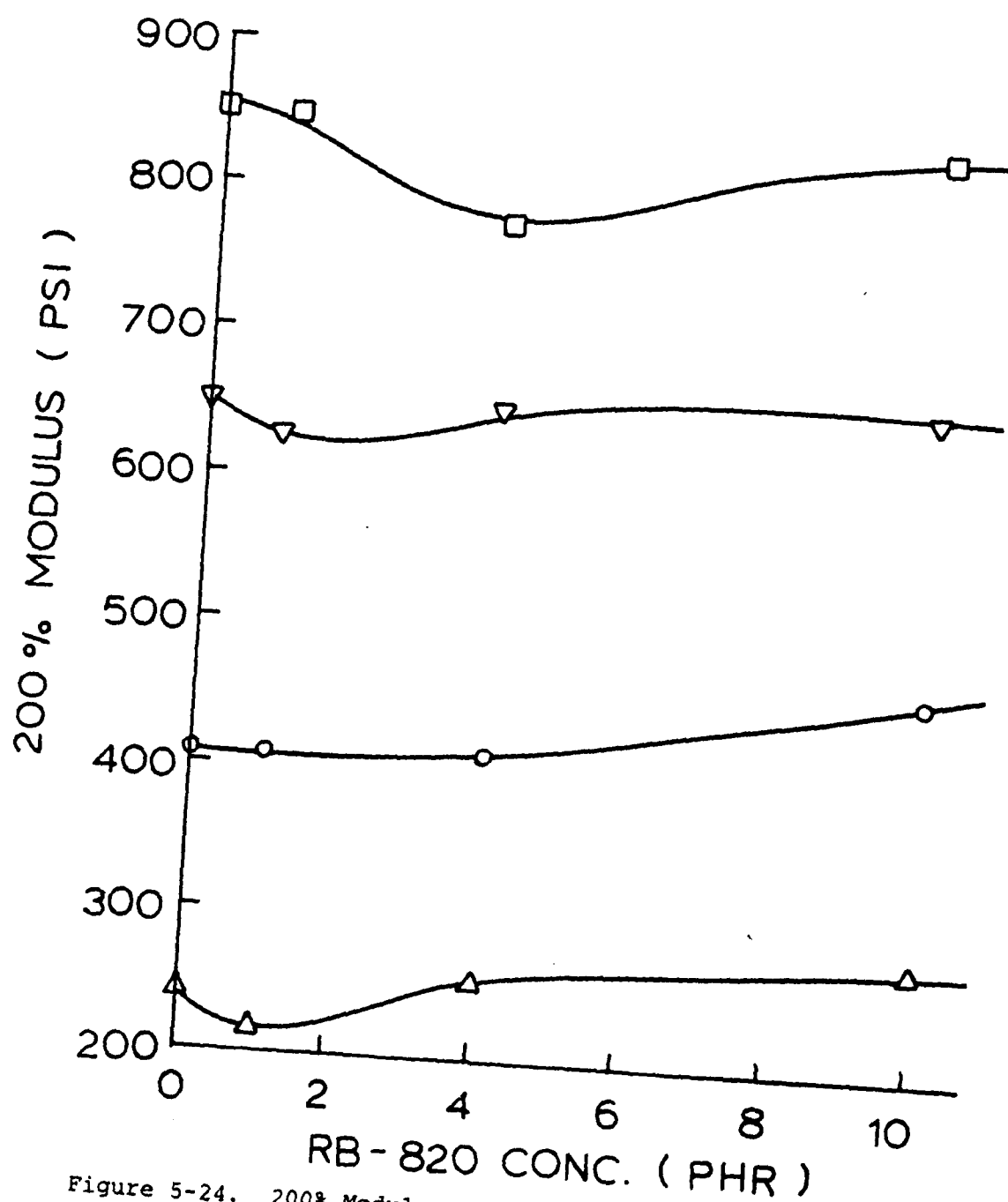


Figure 5-24. 200% Modulus vs. RB-820 Concentration. BR

- (Δ) - 5 Mrad,
- (\circ) - 10 Mrad,
- (∇) - 15 Mrad,
- (\square) - 20 Mrad.

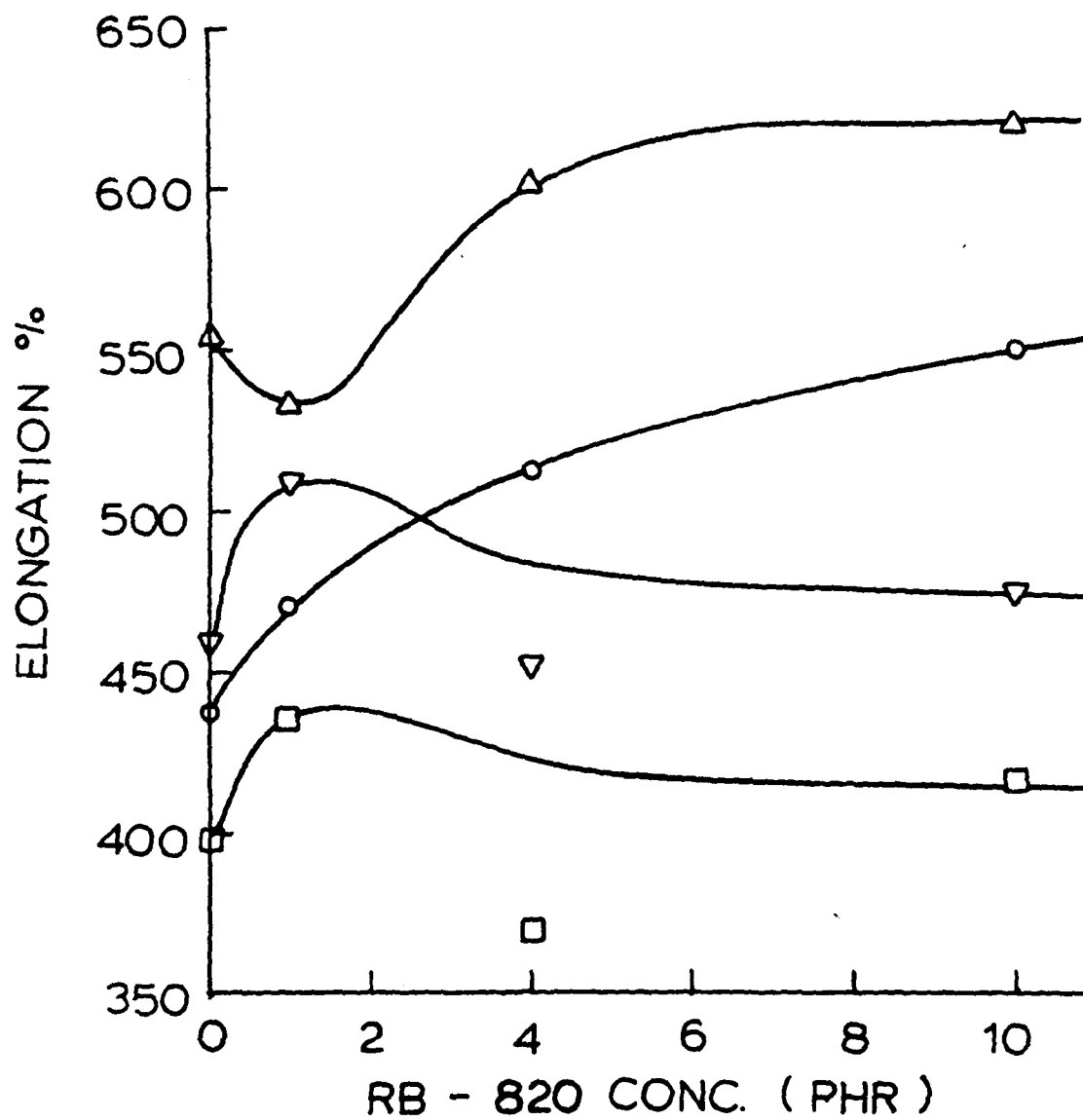


Figure 5-25. Elongation % vs. RB-820 Concentration. BR
 (Δ) - 5 Mrad,
 (○) - 10 Mrad,
 (▽) - 15 Mrad,
 (□) - 20 Mrad.

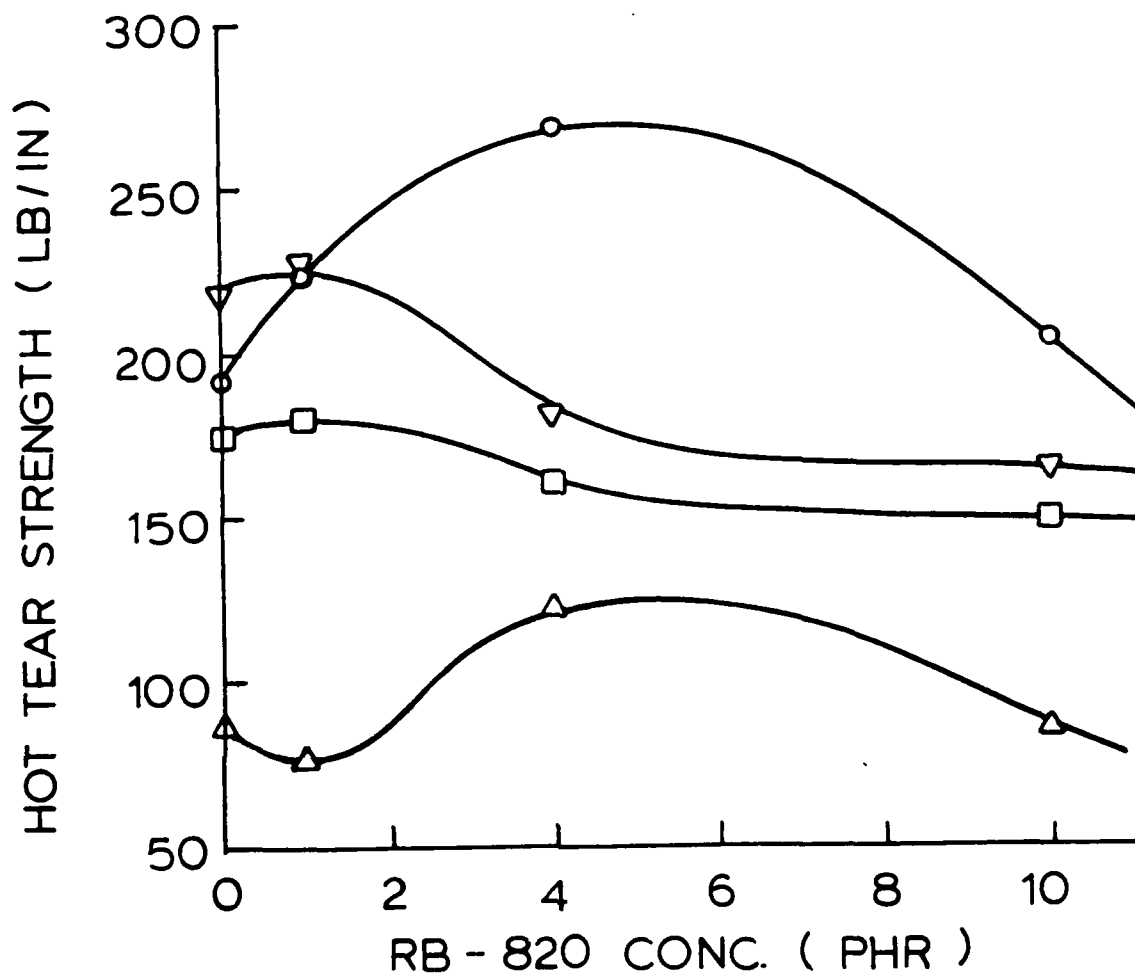


Figure 5-26. Hot Tear Strength vs. RB-820 Concentration. BR
(△) - 5 Mrad,
(○) - 10 Mrad,
(▽) - 15 Mrad,
(□) - 20 Mrad.

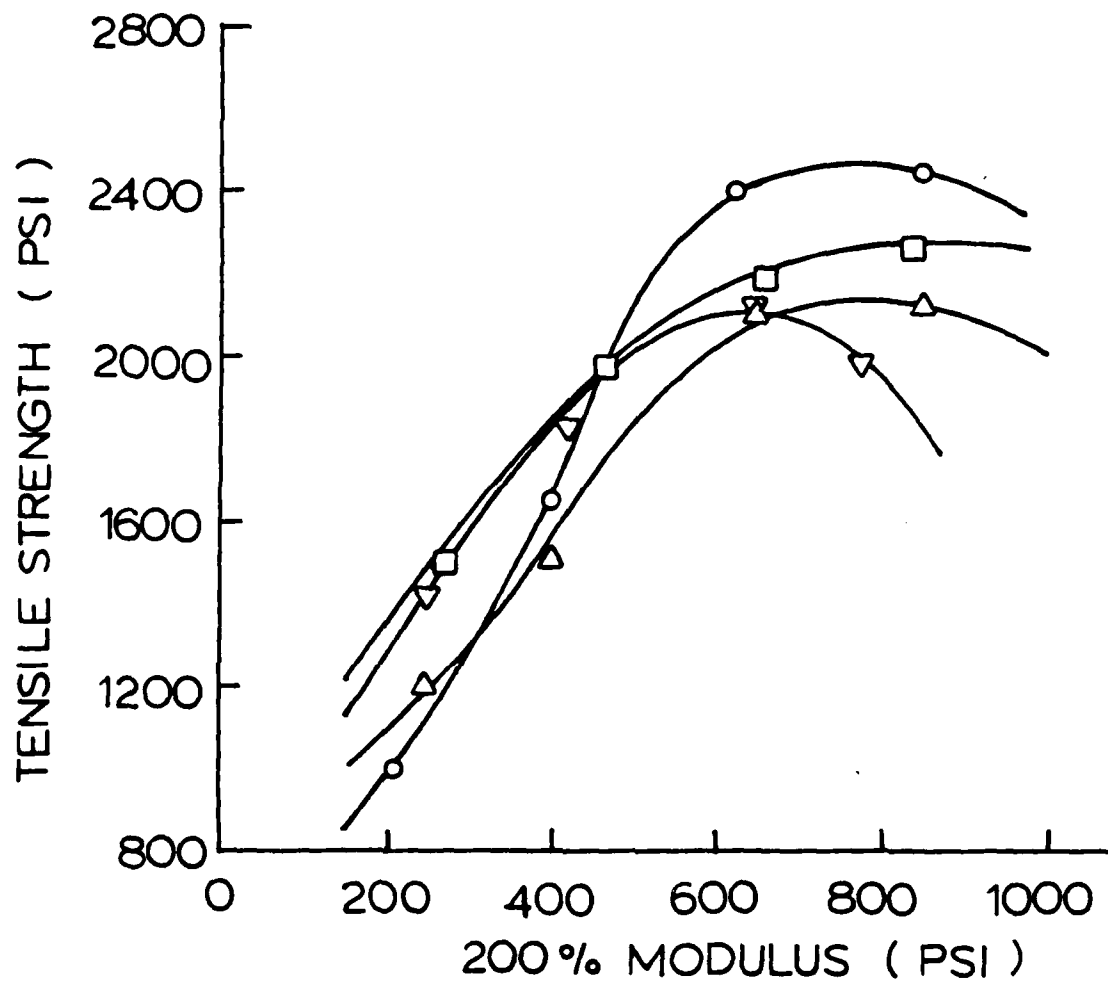


Figure 5-27. Tensile Strength vs. 200% Modulus. BR

- (Δ) - 0 phr RB-820,
- (\circ) - 1 phr RB-820,
- (∇) - 4 phr RB-820,
- (\square) - 10 phr RB-820.

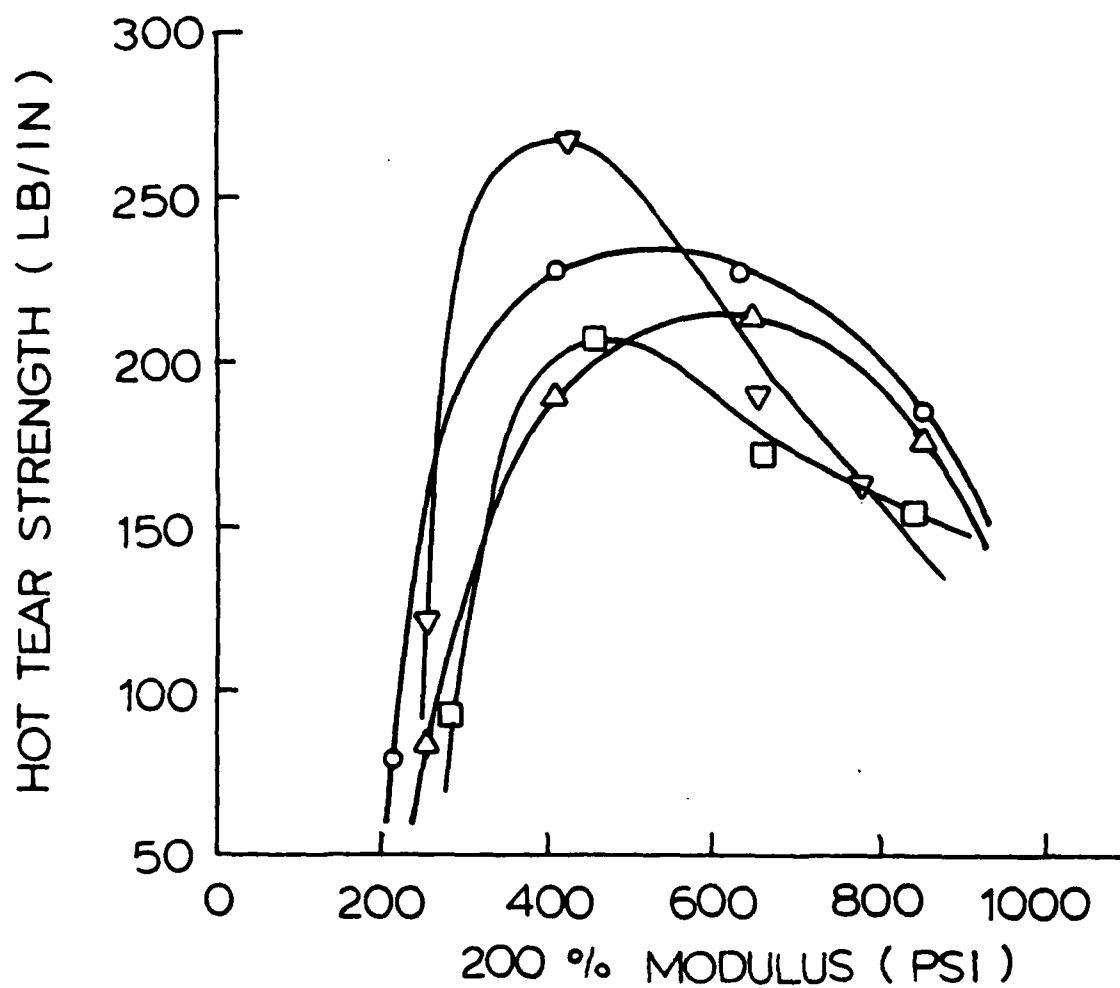


Figure 5-28. Hot Tear Strength vs. 200% Modulus. BR

- (Δ) - 0 phr RB-820,
- (\circ) - 1 phr RB-820,
- (∇) - 4 phr RB-820,
- (\square) - 10 phr RB-820.

modulus increases up to 800-1000 psi. Above 1,000 psi, the tensile strength decreases at an increasing rate as crosslink density increases.

The effect of RB-820 on hot tear strength is similar in that hot tear strength increases as crosslink density increases up to 400-500 psi and then decreases as the crosslink density increases. The optimum RB-820 concentration is 1-4 phr.

The results indicate that the physical properties initially improve as the crosslink density increases, and after achieving a maximum value they then decrease with further increase in the crosslink density. The maximum hot tear strength is obtained at lower dose than tensile strength which coincides with the SBR. Figure 5-29 shows that stress-strain comparison of RBR-20-B to BR-0150. Without any doubt, RBR-20-B is superior to BR.

5.4.4.3. Heat Treatment. Heat treatment of irradiated pure syndiotactic-1,2-PBD has been investigated at the UBE Hirakata Laboratory. A great change in mechanical properties is obtained by irradiation and further improvements are observed after post-irradiation heat treatment above the melting temperature. Heat treatment is found to bring about a remarkable increase in hardness, tensile strength, and elastic modulus.

The RBR-heat treated (RBR-HT) series was heated at 90°C, 120°C, and 200°C for 0.5, 1, and 1 hr respectively in nitrogen atmosphere after a 10 Mrad dose irradiation. Tensile strength, 200 percent modulus, and percent elongation are presented in Table 5-20. Figure 5-30 shows the tensile strength versus RB-820 pphr at different heat treatment levels. Normally it decreases as temperature increases except for the RBR-B-HT-200. This is in agreement with the results from Blow. The percent elongation against RB-820 is plotted in Figure 5-31 and a similar tendency is obtained. The most interesting observation is seen in Figure 5-32 which shows the 200 percent modulus versus RB820 pphr. In this figure the first two curves of 90°C and 120°C have the same trend as mentioned before, but the 200°C heat treatment modulus jumps to twice that of the non-heat treated samples. This phenomenon was observed at the UBE Laboratory. Analyses of infrared spectra of heat treated and untreated samples show that the vinyl groups are seen to decrease while the CH₂ groups increase upon heat treatment (Figure 5-33). Obviously, these structural changes can be assigned to be essentially a cyclization reaction in which the vinyl group plays an important role. Figure 5-31 also shows that an increase in RB-820 concentration increases the 200 percent modulus which gives more evidence of intermolecular cross-linking.

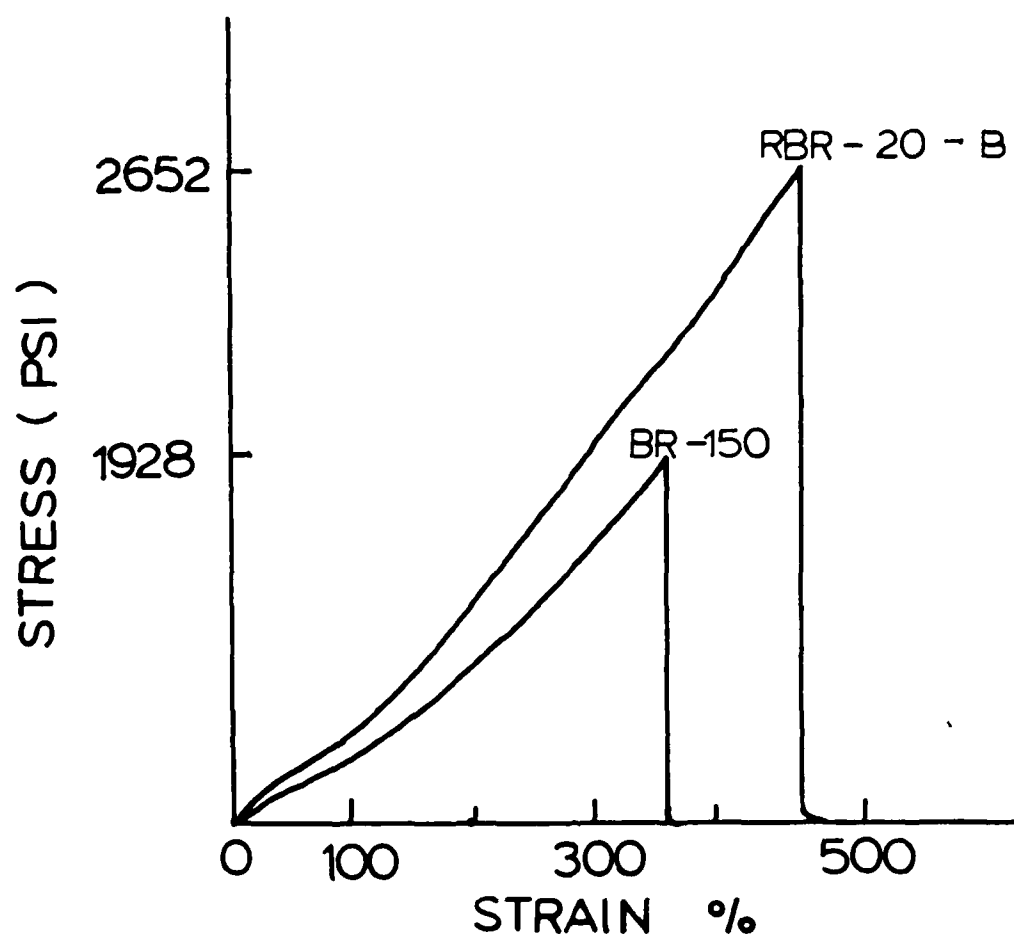


Figure 5-29. Stress-Strain Comparison of RBR-20-B to BR-150

	<u>RBR-20-B</u>	<u>BR-150</u>
Tensile Strength (psi)	2652	1928
200% Modulus (psi)	835	789
Elongation (%)	475	350

Table 5-20. Mechanical Properties of RBR-HT Series

Mechanical Properties	(1)			(2)			(3)		
	RBR-A HT-90	RBR-B HT-90	RBR-C HT-90	RBR-D HT-90	RBR-A HT-120	RBR-B HT-120	RBR-C HT-120	RBR-D HT-120	RBR-A HT-200
200% Modulus (psi)	390 ±20%	236	309	304	345	220	301	287	509
Tensile Strength (psi)	1001 ±12%	951	1087	1252	874 ±8%	777 ±23%	1061	1013	657
Ultimate Elongation (%)	340	435	425	493	353	423	433	470	255
									577
									555
									702
									±16%
									744
									842
									±10%
									240

Note: (1) "RBR-A-HT-90" means Series A under post irradiation heat treatment of 90°C, 1 hour.

(2) "RBR-A-HT-120" means Series A under post irradiation heat treatment of 120°C, 1 hour.

(3) "RBR-A-HT-200" means Series A under post-irradiation heat treatment of 200°C, 1 hour.

(4) All the HT series have a 10 Mrad dose irradiation under nitrogen atmosphere.

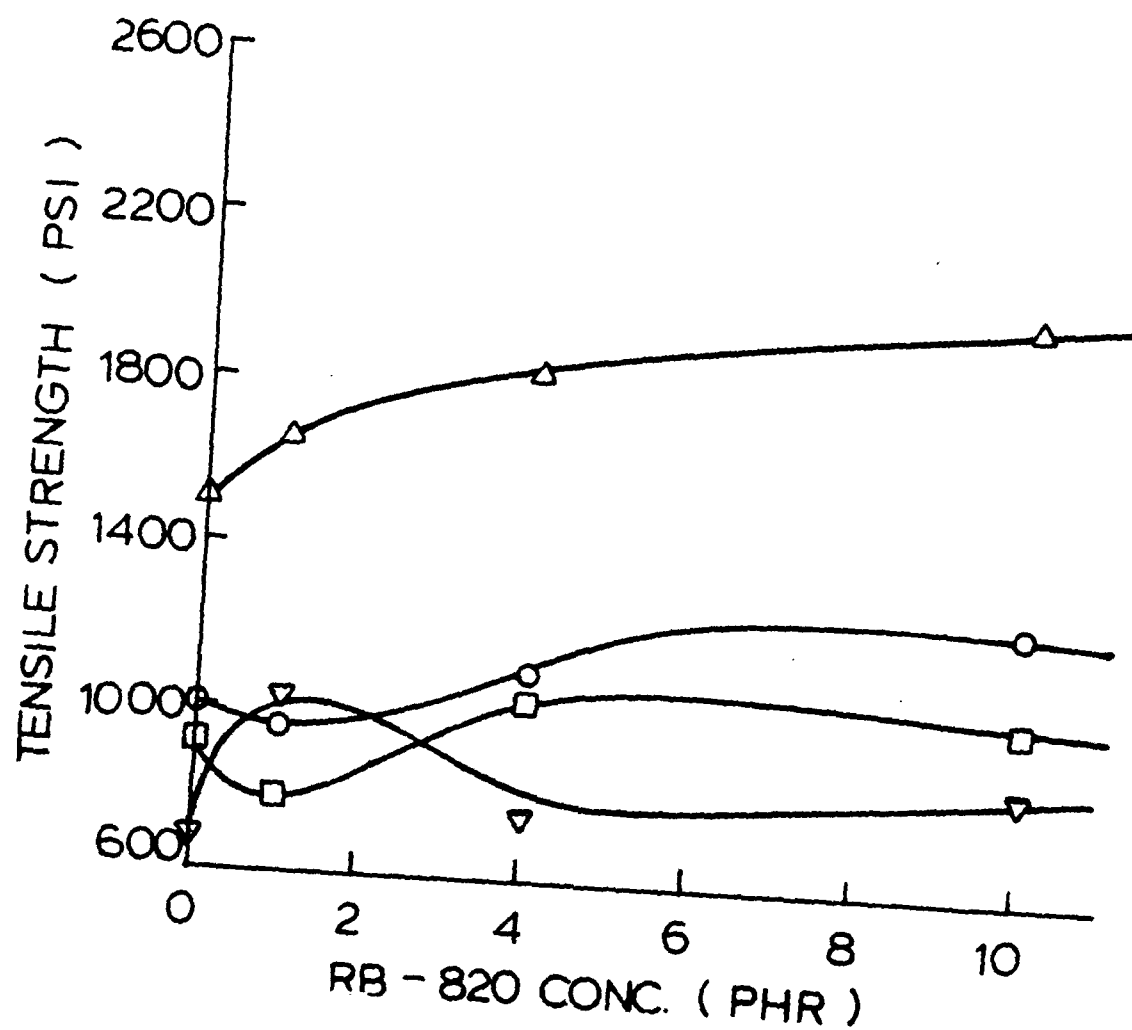


Figure 5-30. Tensile Strength vs. RB-820 Conc. BR (Heat Treatment)

- (Δ) - ambient temperature
- (\circ) - 90°C, $\frac{1}{2}$ hour
- (\square) - 120°C, 1 hour
- (∇) - 200°C, 1 hour

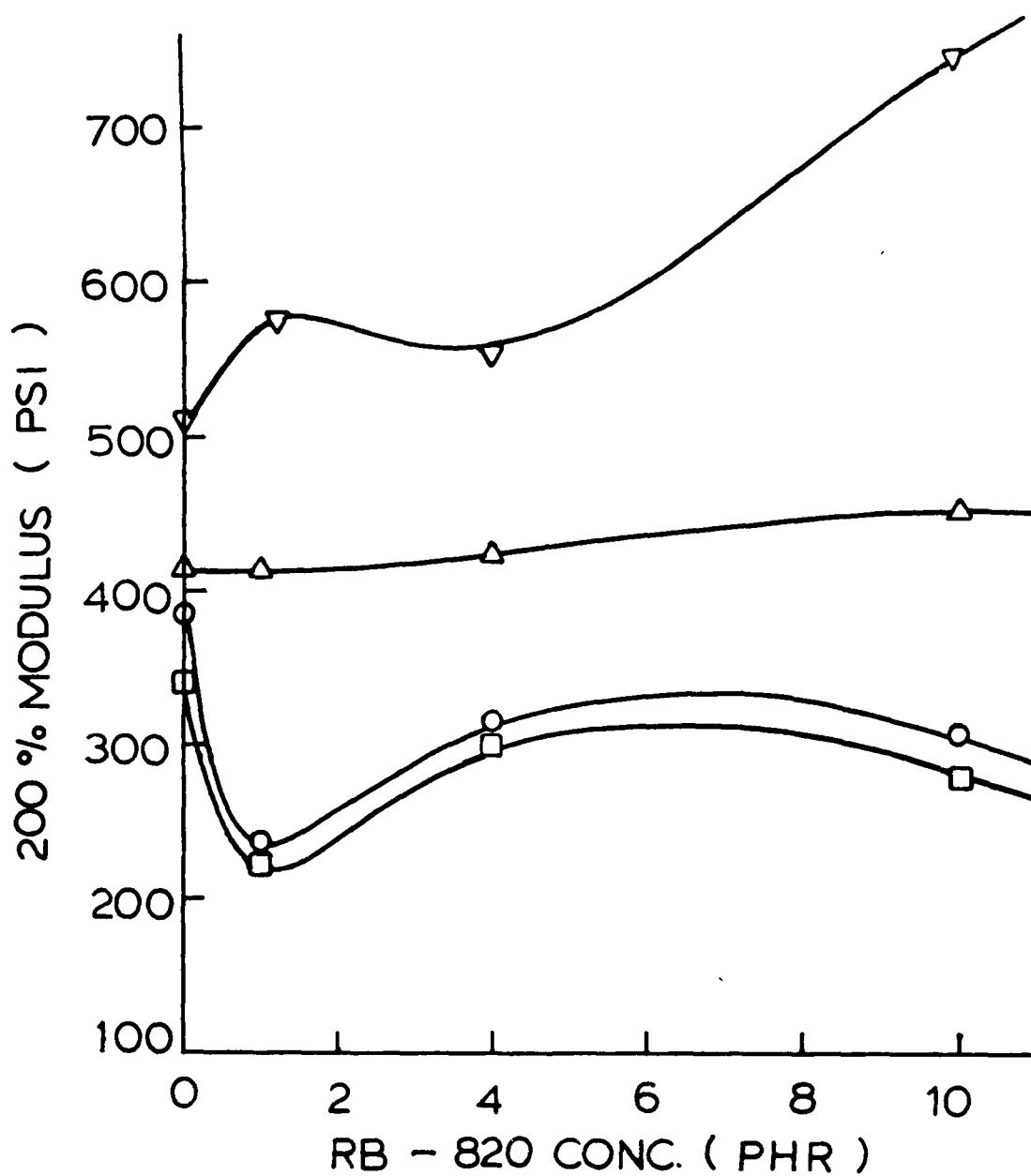


Figure 5-31. 200% Modulus vs. RB-820 Conc. BR (Heat Treatment)

- (Δ) - ambient temperature
- (○) - 90°C, 1/4 hour
- (□) - 120°C, 1 hour
- (▽) - 200°C, 1 hour

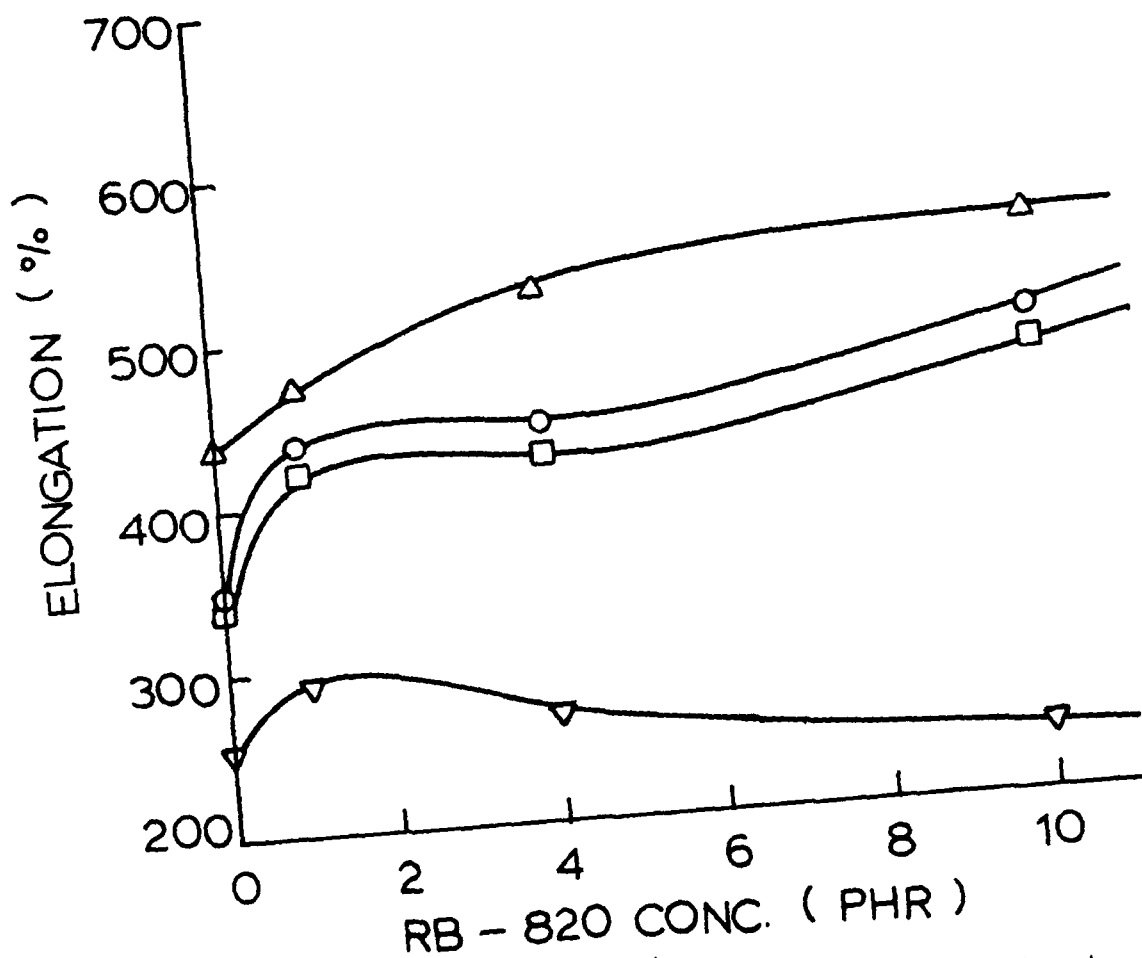


Figure 5-32. Elongation % vs. RB-820 Conc. BR (Heat Treatment)

- (Δ) - ambient temperature
- (○) - 90°C, 1/2 hour
- (□) - 120°C, 1 hour
- (▽) - 200°C, 1 hour

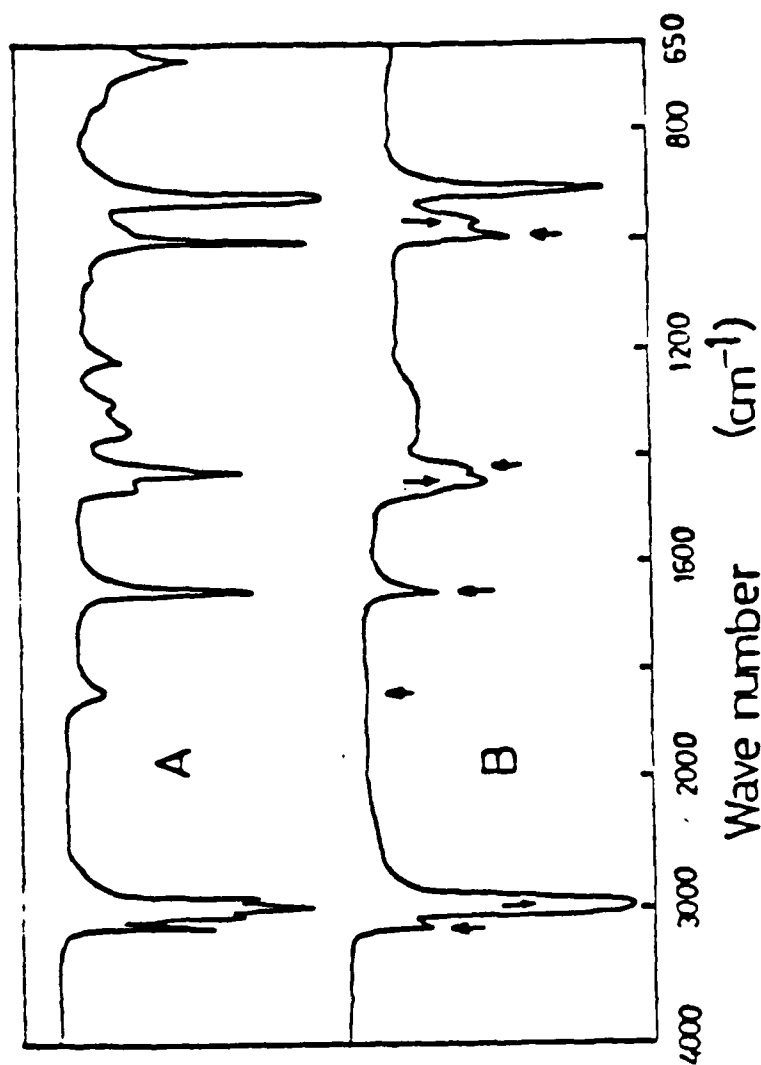
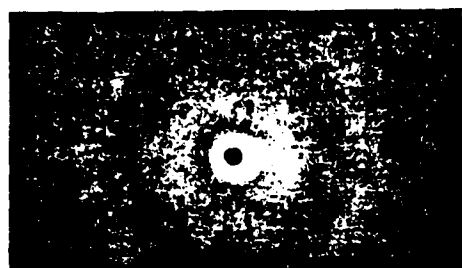


Figure 5-33. Change in infrared spectrum of the irradiated syndio-1,2-PB by heat treatment: sample, B, without BHT; irradiation, $1.0 \mu\text{A}/\text{cm}^2$, 4 Mrad, in vacuo; (A) untreated; (B) heat treatment in vacuo, 275°C , 4.0 hr.

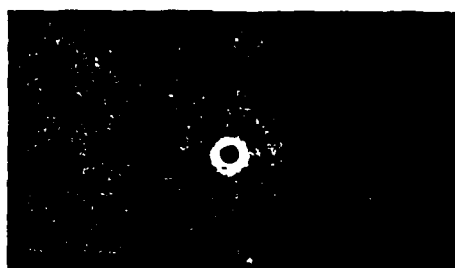
One additional noteworthy observation from Figure 5-19 is that the maximum tensile strength of the radiation-cured RBR sample is 10-15 percent higher than the sulfur-cured sample. This is better than the data reported by Bohm that irradiated elastomers have tensile strength 10 percent lower than that of equivalent sulfur-cured samples. This high tensile strength is probably caused by the crystalline domain of R dispersed in the BR amorphous matrix (as discussed earlier in this section).

5.4.4.4. X-Ray Diffraction. This effect can be illuminated by the X-ray diffraction pattern of the BR and RBR series. Figure 5-34 shows these patterns. The members of the BRS series show the amorphous halo ring for E.R. = 1, 2, 3, and 4; the halo gets dimmer as the extension ratio increases. A surprising result is obtained with the RBR-D series. For extension ratio higher than 2, diffraction spots appear on the equator, the spots getting clearer as the ratio increases. This is excellent evidence that the deformation accelerates crystallization of BR matrix so that when irradiated RBR elastomer confronts the foreign stress, the strain induces the crystallinity. The stronger the foreign stress, the higher the crystallinity. This leads to the requirement of a higher tensile stress and tear stress until break. A further valuable insight is gained when the X-ray diffraction patterns of RBR sulfur-cured formulation B (RBRS-B) and RBR-formulation B (RBR-B) series are compared. The RBR-B series show the diffraction spots on the equator from E.R. = 2, the same effect as RBR-D series, but for RBRS-B series no such effect happened. This is great evidence that the radiation-curing technique has the ability to increase the strain-induced crystallinity while the sulfur-curing system does not. These results were expected as confirmation that the ability of R to induce crystallinity in BR upon extension is the major reason for the improved physical properties of RBR over BR. The unexpected result is that drawn RBRS yields no crystallinity, indicating that the sulfur crosslinks interfere with the formation of crystalline domains in the drawn samples. It is indeed regrettable that these developments did not come at a point when they could be used to specify the formulation for the 200 pad assemblies to be delivered by June 30. It should be emphasized that the achievement of crystallinity in physically blended, radiation-cured elastomers (while sulfur curing inhibits crystallization) is a significant discovery in the morphological studies of radiation curing for pad application. A disclosure document for this new material has been submitted to the U.S. Patent Office. We are considering a patent application. (see APPENDIX A)

5.4.5. Dose Requirements for Partially Sulfur Cured Pads. Firestone informed us at a very late date in the contract



| BRS E.R. = 1



| RBR E.R. = 1



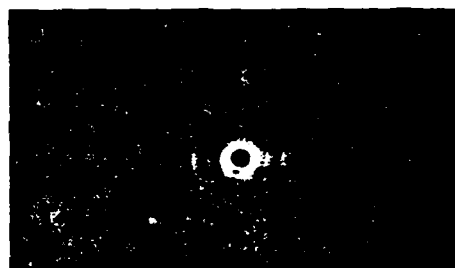
| BRS E.R. = 2



| RBR E.R. = 2



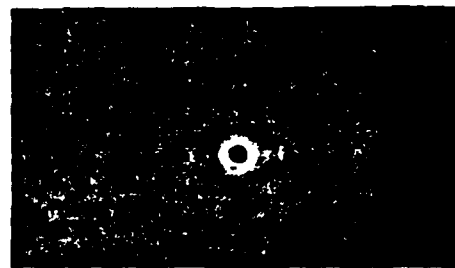
| BRS E.R. = 3



| RBR E.R. = 3

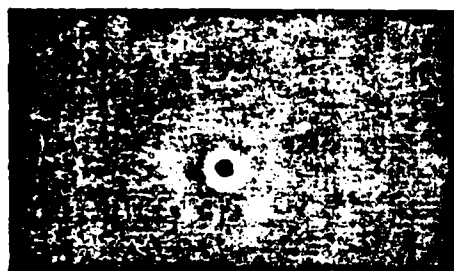


| BRS E.R. = 4



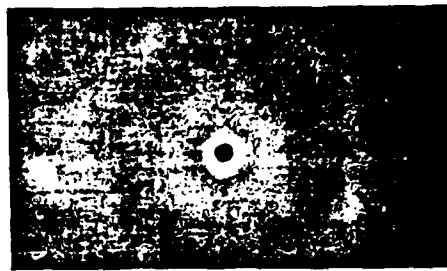
| RBR E.R. = 4

Figure 5-34. X-Ray Diffraction Patterns



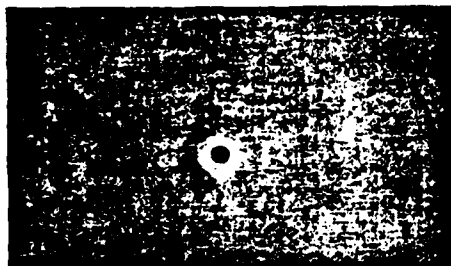
RBRS-B

E.R. = 1



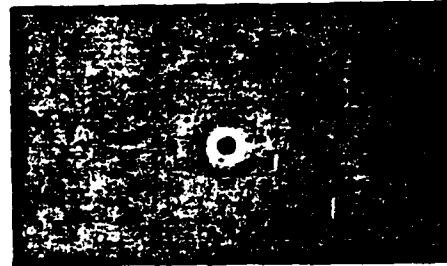
RBR-B

E.R. = 1



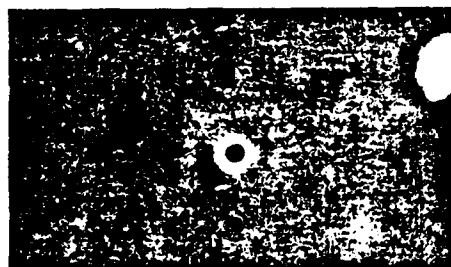
RBRS-B

E.R. = 2



RBR-B

E.R. = 2



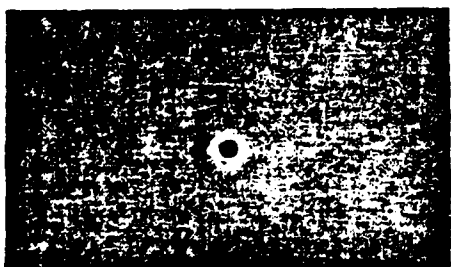
RBRS-B

E.R. = 3



RBR-B

E.R. = 3



RBRS-B

E.R. = 4



RBR-B

E.R. = 4

Figure 5-34. (CONTINUED) X-Ray Diffraction Patterns

that they found it necessary to use one-third of their normal sulfur loading to insure that the pads would be removable from the molds without distortion. This left us with the task of determining the adhesion between pad and backing plate as well as the dose required to complete the cure which the 0.5 phr sulfur loading had commenced. The first step was to determine the mechanical properties of partially cured SBR. These are reported in Table 5-21.

The second step was to irradiate our tank-pad model compound, 26-3, which seemed to fairly well represent the actual pads, to 5 Mrad dose increments and measure the resulting mechanical properties. These are reported in Table 5-22 and plotted in Figure 5-35 through 5-38. Once the tank-pads had been prepared by Firestone, only days before the irradiations were scheduled, we were able to irradiate samples from actual pads to dose increments and measure their mechanical properties to compare with the model compound data. This data is in Table 5-23 and is also plotted in Figure 5-35 through 5-38.

From these data it was decided that a dose of 10 Mrads would be a reasonable initial dose to complete the cure of the tank-pads. At this dose, the 200 percent modulus is over 400 psi, the tensile strength is approaching 3,000 psi and the hot tear strength has reached its optimum plateau. However, we brought back some of the pads irradiated to 10 Mrads and performed additional mechanical properties test as well as irradiating the pads to higher dose increments by electron beam at CRC. (see Table 5-24 and Figure 5-35 through 5-38). We concluded that it would be more reasonable to irradiate one-half of the 200 pads an additional 5 Mrads. The hot tear strength remains high and both 200 percent modulus and tear strength move into what appears to be a more optimum range. As a result, we sent two sets of pads to Yuma for field testing. This should yield the maximum level of information from the field test.

Table 5-21. Mechanical Properties - Partial Sulfur Cure Only

	Fully Cured Analogs 15 SBR 26 etc	(1) NB-907'	(2) 26-3	(3) TP-S
200% Modulus (psi)	550- 750	275	275	215
Tensile strength (psi)	2800-3800	1790	2120	2050
% Elongation	500- 525	820	825	780
Hot Tear (lb/in)	115- 145	---	97	---
R.T. Tear (lb/in)	300- 315	---	---	---
Hardness (IRHD)	65- 70	50	---	---
B. Rebound (%)	35- 40	32	---	---

NOTES: (1) A Firestone formulation similar to 15 SBR 26 with 1/3 of normal S level.
 (2) Tank pad model compound: 0.5 phr S; 0.1 phr DTUD
 (3) Average data from actual pads cured only with sulfur (slices from rubber face $\frac{1}{2}$ of pad).

Table 5-22. 26-3 Plus Radiation Cure

	0 Mrads	5 Mrads	10 Mrads	15 Mrads	20 Mrads	25 Mrads	30 Mrads
Tensile Strength, psi	2120	2636	3070	3395	3580	3770	3680
200 % Modulus, psi	275	370	500	655	780	955	1030
Elongation, %	825	740	665	610	570	525	490
Hot Tear, lb/in, (250°F, 10 min)	97	175 ±15	180 ±5	182 ±6	146 ±24	183	107

Table 5-23. Tank Pads Plus Gamma Rays

	0 Mrads	5 Mrads	10 Mrads
Tensile Strength, psi	2050	2500	2850
200% Modulus, psi	215	265	342
Elongation, %	780	670	640
Hot Tear, lb/in, 250°, 10 min		153	169

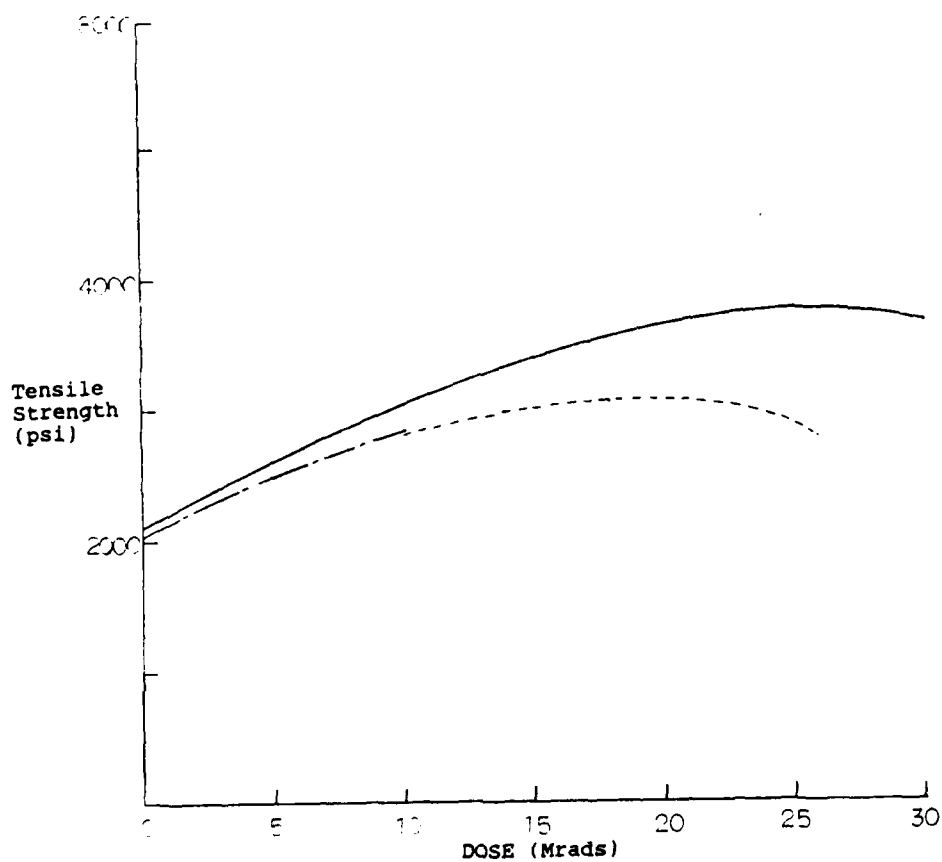


Figure 5-35. Tank Pad and Model Compound - Tensile Strength

— 26-3
--- TP plus gammas
- · - TP plus e⁻ beam

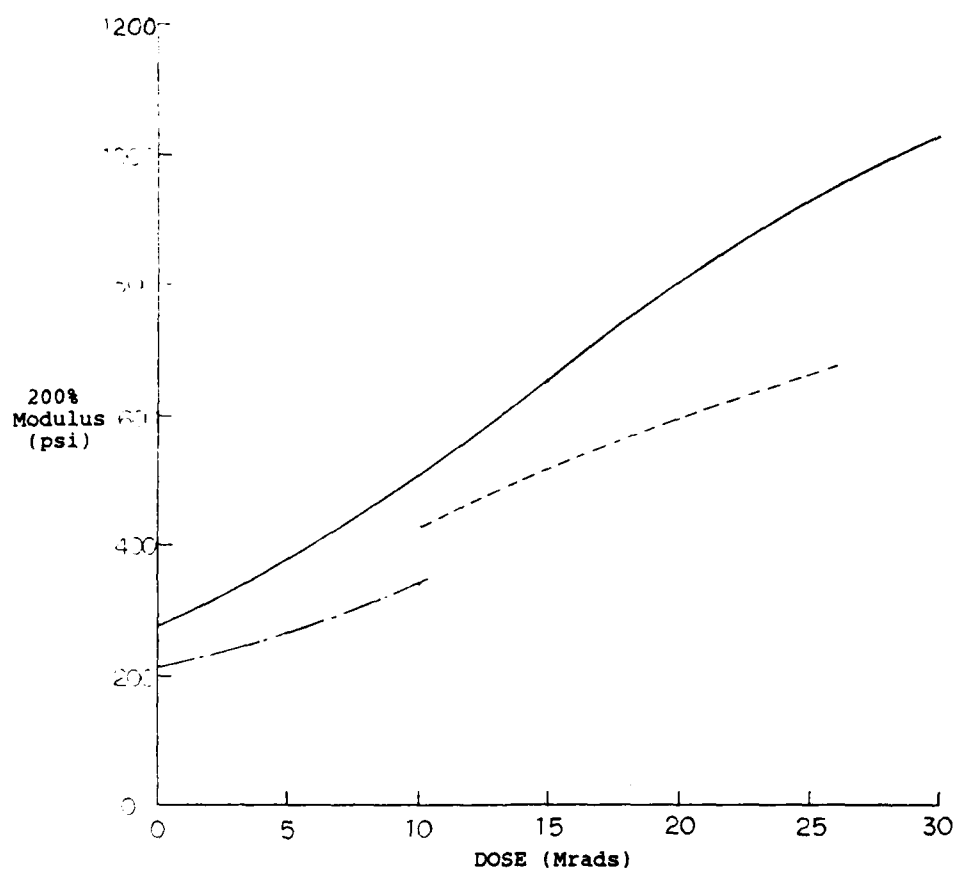


Figure 5-36. Tank Pad and Model Compound - 200% Modulus

————— 26-3
 - - - - - TP plus gammas
 - · - · - TP plus e⁻ beam

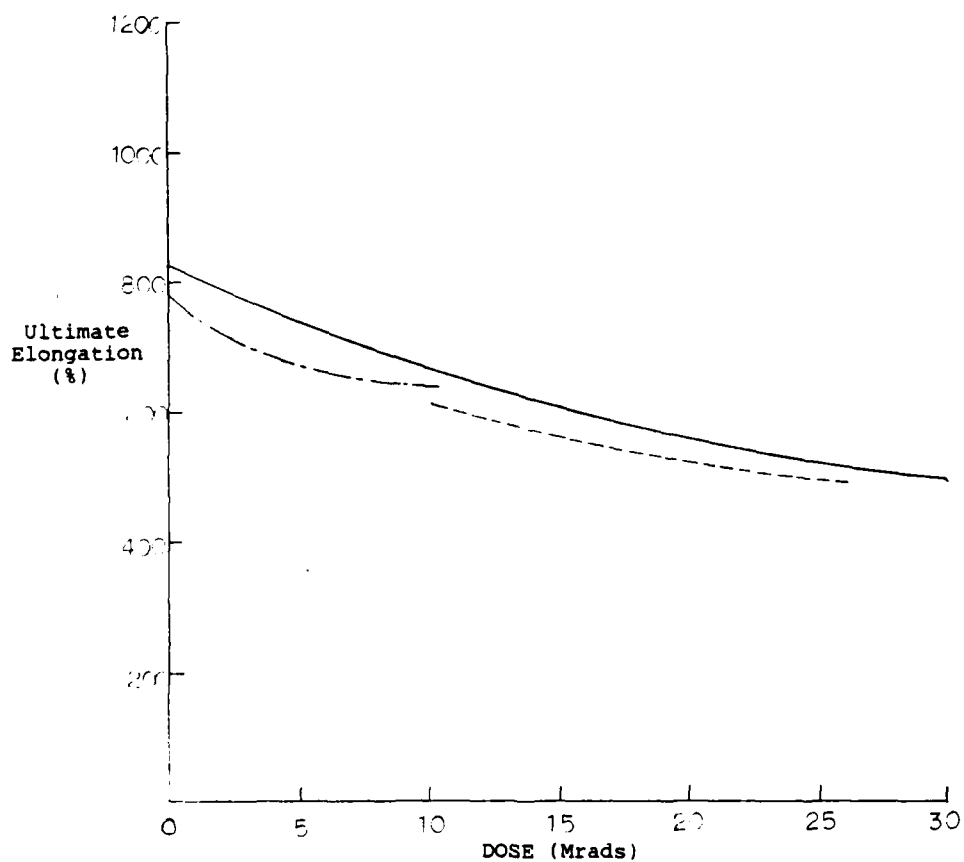


Figure 5-37. Tank Pad and Model Compound - Ultimate Elongation

————— 26-3
 - - - - - TP plus gammas
 TP plus e⁻ beam

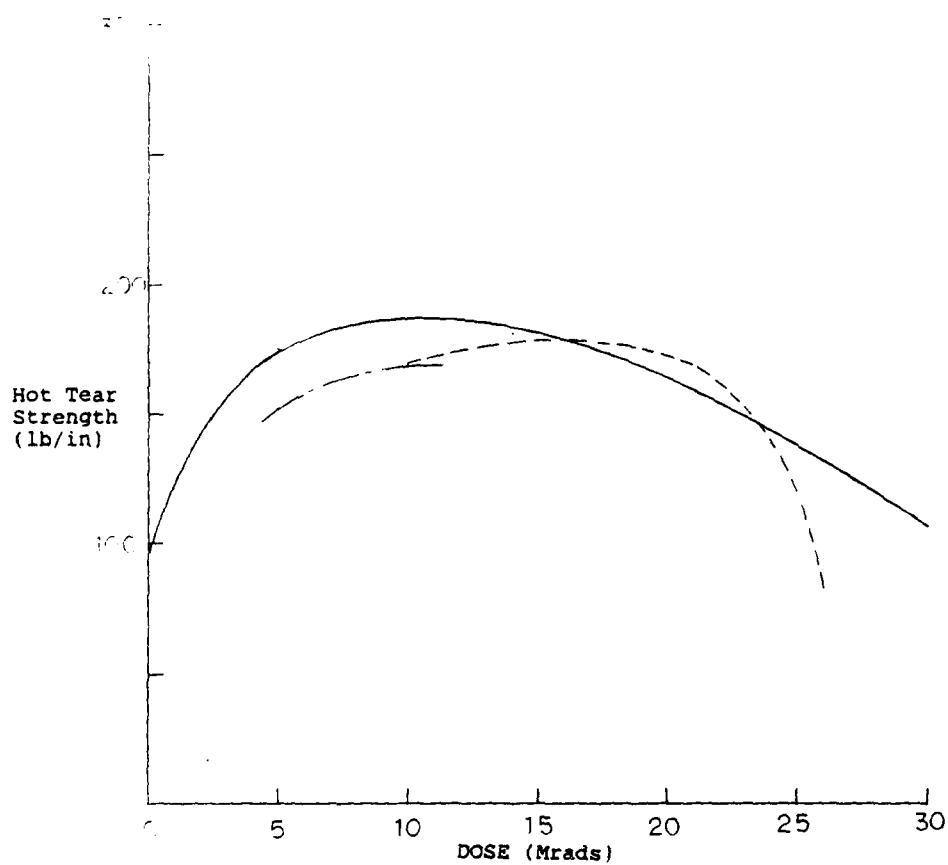


Figure 5-38. Tank Pad and Model Compound - Hot Tear Strength

————— 26-3

----- TP plus gammas

----- TP plus e⁻ beam

Table 5-24. Tank Pads Plus Electron Beam

	10 Mrad (IRT)	14 Mrad (CRC)	18 Mrad (CRC)	22 Mrad (CRC)	26 Mrad (CRC)
Tensile Strength, psi	2820	3000	3055	2790	2906
200 % Modulus, psi	430	503	539	621	673
Elongation, %	610	580	560	500	485
Hot Tear, lb/in, (250°F, 10 min)	170	182	177	165	83

SELECTED BIBLIOGRAPHY

1. G.G.A. Bohm, "The Radiation Chemistry of Macromolecules", Vol. II, M. Dole, Ed., Academic Press, 1973, p. 208.
2. G.G.A. Bohm, M. DeTrano, D.S. Pearson, and D.R. Carter, Radiat. Phys. Chem., 9, 235 (1979).
3. G.G.A. Bohm and J.O. Tveekrem, Rubber Chem. and Techn., 55, 575 (1982).
4. A.N. Gent, JPS: Polymer Symposium #48, "Rubber and Rubber Elasticity", A.S. Runn, Ed., Wiley, NY 1974, p. 1.
5. D.S. Pearson, Radiat. Phys. Chem., 18 (1), 89 (1981).
6. D.S. Pearson and G.G.A. Bohm, Rubber Chemistry and Technol., 45, 193 (1972).
7. J.E. Mark, Rubber Chem. Technol., 55, 762 (1982).
8. L. Bateman, J.I. Cunneen, G.G. Moore, L. Mullins, and A.G. Thomas, "The Chemistry and Physics of Rubber-Like Substances", L. Bateman, Ed., Wiley, NY, 1963, Chapter 19.
9. A.V. Tobolsky and P.F. Lyons, J. Polym. Sci., A2, 6, 1561 (1968).
10. J. Lal, Rubber Chem. Technol., 43, 664 (1970).
11. S.D. Gehman, Rubber Chem. Technol., 42, 659 (1969).
12. V.P. Gordiyenko, N.T. Kartel, K.A. Suprunenko, V.N. Doroshenko, and A.M. Kabakchi, Vysokomol. Soedin, 17 (8), 1737 (1975).
13. W.J. Chappas & J. Silverman, J. Polym. Sci.: Polymer Letters Edition, 17, 5 (1979).
14. J. Bly, J. Ind. Irrad. Technol., 1(1), 51 (1983).
15. G.G.A. Bohm (to Firestone Tire & Rubber Co.) U.S. 4,089,360; May 1, 1978.
16. D.R. Lesuer, S.D. Santor, R.H. Cornell, and J. Patt, UCID Techn. Report #19795, April, 1983.
17. J.R. Beatty and B.J. Miksch, Rubber Chem. Technol., 55, 1531 (1982).

18. G.E. Wardell, V.J. McBrierty, and V. Marsland, Rubber Chem. Technol., 55, 1095 (1982).
19. A. Chapiro, "Polymer Handbook," 2nd Ed., pp. II-481, Wiley Interscience, New York, (1975).
20. G. G. A. Bohm, "Rubber Chemistry and Technology," Vol. 55, 575 (1982).
21. J. Silverman, F.J. Zoepfl, J.C. Randall, and V. Markovic, Radiat. Phys. Chem., 22 (3-5), 583 (1983).
22. G. Odian, B.S. Berstein, J. Polym. Sci., Part A, 2, 2835 (1964).
23. R.F. Grossman, Radiat. Phys. Chem., 9, 659 (1977).
24. A. von Raven and H. Heasinger, J. Polym. Sci., Polym. Chem. Ed., 12, 2255 (1974).
25. JSR RB-820 Catalog.
26. Motowo Takayanagi, "Micromechanics in Heterophase Rubber Systems," reported at IISRP, Hong Kong, (1978).
27. L. E. Nielsen and F. D. Stockton, J. Poly. Sci., A1, 1985 (1963).
28. A. V. Tobolsky, "J. Chem. Phys.," 37, 1139 (1962).
29. C. M. Blow, "Rubber Technology and Manufacture," 2nd Ed., Butterworth Science, Boston, MA, 99 (1982).
30. H. Okamoto and T. Iwai, "Radiat. Phys. Chem.," Vol. 18, No. 3-4, 407 (1981).
31. Byron J. Lambert, Initial Mechanical Property Tests of Radiation Cured SBR Formulations, 23 (1985).
32. Whelan Lee, Developments in Rubber Technology-2, 40, (1979).
33. C. M. Blow, "Rubber Technology and Manufacture," 2nd Ed., Butterworth Scientific, Boston, MA, 135 (1982).

APPENDIX A

DISCLOSURE DOCUMENT FOR RADIATION CURE OF BR
WITH SYNDIOTACTIC-1,2-POLYBUTADIENE

DISCLOSURE DOCUMENT

Radiation Cured Blend of Butadiene Rubber
and Syndiotactic Poly (1,2 Butadiene)

We claim the invention of a new elastomer. It is composed of poly (cis-1,4-butadiene), commonly known as butadiene rubber (BR), blended with a small concentration of poly (syn 1,2 butadiene) and cured by ionizing radiation. Other additives commonly used in the formulation and processing of rubber (carbon black, antioxidants, antiozonants, etc.) may also be present. However, the use of chemical crosslinking agents (sulfur, peroxides, etc.) is unnecessary, although a small concentration may be useful in the molding operation to reduce cold flow.

The new elastomer has physical properties markedly superior to those of sulfur-cured blends of the two components cited above, and to those of sulfur cured BR as well. This is particularly true for such automotive applications as pads for military tank track.

BR filled with carbon black is an excellent elastomer insofar as its heat dissipation properties are concerned. However, its low tensile strength and hot tear strength render it unsuitable as a pad for track of a military tank. The major reason for the failings of BR is that there is little or no crystal formation in extended BR up to the break point. The thermoplastic additive syndiotactic poly 1, 2 butadiene (R) is

AD-A174 455

EVALUATION OF RADIATION TECHNIQUES FOR IMPROVING THE
MECHANICAL PROPERTIES. (U) MARYLAND UNIV COLLEGE PARK
LAB FOR RADIATION AND POLYMER SCIE.

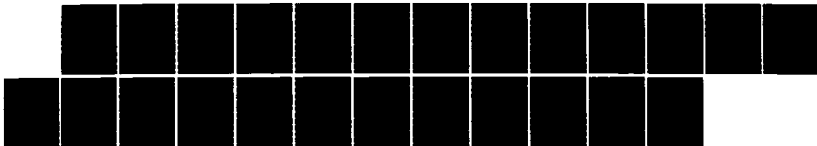
2/2

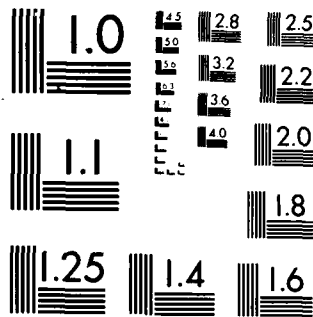
UNCLASSIFIED

B J LAMBERT ET AL. OCT 86 TACOM-TR-13215

F/G 11/10

NL





MICROCOPY RESOLUTION TEST CHART
NATIONAL BUREAU OF STANDARDS-1963-A

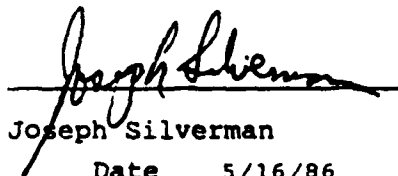
semi-crystalline. Also the pendant vinyl groups on R make it an excellent candidate as a sensitizer for crosslinking. Still further, the syndiotactic arrangement tends to inhibit intra-chain cyclization relative to the formation of inter-chain links. We find that a combination of sulfur and an accelerator performs the expected cure in R-BR blends. Also in blends without these two additives 10-20 Mrad doses of ionizing radiation also produce complete cures. However, our x-ray diffraction studies show that the sulfur-cured blends exhibit no crystallinity even at an extension ratio of 4, while the radiation cured blend has readily detectable crystallinity at extension ratios ≥ 2 . As expected, the tensile strength and especially the hot tear strength of irradiated blend is superior to that of the sulfur-cured equivalent. It appears that the sulfur crosslinks unexpectedly interfere with the formation of crystalline domains in the drawn samples.

The data supporting these observations and conclusions are presented in Tables 1-4.



Kuo Jen Su

Date 5/16/86



Joseph Silverman

Date 5/16/86

APPENDIX B

THEORETICAL ACTIVATION OF IRRADIATED TANK PADS

A. Calculation of Activity

1. 3/4" plywood attenuation

$$a. R = (0.56 \text{ g/cm}^3)(3/4" \cdot 2.54 \text{ cm/in}) = 1.07 \text{ g/cm}^3 \\ = 0.53 E_{\text{attn}} - 0.106$$

$$b. E_{\text{attn}} = 2.2 \text{ MeV}$$

$$c. 12 \text{ MeV} \text{ ---}(3/4" \text{ plywood})\text{---} \rightarrow 9.8 \text{ MeV; No ACTIVATION}$$

2. 1/2" Plywood Attenuation

$$a. \text{ activation Rctn: } M_n^{55}(\gamma-n) \rightarrow M_n^{54}; E_{\text{threshold}} = 9.85 \text{ MeV}$$

b. % steel activated:

$$1. 10.6 \text{ MeV} - 9.85 \text{ MeV} = 0.75 \text{ MeV} \rightarrow x=0.037\text{cm}$$

$$2. 0.037/[1/8" \cdot 2.54\text{cm/in}] \rightarrow 12\% \text{ of steel is activated before } e^- \text{ drop below } E_{\text{threshold}}$$

c. e^- fluence (10 Mrads)

$$D = (\emptyset) \quad (s/p); \\ (\text{dose}) \quad (\text{fluence}) \quad (\text{stopping power})$$

$$\emptyset = D/(s/p) = \frac{(0.63 \cdot 10^{15} \text{ MeV/g})}{(1.5 \text{ MeV cm}^2/\text{g})} \\ = 0.42 \cdot 10^{15} \text{ e}^-/\text{cm}^2$$

d. radioactive M_n atoms (N)

$$N = (N_0) (\emptyset) (\sigma) = \\ (\#Mn/g) \quad (\text{cross section}) \\ \frac{(10^{20} \text{ Mn atoms})}{\text{g steel}} (4.2 \cdot 10^{14} \text{ e}^-/\text{cm}^2) \left(\frac{4 \cdot 10^{-27} \text{ cm}^2}{137} \right) \\ = 1.2 \cdot 10^6 \text{ Mn}^{54}/\text{g steel}$$

e. Activity

$$N'' = (N)(\text{time constant}) = (1.2 \cdot 10^6) [0.693/ \\ 313 \text{ days} \cdot 8.64 \cdot 10^4 \text{ sec/day}]$$

$$= 3 \cdot 10^{-2} \text{ decays/s-g steel [for all of 1/8" steel]}$$

$$N = (3 \cdot 10^{-2})(0.12 \frac{\text{activated steel}}{\text{unaffected steel}}) =$$

$$3.7 \cdot 10^{-3} \text{ decay/s-gm steel}$$

$$= 0.1 \text{ picocuries/g steel}$$

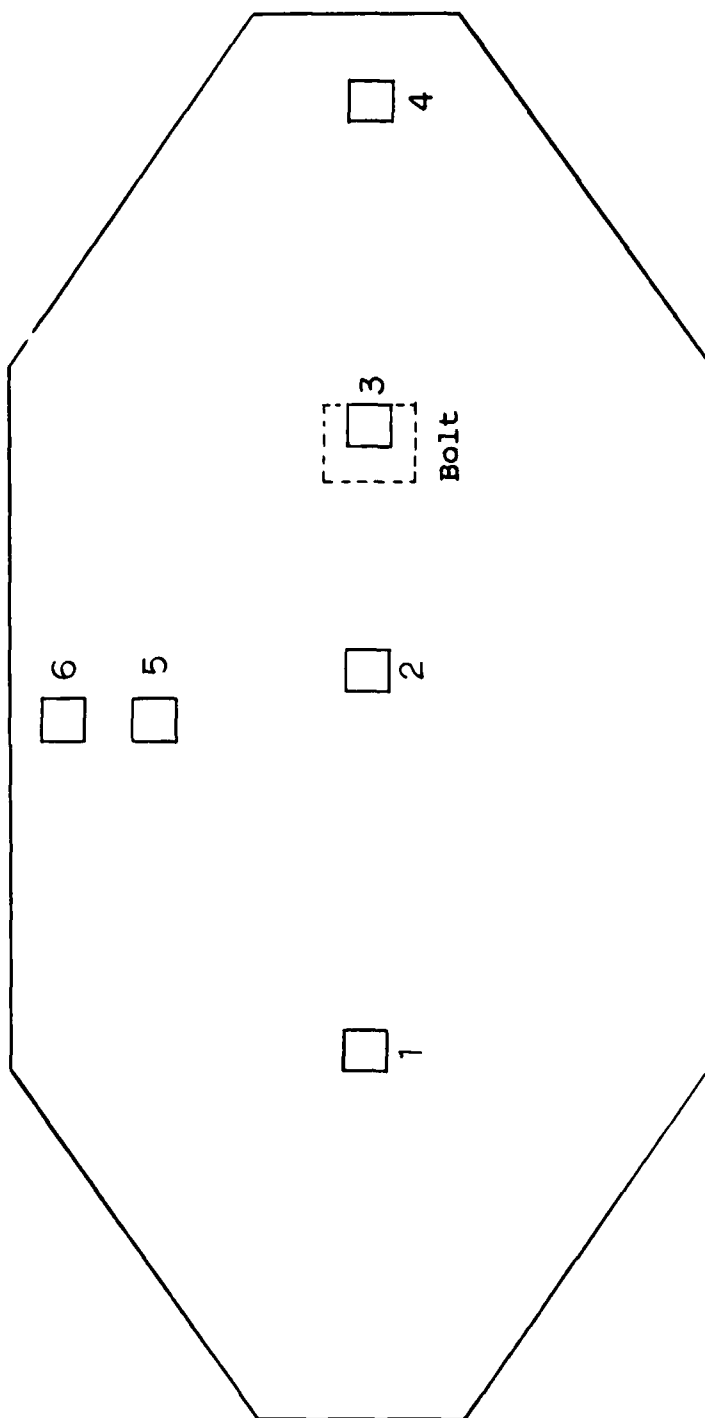
$$= 80 \text{ picocuries/pad} \quad \leftarrow$$

$$= 20 \text{ nanocuries/250 pads}$$

NOTE: NBS Data: $s/p(\text{Mn}) = 1.5 \text{ MeV cm}^2/\text{g}$; $\sigma \leq 4 \cdot 10^{-27} \text{ cm}^2$ ($\gamma-n$ 10.6-9.8 MeV); 10 Mrads = $0.63 \cdot 10^{15} \text{ MeV/g}$; fine structure cont. = 1/137 for (e^-n) reaction.

APPENDIX C

DOSE DEPTH EXPERIMENTAL MEASUREMENTS



Horizontal Positioning of Dose Depth Dosimeters

<u>Pad Level</u>	<u>Dose</u> (Mrads)	<u>Depth</u> (mm)
1.1	3.10 3.03 2.94 2.92 2.99 3.14	0.0 0.0 0.0 0.0 0.0 0.0
1.2	3.50 3.35 3.09 3.26 3.22 3.42	9.3 11.8 11.0 11.8 9.7 6.3
1.3	3.63 3.67 3.58 3.51 3.41 3.59	26.3 27.6 24.4 26.1 24.2 18.0
1.4	--- --- --- --- 3.29 3.57	--- --- --- --- 29.7 26.1
1.5	3.75 3.81 MAX 3.43 3.20 2.52 3.72	33.1 35.2 35.9 36.4 37.2 30.1
1.6	3.50 3.26 3.01 2.52 0.916 3.69 MIN	41.1 43.9 50.8 46.5 45.7 38.6

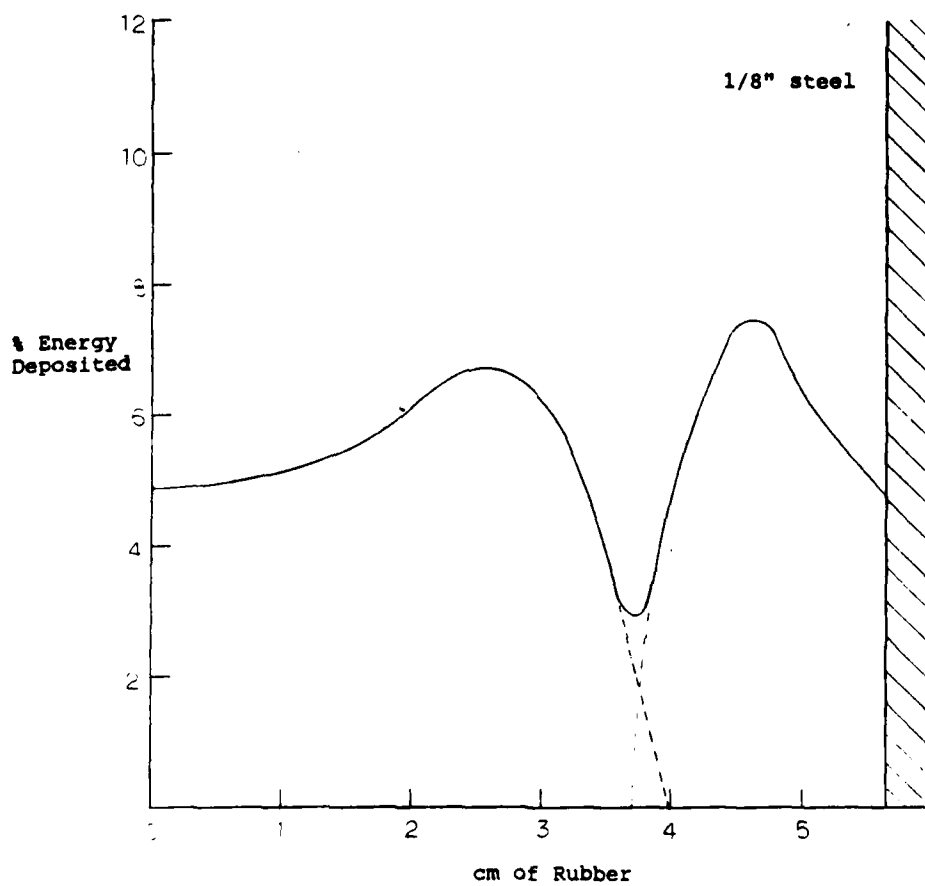
Experimental Dose Depth Data. 1/4" plywood on each side of the pad (Pad No. 1). 12 MeV electron beam.

<u>Pad Level</u>	<u>Dose</u> (Mrads)	<u>Depth</u> (mm)
2.1	<div> 3.06 2.86 2.94 2.86 2.98 3.08 </div>	<div> 0.0 0.0 0.0 0.0 0.0 0.0 </div>
2.2	<div> 3.21 3.20 3.02 3.24 3.26 3.30 </div>	<div> 9.7 11.8 7.3 13.2 13.8 8.2 </div>
2.3	<div> 3.38 3.44 3.30 3.45 3.32 3.51 </div>	<div> 20.9 23.0 19.1 23.9 23.7 18.1 </div>
2.4	<div> 3.41 3.58 3.54 3.66 3.12 3.54 </div>	<div> 29.5 31.6 32.1 33.7 34.5 28.3 </div>
2.5	<div> 3.28 3.56 MAX 3.25 3.31 2.10 3.38 </div>	<div> 36.6 39.2 38.5 41.8 42.1 37.2 </div>
2.6	<div> 3.54 3.53 MIN 2.90 3.01 0.955 3.16 </div>	<div> 41.5 42.5 45.3 44.5 47.0 47.1 </div>

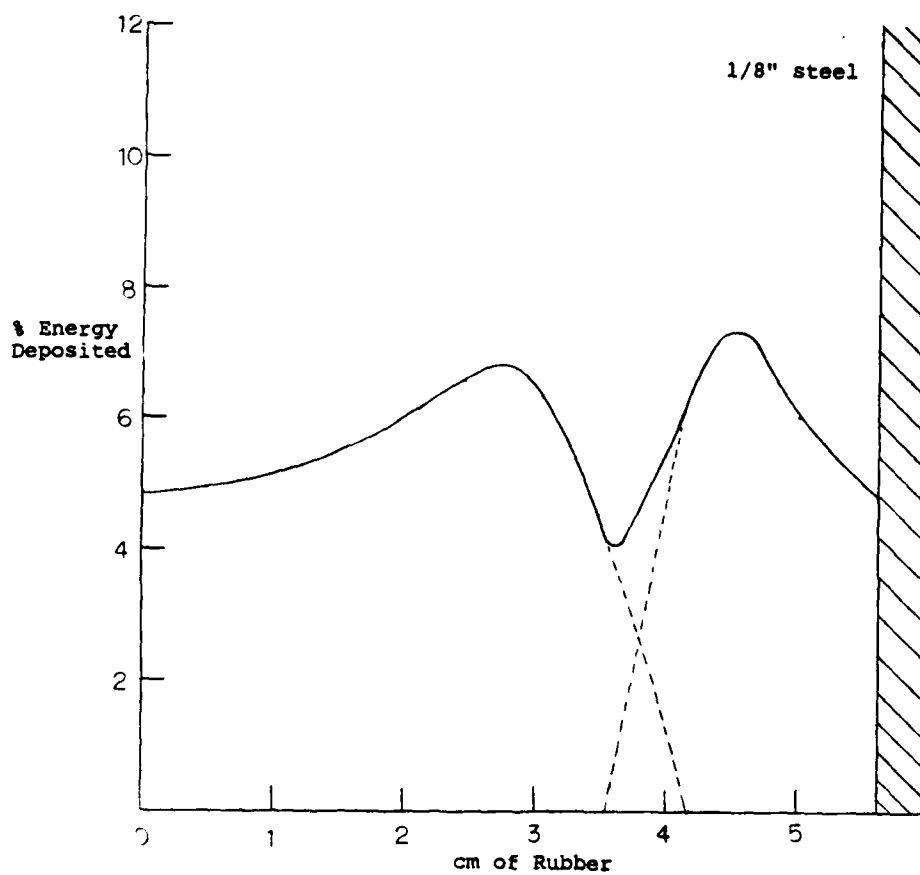
Experimental Dose Depth Data. 1/4" plywood on rubber face and 3/4" plywood on steel face (Pad No. 2). 12 MeV electron beam.

APPENDIX D

DOSE DEPTH THEORETICAL PROFILES

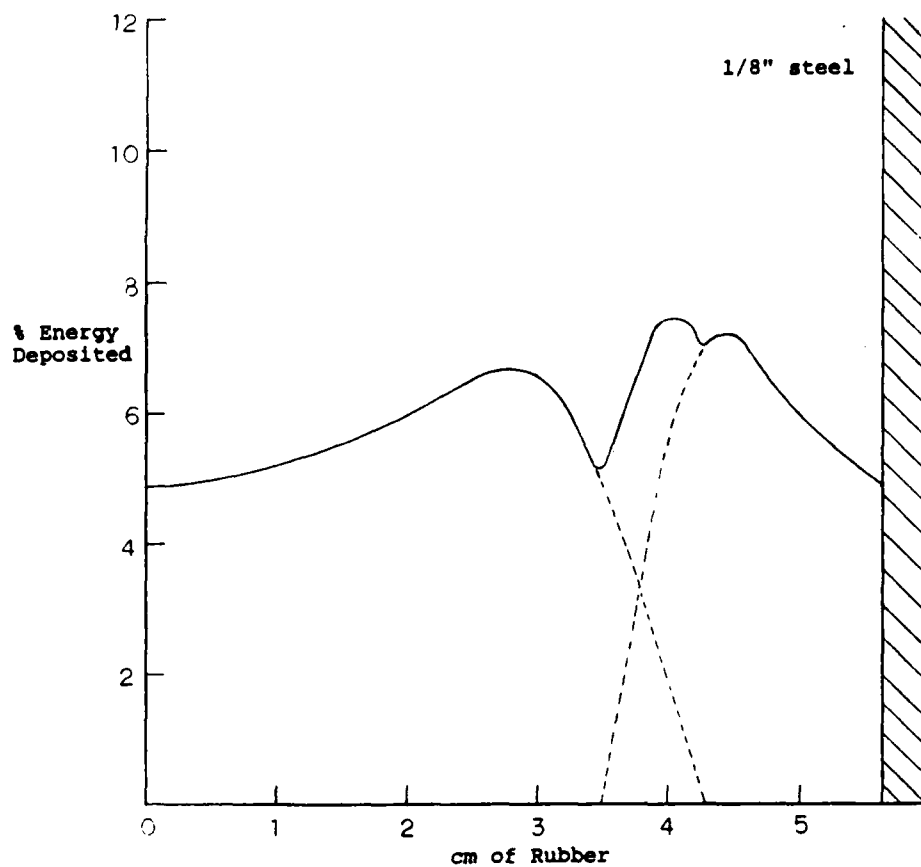


Theoretical Dose Depth Profile. 10.0 MeV
 $D_{\text{max}}/D_{\text{min}} = 2.55$ $D_{\text{max}}/D_{\text{surface}} = 1.51$



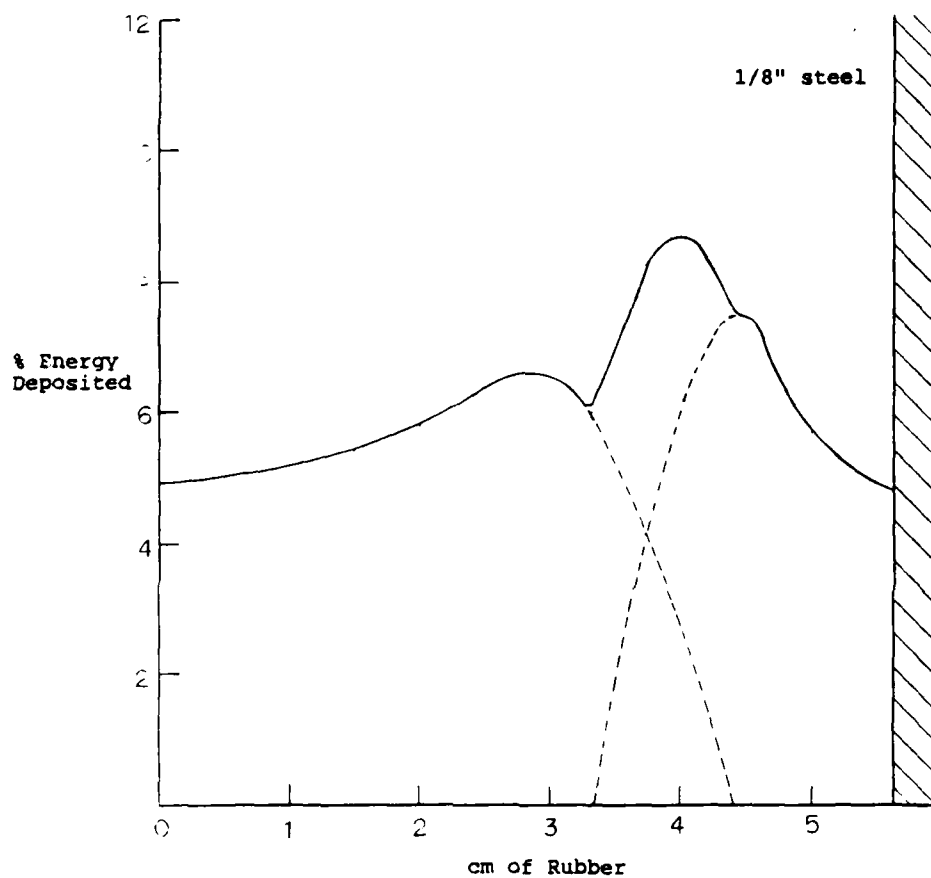
Theoretical Dose Depth Profile. 10.25 MeV

$D_{\text{max}}/D_{\text{min}} = 1.76$ $D_{\text{max}}/D_{\text{surface}} = 1.51$



Theoretical Dose Depth Profile. 10.5 MeV

$D_{\max}/D_{\min} = 1.53$ $D_{\max}/D_{\text{surface}} = 1.53$



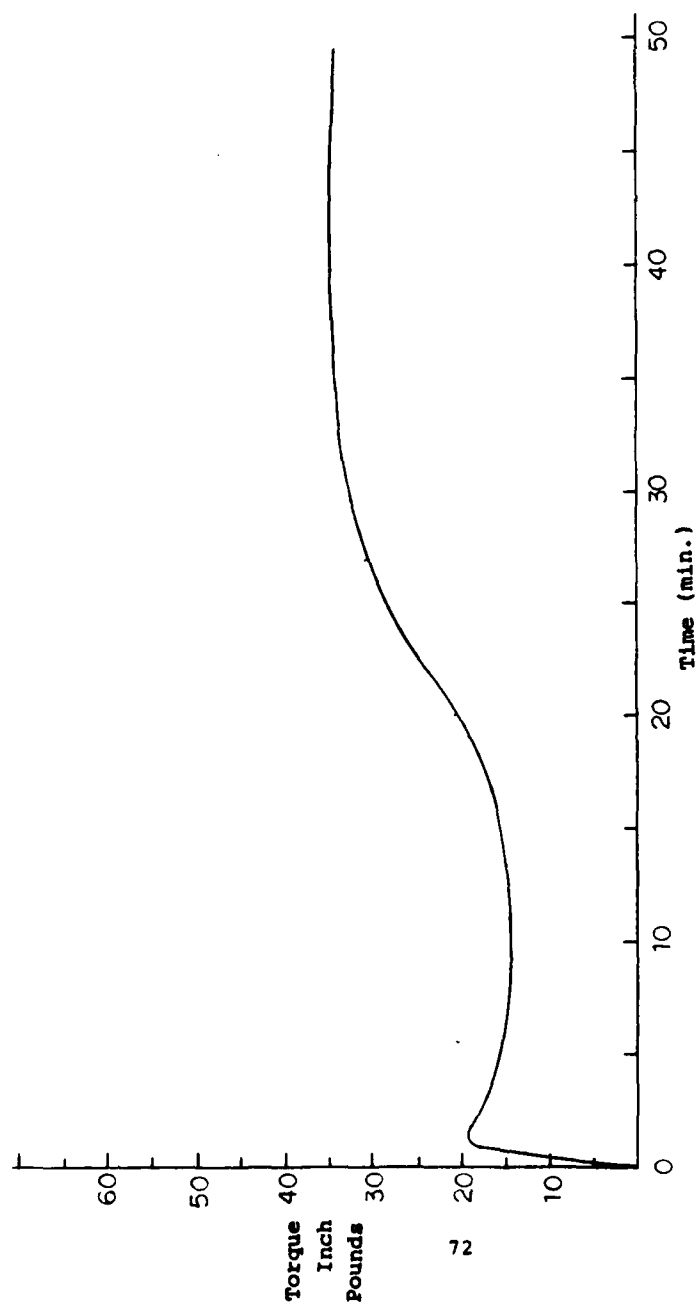
Theoretical Dose Depth Profile. 10.75 MeV
 $D_{\max}/D_{\min} = 1.80$

APPENDIX E

PAD FORMULATION AND RHEOMETER CURVE

Pad Formulation

<u>Firestone Code</u>	<u>Material</u>	<u>Weight</u>	
		<u>(pphr)</u>	<u>Weight</u>
5750 mb			
S-1500	SBR	100.00	280.00
677	N-110 carbon black	45.00	126.00
660	Zinc oxide	4.00	11.20
54	Steric acid	2.00	5.59
12,202	Antiozite 2	3.00	8.39
1205	Agerite white	0.50	1.40
4,340	Agerite resin D	1.00	2.80
		155.50	435.38
5750 mb		155.50	430.00
*EP553	Special Ingredient (DTUD)	0.10	0.28
11	Sulfur	0.50	1.38
	Accelerator (proprietary)	0.50	1.38
	Accelerator (proprietary)	0.70	1.94
		157.30	434.98



Pad Rheometer Curve

T = 380°F

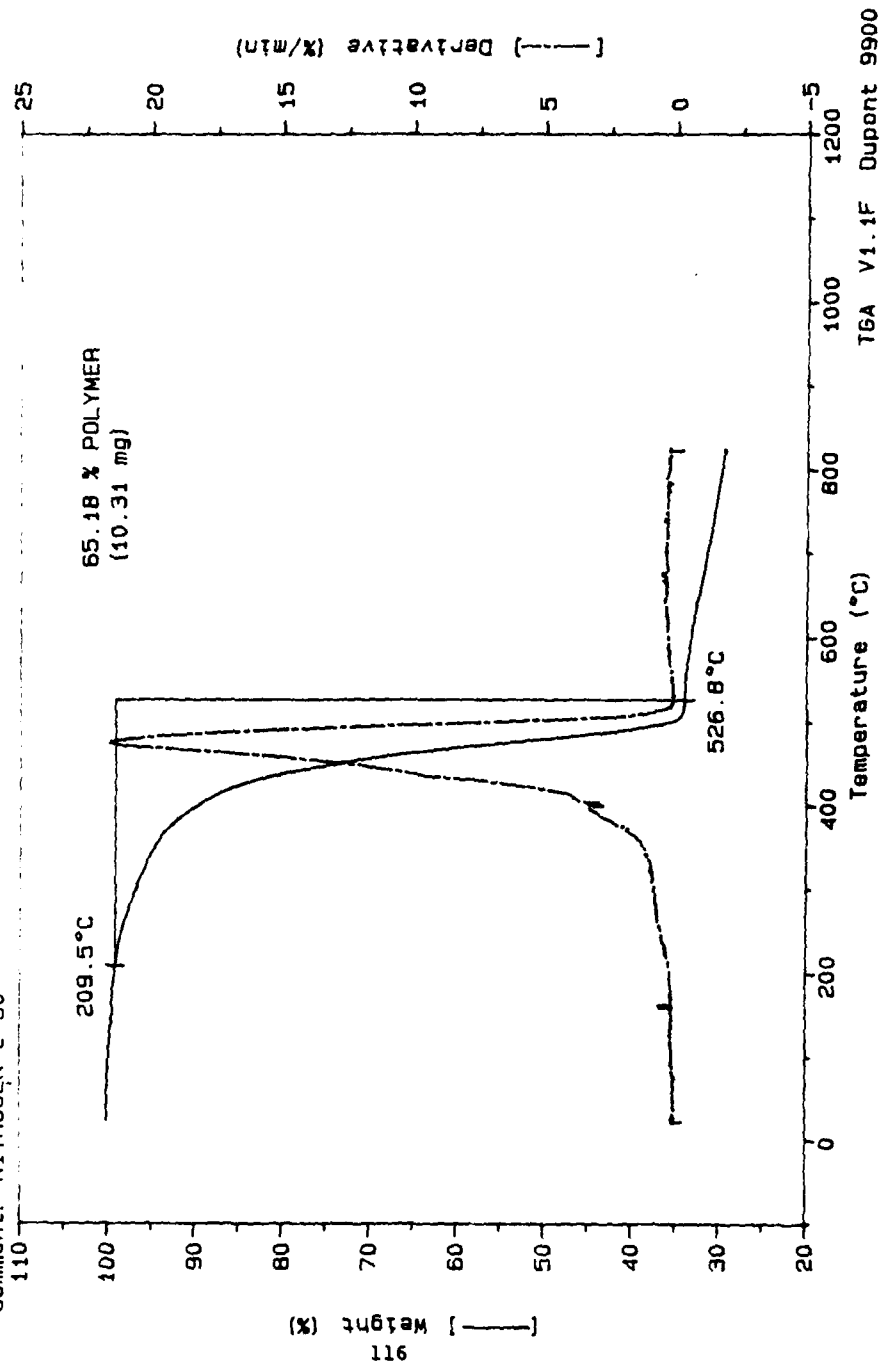
APPENDIX F

THERMAL GRAVIMETRIC ANALYSIS CURVES

Sample: 26-3-10
Size: 15.82 mg
Method: 25-800 TEMP SCAN
Comment: NITROGEN @ 50

File: BL26-3-10.01
Operator: PL
Run date: 07/16/86 13:02

TGA



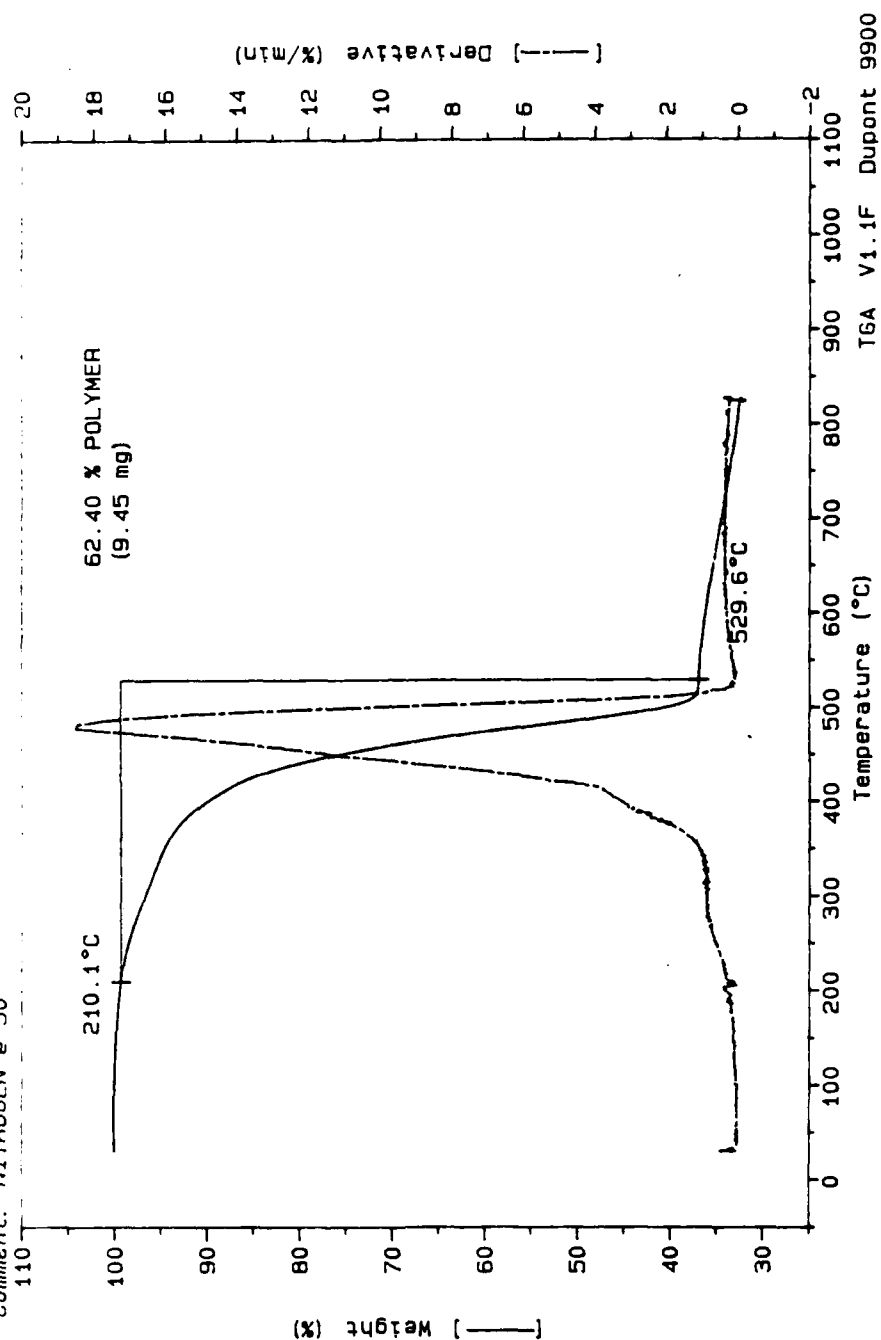
Sample: TP10
 Size: 15.15 mg
 Method: 25-B00 TEMP SCAN
 Comment: NITROGEN @ 50

File: BLTP10N/H6.01

Operator: PL

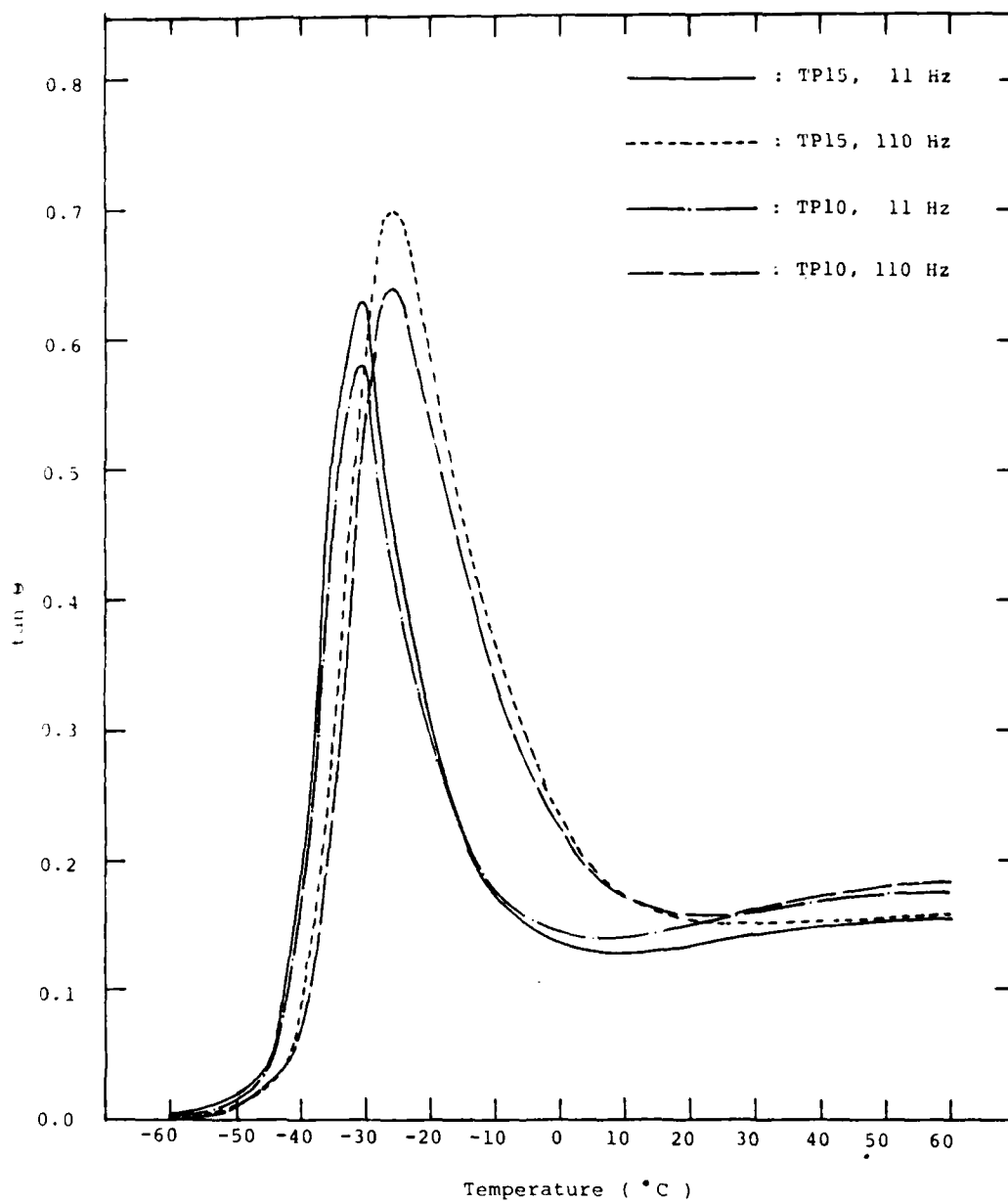
Run date: 07/16/86 10:45

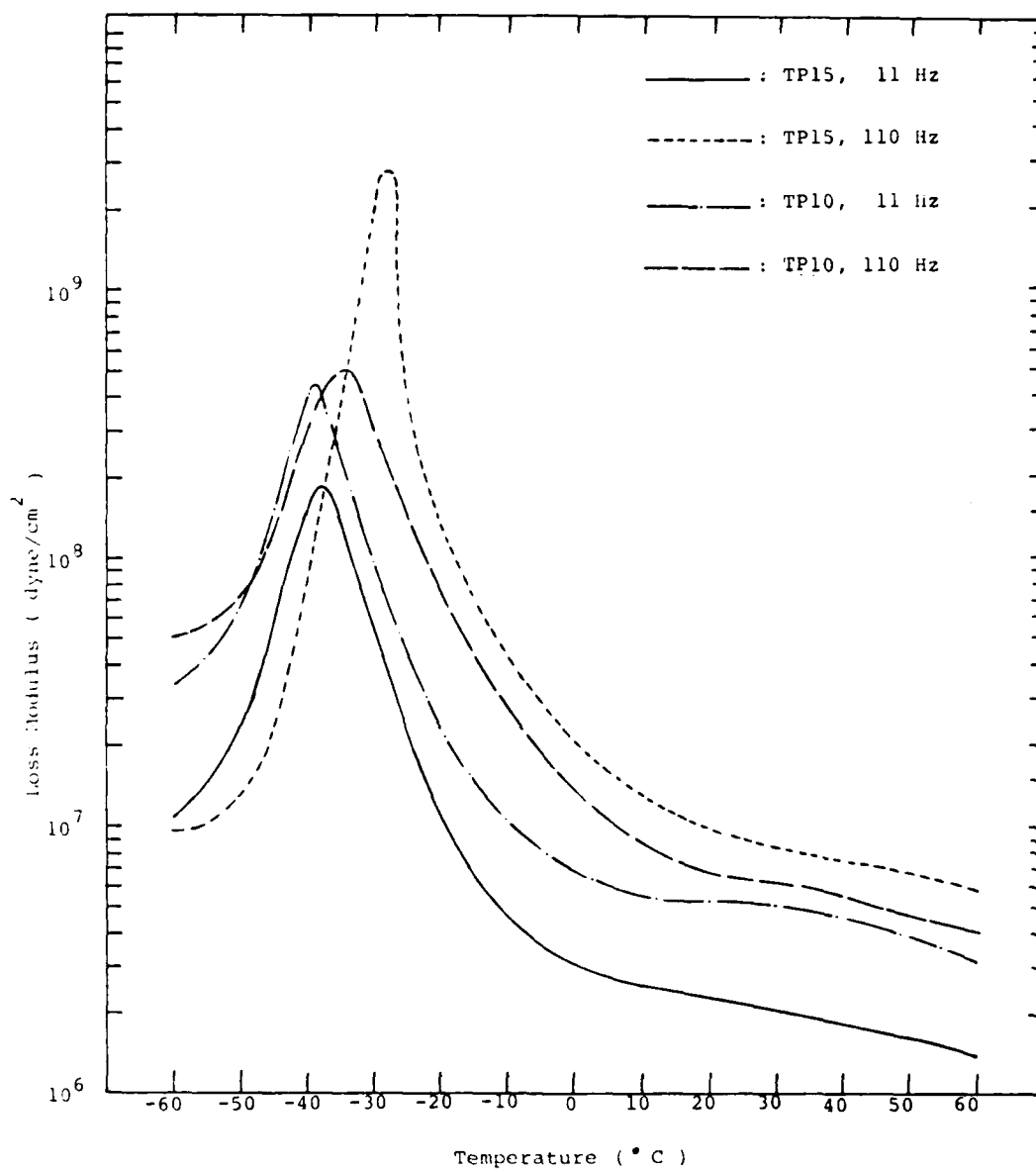
TGA

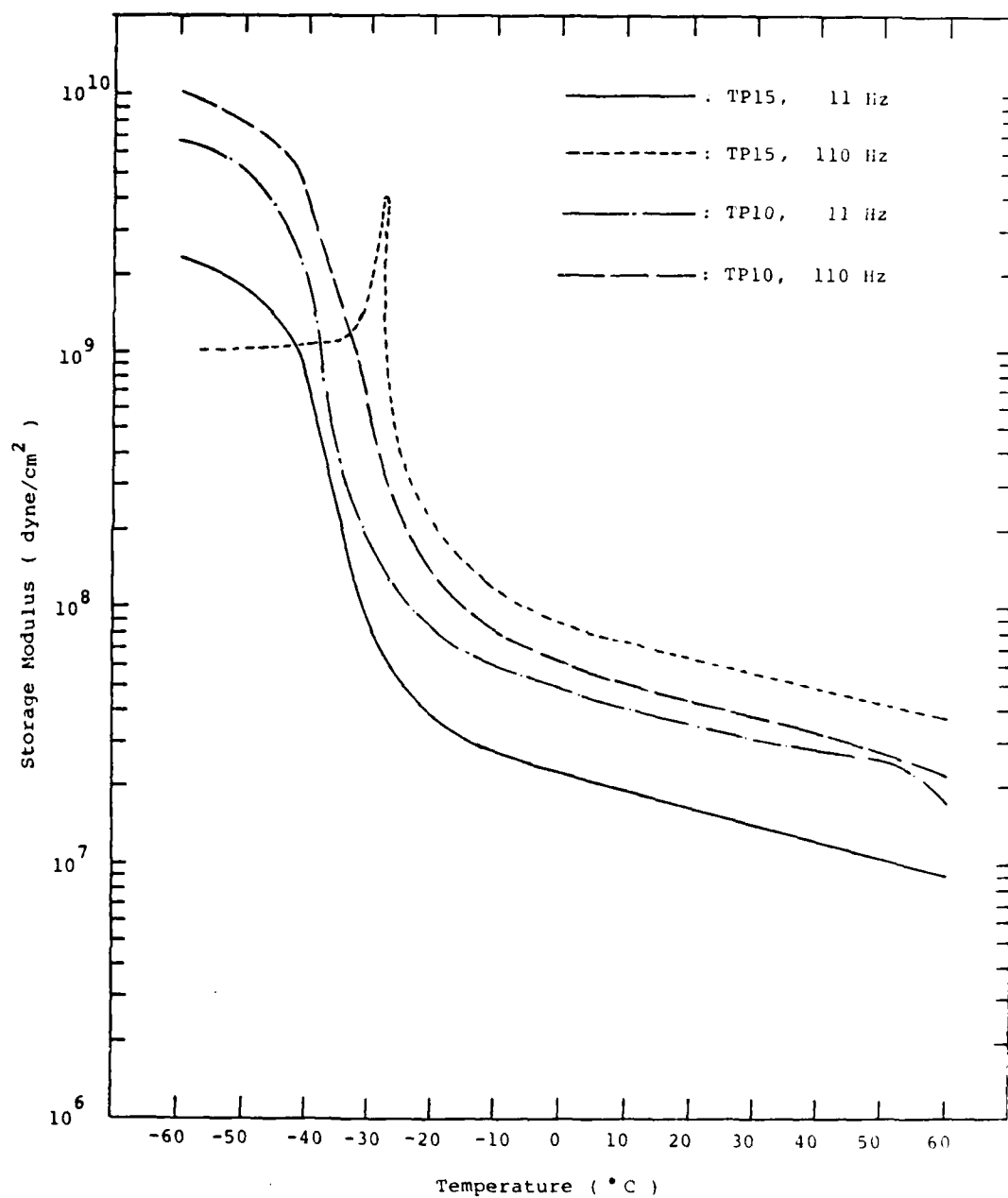


APPENDIX G

RHEOMETER CURVES: TAN AND LOSS MODULUS







DISTRIBUTION LIST

	Copies
Commander Defense Technical Information Center Bldg. 5, Cameron Station ATTN: DDAC Alexandria, VA 22314	12
Manager Defense Logistics Studies Information Exchange ATTN: AMXMC-D Fort Lee, VA 23801-6044	2
Commander U.S. Army Tank-Automotive Command ATTN: AMSTA-DDL Warren, MI 48397-5000	2
Commander U.S. Army Tank-Automotive Command ATTN: AMSTA-CF (Mr. Charles Salter) Warren, MI 48397-5000	1
Mr. Jack Patt U.S. Army Tank-Automotive Command ATTN: AMSTA-RCKT East Eleven Street Warren, MI 48090	35

END

12-86

DTIC